SPATIOTEMPORAL DYNAMICS OF RIPARIAN GREENHOUSE GAS FLUXES AND SOIL CARBON STOCKS IN THE BURA AND WUNDANYI CATCHMENTS, KENYA

GODFREY BARASA OWUOR

A THESIS SUBMITTED TO THE SCHOOL OF AGRICULTURE AND BIOTECHNOLOGY IN PARTIAL FULFILMENT OF THE REQUIREMENTS FOR THE AWARD OF THE DEGREE OF MASTER OF SCIENCE IN SOIL SCIENCE, UNIVERSITY OF ELDORET, KENYA

2025

DECLARATION

Declaration by the candidate

This thesis is my original work and has never been presented for the award of an academic degree in any other university and should not be copied or reproduced in any format without written authority from the author and/or the University of Eldoret.

GODFREY BARASA OWUOR

Signature: ……  ……... **Date:** 4/11/2025

SAGR/SOS/M/001/20

Approval by the supervisors

This thesis has been submitted with our approval as university supervisors.

Signature: …… 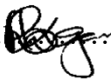 ……. **Date**: 4/11/2025

DR. RUTH NJOROGE

School of Agriculture and Biotechnology
Department of Soil Science
University of Eldoret, Eldoret, Kenya

Signature: ……  ……. **Date:** 4/11/2025

DR. ABIGAEL OTINGA

School of Agriculture and Biotechnology
Department of Soil Science
University of Eldoret, Eldoret, Kenya

Signature: ……  …… **Date:** 4/11/2025

DR. FRANK MASESE

School of Environmental Sciences and Natural Resources
Department of Fisheries and Aquatic Sciences
University of Eldoret, Eldoret, Kenya

DEDICATION

This work is dedicated to the pursuit of science that bridges knowledge and action for a resilient Africa. It honours the farmers, pastoralists, and land stewards of Sub-Saharan Africa whose daily efforts sustain both people and ecosystems, often under the pressure of changing climates and limited resources. Their lived experiences remind us that climate resilience begins in the soil, the unseen processes of carbon storage and greenhouse gas exchange that define the health of our lands.

To academicians and young scientists, including myself, why is most research not beneficial to the smallholder farming communities in SSA? I believe, among many possibilities, that it is not just about data and publications, but the future of food, landscapes, livelihoods, and the sustainability of our shared planet.

To the everyday farmer and reader, this work is a testament that small, informed actions, better soil care, thoughtful livestock management, and respect for nature can contribute to a more sustainable, more productive, and more prosperous global living.

ACKNOWLEDGEMENT

I thank the Global Research Alliance on Agricultural Greenhouse Gas Emissions (GRA), which, jointly with RUFORUM, funded the Greenhouse Gas Emissions, Soil Carbon Stocks, and Livestock Watering Points in Agropastoral Rangelands of Taita Taveta Hills, Kenya (GRESOL) project, through which we accomplished this work. Expert inputs from the Mazingira Centre (ILRI), the Institute for Water Research (IHE-Delft), and TERRA (Taita Research Station, Kenya, of the University of Helsinki) in the form of advisories, mentorship, analyses, and guidance were crucial to the success of this work. I am thankful to my field personnel, Mr Benson Mwakachola Lombo, who ensured a smooth running of my fieldwork. I also thank the farmers and residents of Taita Taveta for allowing me to conduct my fieldwork efficiently. I sincerely appreciate my laboratory technicians, Mrs Mary Nekesa Pepela and Mrs Scholastica Mutua, for their long hours of technical and analytical support.

To all those whose contributions in the many possible ways may not be mentioned here, please accept my heartfelt gratitude. May you be abundantly rewarded.

ABSTRACT

Agropastoral riparian zones are globally linked to increased greenhouse gas (GHG) emissions and soil organic carbon (SOC) depletion, but the Kenyan cases are underrepresented in global datasets. The study investigated variations in GHG fluxes and SOC stocks across three livestock production density levels in the Bura and Wundanyi sub-catchments. Eighteen (18) riparian sites (high livestock density (HLD *n=7*), low livestock density (LLD *n=4*), and zero density (ZLD *n=7*) were sampled between 2021 and 2022 in 2 dry seasons and 2 wet seasons in three topographies [(Upland at >1000 masl), (Midland 700 - <1000 masl), and (Lowland <700 masl)]. Results from Wundanyi showed higher CH_4 fluxes under HLD, particularly in the midland zones, where emissions reached 302.5 µg CH_4 m^{-2} d^{-1}. In contrast, ZLD sites acted as net CH_4 sinks. The mean CH_4 flux for Wundanyi was 30.21 mg CH_4-C m^{-2} d^{-1}. Consistently high CO_2 fluxes were recorded in Wundanyi with a mean of 900.17 mg CO_2-C m^{-2} d^{-1}. The highest mean was observed at the ZLD sites, Upland (1146.75 mg CO_2-C m^{-2} d^{-1}) and Midland (1003.25 mg CO_2-C m^{-2} d^{-1}). SOC stocks in Wundanyi averaged 6.91 Mg C ha^{-1}, with higher concentrations recorded in Upland areas (8.01 Mg C ha^{-1}). These stocks were greater during wet seasons (8.47 Mg C ha^{-1}) and showed an increasing trend with livestock density: 6.67, 7.03, and 7.40 Mg C ha^{-1} in ZLD, LLD, and HLD, respectively. In Bura, CH_4 fluxes were predominantly negative with mean absorptions in Midland LLD and Upland HLD areas (-169.27 and -256.63 mg CH_4-C m^{-2} d^{-1}), respectively. CO_2 emissions were moderate, with a mean of 527.07 mg CO_2-C m^{-2} d^{-1}, remaining <700 mg CO_2-C m^{-2} d^{-1} across sites and livestock systems. N_2O fluxes in Bura were moderate, peaking at 155.93 µg N_2O-N m^{-2} d^{-1} in Midland zones under HLD. SOC stocks were highest in the Midlands at 8.29 Mg C ha^{-1}, with values increasing alongside livestock density (7.13, 7.78, and 9.16 Mg C ha^{-1} for ZLD, LLD, and HLD, respectively. Bura was a strong methane sink, while Wundanyi recorded CH_4 emissions in grazed areas and net uptake in ZLD. The upland and ZLD areas were significant CO_2 sources. This study confirms that increasing livestock densities depleted SOC stocks with appreciable human disturbance contributions. Livestock production densities are dictated by topography, and GHG emissions are often part of natural exchange processes. To realise sustainability in livestock systems, sustainable stocking densities, protecting riparian strips, and enhancing vegetative cover should be practised. Long-term catchment-level research to document seasonal nutrient input-output dynamics would improve GHG inventories for sub-Saharan Africa.

TABLE OF CONTENTS

LIST OF TABLES

LIST OF FIGURES

LIST OF PLATES

LIST OF APPENDICES

LIST OF ABBREVIATIONS, ACRONYMS, AND SYMBOLS

AFOLU - Agriculture, Forestry, and Other Land Use

CIDP - County Integrated Development Plan

CH_4 - Methane, GHG with GWP-100 = 28-30 under IPCC AR5

CO_2 e - Carbon Dioxide Equivalent

CSA - Climate Smart Agriculture

EDGAR - Emissions Database for Global Atmospheric Research

EF - Emission Factor

FAO - Food and Agriculture Organisation

GHG - Greenhouse gas

GWP - Global Warming Potential

GDP - Gross Domestic Product

HLD - High Livestock Density

ILRI - International Livestock Research Institute

IPCC - Intergovernmental Panel on Climate Change

KCSAS - Kenya Climate-Smart Agriculture Strategy

LCA - Life Cycle Assessment

LPS - Livestock Production System

LULCC - Land Use and Land Cover Change

LULUCF - Land Use, Land Use Change, and Forestry (IPCC)

LPS - Livestock Production System

LLD - Low Livestock Density

N_2O - Nitrous oxide, GHG with GWP-100 = 265 under IPCC AR5

NAMA - Nationally Appropriate Mitigation Action for Dairy

RCBD - Randomised Complete Block Design

SIC - soil inorganic carbon

SOC - Soil organic carbon

UNFCC - United Nations Framework Convention on Climate Change

ZLD - Zero Livestock Density (No Livestock

CHAPTER ONE

INTRODUCTION

1.1 Background information

Human civilisation, its current and future sustainability, has immensely increased pressure on the utilisation of natural resources (van Gestel *et al.*, 2018; Wiesmeier *et al.*, 2019). Studies estimate that about 50 million km² of soil are under human utility for either food, fibre, or livestock production (Viaud, 2018; Wachiye *et al.*, 2020a). Anthropogenic influence on soil resources is far detrimental, ranging beyond soil fertility depletion, soil erosion (Mesele *et al.*, 2025), acidification, soil and water pollution (Bhattacharyya *et al.*, 2022), loss of biodiversity, but chiefly, loss of soil carbon (Gross & Harrison, 2019; Lal, 2025) and elevated greenhouse gas (GHG) emissions (Wachiye *et al.*, 2020b). Despite extensive research on soil organic matter (SOM) and soil organic carbon (SOC), which is the most crucial facet of SOM, there are complicating factors (Nganga *et al.*, 2020) that hinder progress in the implementation of sound land management strategies aimed at rebuilding SOC stocks (Paustian *et al.*, 2016; Wiesmeier *et al.*, 2019). The conversion of native non-agricultural soils and ecosystems to agricultural utilities accelerates the decline in SOC (Sainepo *et al.*, 2018; Vermeulen *et al.*, 2019). The rate and extent of this decline vary in space and time, due to differences in soil properties, climate, specific land-use type (LUT), and importantly, the specific management options adopted within each case (Wei *et al.*, 2015). The riparian zones account for approximately 15 % of the Earth's total reservoir surface area and are primary sources of GHG emissions through the anaerobic decomposition of SOC (Cheng *et al.*, 2025). GHG emissions in riparian zones are strongly influenced by vegetation type and various environmental factors, which jointly determine the magnitude and dynamics of emissions (Dlamini *et al.*, 2022).

Livestock production systems alter the natural nutrient cycles in the ecosystem when feeding, defecating, and urinating. They are directly linked to reduced plant litter inputs (Iteba *et al.*, 2021) and are key drivers of GHG emissions (Tiegs *et al.*, 2019). Livestock further transfer appreciable amounts of organic matter (OM) from the savanna grasslands (forage fields) into riparian ecosystems (watering sites) (Reisinger & Clark, 2018) through defecation and urination (Iteba *et al.*, 2021; Wachiye *et al.*, 2022). It is estimated that about 2.4 to 5.1 PG C y-1 is exported from land to rivers globally, with a significant portion going through microbial metabolism before reaching oceanic sinks (Iteba *et al.*, 2021; Rowland *et al.*, 2025). Soils have the potential to sequester three hundred times as much carbon produced from the burning of fossil fuels (Schuman *et al.*, 2002; Smith *et al.*, 2020; Bhattacharyya *et al.*, 2022). SOC plays an important energy-balancing role in the natural carbon cycle (Van Oost *et al.*, 2007). Rangelands with the least significant increase in SOC reserves have the potential to mitigate climate change due to their large global coverage (Lal, 2025; Schuman *et al.*, 2002).

Furthermore, SOC contains organic compounds rich in carbon and may include plant, animal, and microbial remains in any stage of decay (Vermeulen *et al.*, 2019; Lal, 2025). Livestock production initiatives directly affect SOC stocks, but with the influence of lithology, climate, edaphic factors, and biotic factors (Dahl *et al.*, 2023; Don *et al.*, 2011), which regulate input-output dynamics. Estimates of SOC losses have been reported in recent studies (Munoz-Rojas *et al.*, 2015), likely to increase with demand for food by growing populations, leading to increased pressure on rangelands (Perreira *et al.*, 2010). Livestock excreta (dung and urine) undergo microbial processing and mineralization to enhance SOC stocks and minerals, but erosion, plant uptake, and hydroclimatic limitations

work conversely. The daily forage intake by livestock is higher than their excreta can replenish, thus net carbon removal through overgrazing is a common limitation to natural ecosystem restoration efforts.

Primary land use types, anthropogenic factors, and land cover changes are the major factors that influence carbon fluxes between the Earth's surface and the atmosphere (IPCC, 2013). Land use changes and land cover changes (LULCC), particularly the conversion of riparian lands to crop production, are drivers of losses in biodiversity and ecosystem modification through carbon cycling (Munoz-Rojas *et al.*, 2015; Wei X *et al.*, 2014). Anthropogenic activities in catchments and along riparian systems have continuously replaced natural vegetation with agriculture and pastures (Gubamwoyo *et al.*, 2025; Zandalinas *et al.*, 2021). These activities escalate biodiversity losses, terminally altering natural ecosystem energy dynamics, nutrient cycling, and exacerbating erosional processes (Evangelou & Giourga, 2024; Hohenthal *et al.*, 2015). Agricultural activities, biased to livestock production, have been linked to elevating nutrient depositions and reducing plant litter inputs (Hinshaw & Wohl, 2023). Overstocking and harvesting plant residues for livestock feed contribute to increased soil erosion and loss of organic carbon to rivers and other water bodies. The organic carbon fractions within river and riparian ecosystems meet one of many fates: mineralisation and incorporation into food webs or routed downstream into long-term storage pools in aquatic sediments (Bhattacharyya *et al.*, 2022; van Gestel *et al.*, 2018).

Both livestock and wildlife transfer considerable amounts of organic matter and nutrients from the savannah grasslands into riparian ecosystems alongside similar contributions by zebra, elephant, and buffalo through direct defecation and urination (Masese *et al.*, 2017;

Tiegs *et al.*, 2019; Wachiye *et al.*, 2020a). Godde *et al.* (2020) reported a decline in the numbers of large herbivorous wildlife owing to extinction, poaching, diseases, wildfires, and human invasion, among other factors. wildlife have often been replaced by livestock (FAO, 2018; Reisinger & Clark, 2018; Rust & Rust, 2013), which ensures the continuity of this undesirable cycle.

1.2 Statement of the problem

About 42 % of agricultural soil-based greenhouse gas (GHG) emissions are reported from tropical countries (FAOSTAT, 2014a), which are underrepresented in global datasets. Despite the reported decline in the relative impacts of agro-based emissions compared to other GHG sources like the industries and transport (IPCC, 2023; Sapkota *et al.*, 2021), the quantity of agricultural emissions in absolute terms has increased and is expected to further increase with population and dietary shifts (Abera *et al.*, 2022; Kim *et al.*, 2016). Declining soil organic carbon stocks (SOC) in sub-Saharan Africa (SSA) are an indicator of increasing greenhouse gas (GHG) emissions, especially CH_4 and CO_2. Together, these factors exacerbate climate change. An urgent need to rebuild SOC stocks through carbon (C) sequestration is key to climate change mitigation and sustainability in the agricultural sector. This study will document soil-related GHG emissions and SOC measurements as would be influenced by different livestock production systems (LPS).

1.3 Justification of the study

SOC impacts the chemical, physical, and biological ecosystem functions of soil. Therefore, SOC is a strong indicator of soil quality (Evangelou & Giourga, 2024; Sainepo *et al.*, 2018). Grazing intensity contributes to soil carbon removal, which is linked to species composition and function (Gitau *et al.*, 2021). The SOC reserve includes the labile and

stable carbon fractions, with the former being more manageable. Kenya's SOC stocks have reportedly declined over the years with the expansion of ASALS (**Figure 1Figure 1**). Heinrich (2025) reports that only 25 % of the land in Kenya is suitable for crop production (based on overall soil health), and thus justifies encroachment into the riparian zones. Taita Taveta, highlighted in black, falls in one of the most hit areas with deficient SOC (<1.3 %), degraded lands, encroached riparian zones, and high sand harvesting (Taita Taveta County Government, 2018, 2023).

Elevated atmospheric CO_2 inputs are associated with degrading anthropogenic activities such as overgrazing and deforestation. (Gitau *et al.*, 2021; Gross & Harrison, 2019). In Kenya, the agricultural sector accounts for 58.6 % of the country's total GHG emissions, and livestock production is responsible for 96.2 % (Reisinger & Clark, 2018; Sapkota *et al.*, 2021). GHG mitigation options for the livestock sector in Kenya would include improved feeds with fodder and hay production (1.57 Mt $CO_2e\ y^{-1}$), manure management using biogas plants (0.09 Mt $CO_2e\ y^{-1}$), breed improvement production (1.2 Mt $CO_2e\ y^{-1}$), dairy processing plants retrofit (0.14 Mt $CO_2e\ y^{-1}$), and reduction of milk loss and waste (2.9 Mt $CO_2e\ y^{-1}$) (IPCC SPM, 2023; Khatri-Chhetri *et al.*, 2020; Herrero *et al.*, 2016a).

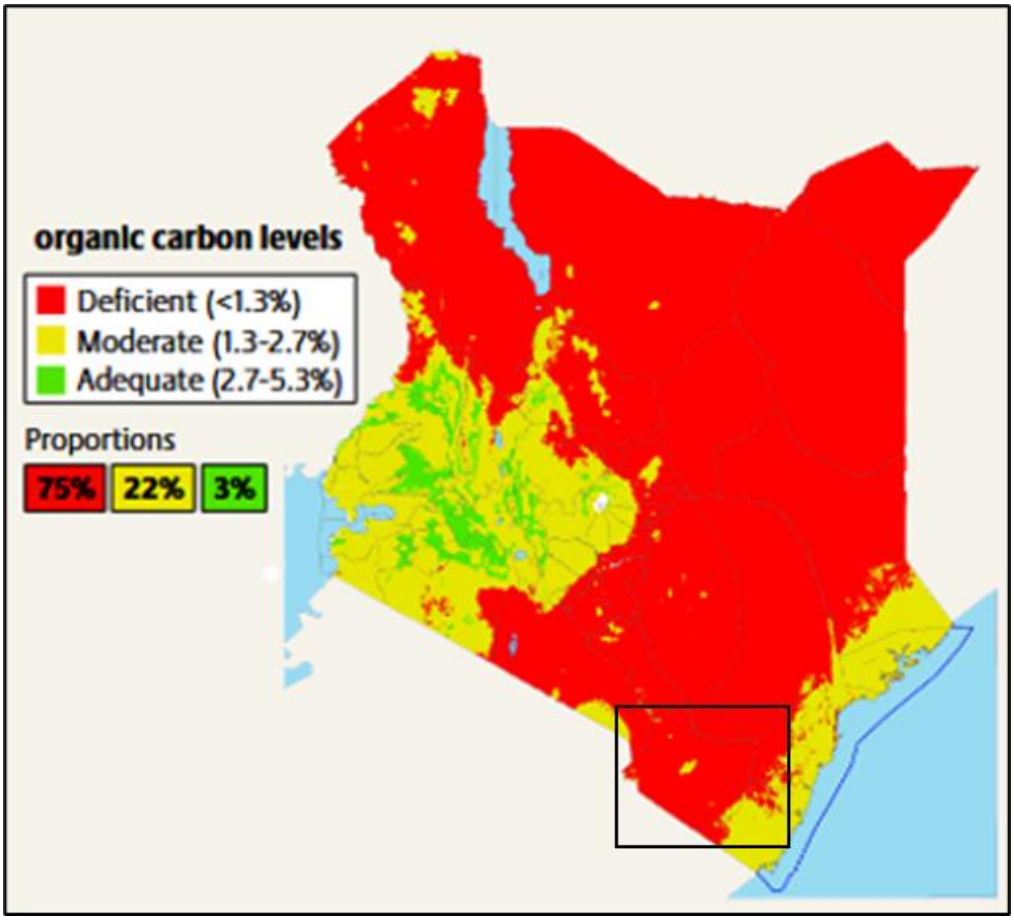

Figure 1: **Soil organic carbon (SOC) distribution map of Kenya. About 25 % of Kenya is suitable for crop production. The black border south of Kenya shows the Taita Taveta County. Adapted from The Soil Atlas Kenya Edition (Heinrich, 2025).**

The cost of GHG emissions abatement using these options ranges from 63$/t$CO_2$ in improved feed to 80$/t$CO_2$ in dairy plants (Khatri-Chhetri *et al.*, 2020; Ndung'u *et al.*, 2020). But, how about the free-range systems? Livestock, as the major consumer of primary production in Kenya's ASAL rangelands (Iteba *et al.*, 2021; Wachiye *et al.*, 2022), are often dependent on the cultural and economic interests of the major ethnic group occupying the area, although they are often interconnected. Herd sizes and compositions vary spatially and culturally, but neither depends on land suitability nor sustainability scores (FAO, 2018; Rust & Rust, 2013; Sapkota *et al.*, 2021).

FAOSTAT (2024) reported increasing GHG emissions in Kenya (**Figure 2**) with livestock production (Reisinger & Clark, 2018) accounting for more than 60% of national GHG emissions from agriculture. Livestock production notably contributes significantly to food security, nutrition, and poverty alleviation (FAO, 2018; Rayne & Aula, 2020). The two primary sources of GHG emissions are feed production and processing, enteric fermentation, and manure management (Khatri-Chhetri *et al.*, 2020). FAO reported that enteric fermentation and manure management are expected to raise global methane (CH_4) and nitrous oxide (N_2O) emissions by 13.5 % by 2030 (FAO, 2018).

Kenya is a signatory to the Paris Agreement (2015) and a party to the UNFCCC. She has achieved significant progress in mainstreaming climate change mitigation and adaptation initiatives through policies like the National Climate Finance Policy and the Green Economy Strategy and Implementation Plans (2016-2030), Climate Act (2016), Kenya Climate-Smart Agriculture Strategy (KCSAS-2017), Dairy Nationally Appropriate Mitigation Action (NAMA-2017), among others.

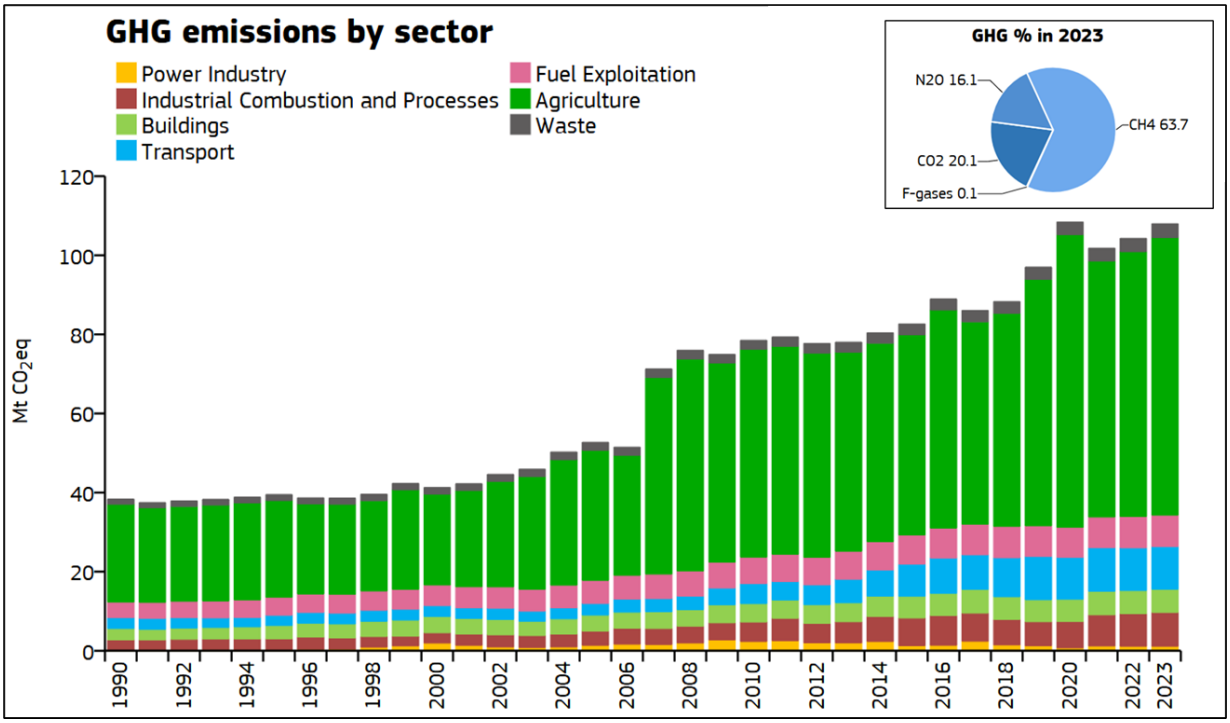

Figure 2: Kenya's sectoral GHG emission trend between 1990 and 2023. Emissions decreased in 2021 and increased continuously thereafter. Kenya's GHG emissions are methane-driven (63.7%). Adapted from (FAOSTAT, 2024).

1.4 Objectives of the study

1.4.1 Broad objective

This study aimed at investigating and documenting the contribution of livestock to seasonal GHG emissions and SOC dynamics on riparian lands along the Afromontane River basin in Taita Taveta County, Kenya.

1.4.2 Specific objectives

The specific objectives of this research are to:

1. Quantify and compare seasonal greenhouse gas (GHG) fluxes on riparian strips as influenced by livestock density classes along the Bura and Wundanyi sub-catchments.

2. Determine and document seasonal changes in riparian soil organic carbon (SOC) stocks as influenced by livestock density classes in the Bura and Wundanyi sub-catchments.

1.5 Hypotheses

The following hypotheses were considered for this study:

1. Increasing livestock nutrient loading (urination and defecation) on riparian strips augments greenhouse gas (GHG) emissions in the Bura and Wundanyi sub-catchments.

2. Increasing livestock densities exacerbate soil organic carbon (SOC) depletion through high forage intakes in the Bura and Wundanyi sub-catchments.

CHAPTER TWO

LITERATURE REVIEW

2.1 Background to soil organic carbon (SOC)

The dead fraction of the soil consisting of plant and/or animal tissues in various stages of decomposition is often referred to as the soil organic matter (Six *et al.*, 2001; Yang *et al.*, 2025). For ideal agricultural soils, the threshold of soil organic matter (SOM) content constitutes up to 6% of a soil's dry weight (Brady & Weil, 2016); below this threshold, rigorous management options are recommended to replenish the SOM content. Due to climate variability and site-specific management initiatives, SOM ranges are varied, especially for cultivated soils (Nganga *et al.*, 2020; Rotich *et al.*, 2020). Soil organic matter can be classified into three (3) broad categories: *i*. living microbial biomass and plant residues, *ii*. the active detritus soil organic matter, and *iii*. the stable, fully degraded organic matter (humus) (Gitau *et al.*, 2021; Six *et al.*, 2001). When these OM fractions decompose, primary nutrients (e.g., N, P, and K) are released and thus directly contribute to soil fertility. Humus is the end product of decomposition and mainly contributes to soil physical attributes (e.g., soil structure, tilth, and electroconductivity (EC)) critical in soil health assessment (Gul & Whalen, 2022).

2.2 Soil organic matter (SOM) and soil organic carbon (SOC) – the contrast

Soil organic carbon (SOC) is a component of soil organic matter (SOM). SOM is primarily made up of carbon (58 %), with the remaining mass consisting of water and mineral nutrients. Carbon occupies the largest fraction of SOM and is relatively easier to quantify and report through a standard test in the laboratory. (Sainepo *et al.*, 2018; Vermeulen *et al.*, 2019). As a standard soil testing protocol, any organic matter >2.0 mm is not

sufficiently degraded and is not considered part of the SOM. Such are referred to as (plant or animal, buried or surface) residues. Decomposition is a biological process that includes the physical breakdown and biochemical transformation of complex molecules into simpler molecules that are easily absorbed in the rhizosphere (Carter, 1995; Lavallee *et al.*, 2020). The breakdown of SOM, root growth, and decay also contribute to these biochemical and physical transition processes (Muñoz-Rojas *et al.*, 2015). Carbon cycling is the continuous transformation of organic and inorganic carbon compounds by plants and micro- and macro-organisms between the soil, plants, and the atmosphere (Gross & Harrison, 2019; Rotich *et al.*, 2020). SOM is ordinarily estimated to contain 58 % C, and soil organic carbon (SOC) is often used as a synonym for SOM, with measured SOC content used as a proxy for SOM. Soil represents one of the largest C sinks on Earth and is significant in the global carbon cycle and therefore for climate change mitigation (He, 2020; Lavallee *et al.*, 2020).

2.3 The soil organic and inorganic carbon pools

Soil inorganic carbon (SIC) and organic carbon (SOC) are important carbon reservoirs and, therefore, precursors to GHG emissions in agroecosystems (**Figure 3**). The estimated global SOC storage varies within 1220-1576 Pg in the top 100 cm^3, and the SIC storage is 700-1700 Pg (Guo *et al.*, 2016). Soil inorganic carbon, primarily calcium (and often magnesium) carbonate, is formed mainly through the following two reactions:

Equation 1

$$CO_2 + H_2O \leftrightarrow HCO_3^- + H^+ \qquad \text{…. (i)}$$

$$Ca_2^+ + 2HCO_3^- \leftrightarrow CaCO_3 + H_2O + CO_2 \qquad \text{…. (ii)}$$

From these reversible equations, the formation of calcium carbonate ($CaCO_3$) is affected by soil carbon dioxide (CO_2) concentration, pH, calcium ions (Ca^{2+}) content, and water (H_2O) availability. Increasing soil pH (decrease in H^+) would drive the reaction (i) to the right, producing more HCO_3^-. When there is no limitation of soluble Ca^{2+}, $CaCO_3$ is precipitated. On the other hand, an increase in soil CO_2 or a decrease in soil pH would drive the reaction (2) to the left to attain equilibrium. Therefore, inherent acidic conditions could lead to the dissolution of carbonates, causing a decrease in SIC, whereas an alkaline environment would favour the formation of carbonates (Guo *et al.*, 2016). There are limited local studies assessing how these environmental conditions regulate SIC dynamics (see **Figure 3**). In particular, little information is available on the relationship of Ca^{2+} (or Mg^{2+}) with SIC stock (Lu *et al.*, 2020). According to the Africa Climate Reality Project, African soils stored 154.6 billion tons of CO_2 in 2014, representing 9 % of the global soil carbon stocks.

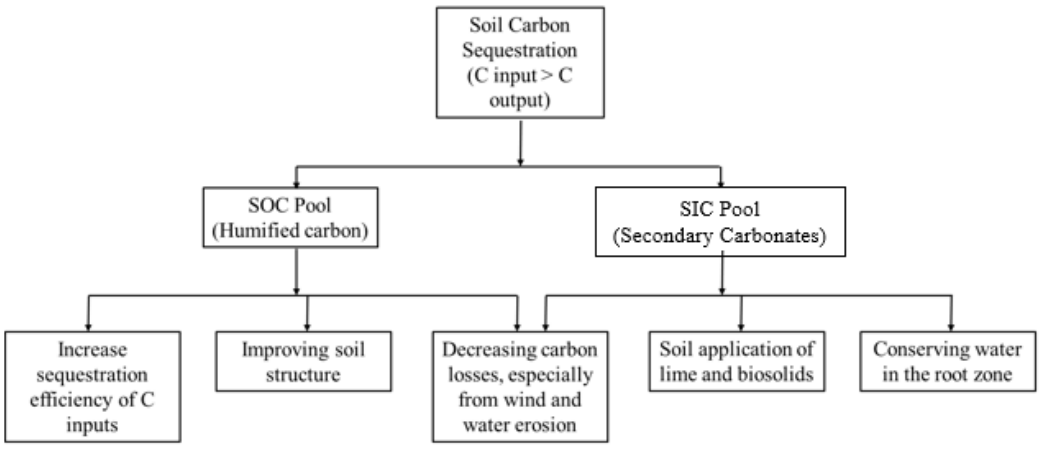

Figure 3: Soil carbon sequestration strategies. SIC is the soil inorganic carbon pool depicted as secondary carbonates, while SOC (soil organic carbon) is referred to as humified carbon. Source (Morgan *et al.*, 2010).

2.4 Sources and roles of soil organic matter (SOM)

2.4.1 Agricultural Sources of SOM

Application of organic materials over time can increase stable soil organic matter levels. The quickest increases are obtained with sources high in carbon, such as compost or semi-solid manure (He, 2020). Sources of organic materials include:

1) Crop residues, including stalks, straws, pods, leaves, flowers, etc.
2) Animal manure, including cow dung, donkey, goat, sheep, rabbit, and chicken droppings
3) Composts that include every bit of all these items.
4) Cover crops (green manure) like potato vines and clover
5) Perennial grasses and legumes.

2.4.2 Agroecological importance of SOM

There are numerous benefits to having a relatively high, stable organic matter level in agricultural soils (Carter, 1995; Lavallee *et al.*, 2020). With careful management, the preservation and accumulation of soil organic matter can help to improve soil productivity, resulting in greater farm profitability (He, 2020). The benefits of SOM result from several complex, interactive, and edaphic factors (**Figure 3**), which can be grouped into three broad categories:

2.4.2.1 SOM and physical soil attributes

1) Enhances aggregate stability, improving water infiltration and soil aeration, reducing runoff.

2) Improves water holding capacity.
3) Reduces the stickiness of clay soils, making them easier to till.
4) Reduces surface crusting, facilitating seedbed preparation.

2.4.2.2 SOM and chemical soil attributes

1) Increases the soil's CEC or its ability to hold onto and supply over time essential nutrients such as calcium, magnesium, and potassium.
2) Improves the ability of a soil to resist pH changes or soil pH buffering.
3) Accelerates decomposition of soil minerals over time, making the nutrients in the minerals available for plant uptake.
4) Absorption and retention of pollutants, consider heavy metals and plant usable nutrients.

2.4.2.3 SOM and biological soil attributes

1) Provides food and habitat for the living organisms in the soil.
2) Enhances soil microbial biodiversity and activity, which can help in the mineralisation processes as well as the suppression of diseases and pests.
3) Enhances pore space through the actions of soil microorganisms. This helps to increase infiltration and reduce runoff.
4) Heat and water retention – important in temperature regulation for optimised microbial activities.

2.5 Influences of anthropogenic activities on SOC

Approximately 50 million km^2 of soil are under human utility for either food, fibre, or livestock production under significantly variable scales and intensities (Don *et al.*, 2011,

2011; Gubamwoyo *et al.*, 2025). Humanity, therefore, impacts the natural ecosystem functioning in the quest to meet global population food and fibre demands (**Plate II**). A dramatic reworking of the regional distribution and quantity of greenhouse gas (GHG) sources and sinks occurs as a result of unprecedented expansion in energy consumption and rapid land use changes (Calle *et al.*, 2016). Even though fossil fuel combustion accounts for the majority of anthropogenic carbon emissions in Asia (Wei *et al.*, 2015), land transformation in this region is among the quickest in the world, with substantial spatial contrast between deforestation and reforestation aspects (Hansen *et al.*, 2013; He, 2020). Global net carbon emissions from land use and land cover change (LULCC) are around 1.0 ± 0.8 Pg C yr^{-1} (Le Quéré *et al.*, 2015).

Typically, the Afrotropical riparian strips are often fertile due to alluvial deposits, and the availability of moisture supports vegetation buildup. The government of Kenya has enacted riparian zone protection acts to inhibit encroachment by humans, but high demand for food and fiber has made this a difficult task. Humans have evidently established food crops, sand harvesting, agroforestry, and pasturelands along these river systems, altering the natural agroecological nutrient cycling, OM processing, and eventually increasing GHG emissions. Such initiatives are considerably difficult to regulate despite the existence of legal measures (from the County administration), particularly because these lands are lucrative sources of livelihood, and leaving them ‘idle’ does not seem right according to a local informant.

The readily usable biomasses like wood, leaves & roots, and associated land-management practices (e.g., slash and burn, shifting cultivation, permanent agriculture) influence the

extent of net CO_2 fluxes with respect to changes in land use and land cover (LULC) (Muñoz-Rojas *et al.*, 2015). According to the Intergovernmental Panel on Climate Change Assessment Report 5, worldwide LULCC carbon emissions declined between the 1990s (1.5 - 0.8 Pg. C yr^{-1}) and the 2000s (1.0 Pg. C yr^{-1}) (Calle *et al.*, 2016). In their study, Kim *et al.* (2016) reported significant ambiguities surrounding the magnitude of change and the spatial attribution of carbon flows. LULCC fluxes are needed to limit the global carbon shifts and, further, to internalise the role of terrestrial ecosystems in Africa in contributing to and moderating GHG concentration rises (Gitau *et al.*, 2021; Hou *et al.*, 2016).

2.6 Land use classification for the Taita Taveta landscape

2.6.1 Land use and cover classification in Taita Taveta

LULC classifications and mapping for Taita Taveta County have developed over time. Cropland, shrubland, thicket, grassland, woodland, exotic plantation forest, water, indigenous evergreen moist montane forest, bare rock, bare soil, built-up areas, and burned areas were the twelve (12) land cover classes obtained from the 1987, 1992, and 2003 SPOT scenes (Clark & Pellikka, 2009). As shown in **Figure 4**, Taita Taveta mainly comprises croplands and shrublands in the highland valley bottom wetland (HVBW) regions. Built-up regions and bare soil classes were grouped since charred portions were absent. This resulted in ten categories in 2011. (Pellikka *et al.*, 2013b, 2018a). Gubamwoyo *et al.* (2025) mapped out six consolidated LULC classes in Taita Taveta, comprising: *i*. cropland and agroforestry, *ii*. water, *iii*. shrubland, *iv*. road-leaved forests, grassland and thicket, *v*. buildings, bare rock, and bare soil, and *vi*. plantation forests.

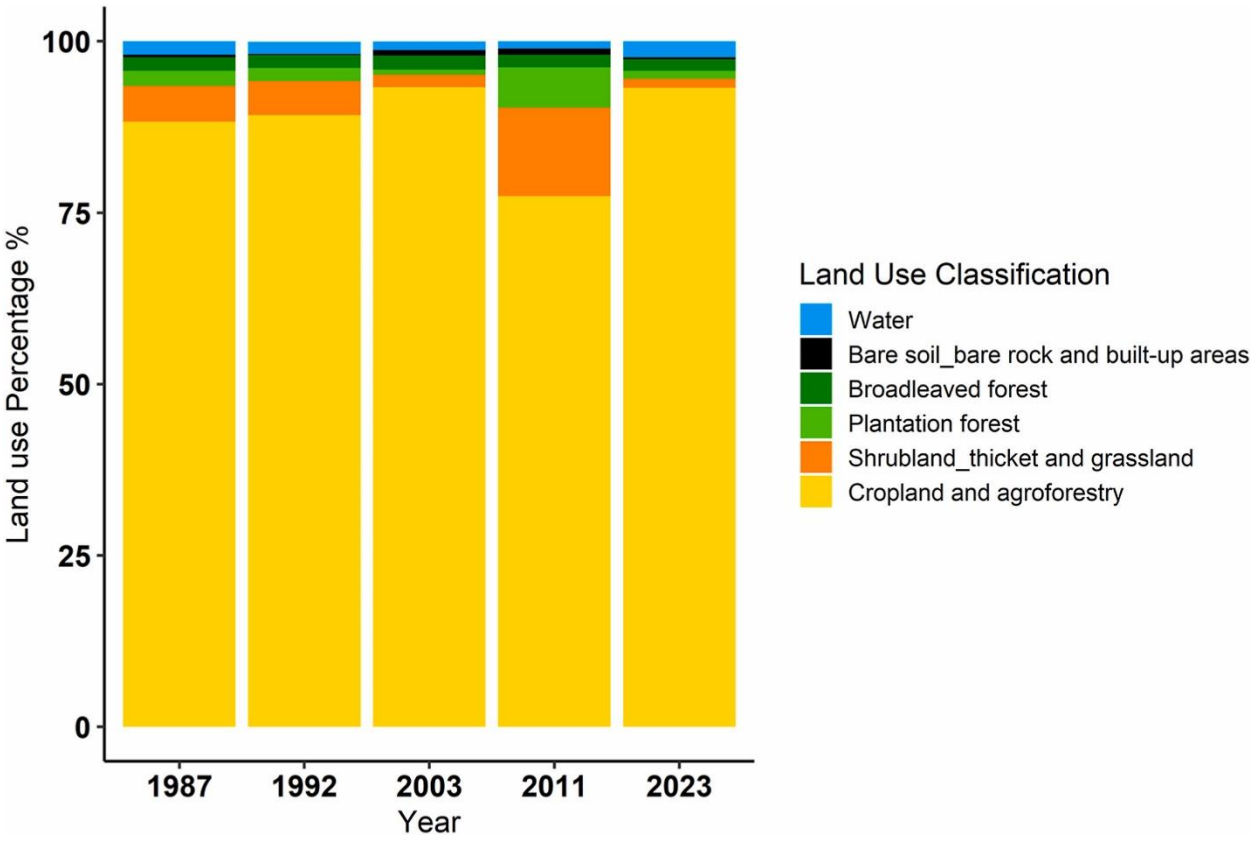

Figure 4: **Land use and cover changes in Taita Taveta. Percentage coverage of LULC classes in five years in Taita Hills HVBW from 1987 to 2023. Adapted from (Gubamwoyo *et al.*, 2025)**

2.6.2 Satellite imagery for LULC in Taita Taveta

Early LULC maps were created in 1987, 1992, and 2003, utilising an object-oriented technique known as the multi-scale segmentation and object relationship modelling (MSS/ORM) methodology (Clark & Pellikka, 2009). The MSS/ORM approach was further utilised for processing and categorisation of the SPOT 4 HRVIR picture from October 2011, see **Plate *I***.

Plate I: Some LULC classifications in Taita Taveta. Land utilisation types in Taita Taveta. A) Cropland over 1220 m asl characterised by tree cover, B) Cropland below 1220 m asl on alluvial plane, C) Indigenous moist evergreen montane forest, D) Cropland over 1220 m asl with Grevillea Robusta trees. Source: (Pellikka *et al.*, 2018b).

2.7 Effects of livestock production on soil organic matter

Rangelands constitute about 50 % of the global landmass and approximately 69 % of the world's agricultural land (Gitau *et al.*, 2021; Rotich *et al.*, 2020). Rangelands are important habitats for wild macroflora and macrofauna and are additionally key to domestic livestock production (Bird *et al.*, 2002; Pulido *et al.*, 2018; Waters *et al.*, 2017). In Kenya, livestock production is often attractive to the arid and semi-arid lands (ASALs) through pastoralism and ranching systems (**Plate IV**). An estimated 25 million pastoralists and 240 million agro-pastoralists primarily depend on livestock production for their income (FAO, 2018; Gerber *et al.*, 2013; Rust & Rust, 2013). Livestock movement and feeding are important

components of land management in this sector (Rayne & Aula, 2020). Recently, rapid losses of soil C associated with intensive livestock grazing have been reported for tropical savannah (Slosson *et al.*, 2025; van Gestel *et al.*, 2018).

To compare soil carbon of grazed and protected areas, about 40 % of data sets indicated an increase in soil carbon due to grazing, and about 60 % showed a decrease or no response to grazing (Rayne & Aula, 2020; Reisinger & Clark, 2018). Additionally, the impact of grazing on ecosystem functioning was influenced by the extent of the removal of photosynthetic biomass, i.e., defoliation, which is partially determined by livestock grazing intensities; trafficking and faecal and urine depositions (Godde *et al.*, 2020; Herrero *et al.*, 2016a). Overstocking and poor grazing patterns reduce pasture (grasses, herbs, and shrubs) growth and productivity. This becomes a socioeconomic threat, especially in the dry seasons, when forage demand is high (Pulido *et al.*, 2018; Rotich *et al.*, 2020). Grazing influences carbon dynamics in the rangelands through defecation (dung and urine), which alters nutrient distributions, biomass, and biodiversity (Pulido *et al.*, 2018).

2.7.1 Management of SOC in pasturelands

Livestock are large mammalian herbivores, foraging on plant biomass in the tropics with different seasonal feeding patterns (Rust & Rust, 2013). Carbon sequestration rates decline over time due to unsustainable grazing patterns. Additional inputs are needed to enhance carbon sequestration on tropical pasturelands (Zuo *et al.*, 2018). Tropical pasturelands may store twice as much carbon as farmlands through sustainable stocking rates, plant biodiversity, and soil erosion management (Pulido *et al.*, 2018). Under optimum

management techniques, rates of SOC sequestration for rangelands in the US reportedly ranged from 0.070 to 0.30 Mg C ha^{-1} yr^{-1} (62 to 270 lb. C ac-1 yr-1) and for pastures from 0.30 to 1.4 Mg C ha^{-1} yr^{-1} (270 to 1200 lb. ac^{-1} yr^{-1}) (Herrero *et al.*, 2016a; Reisinger & Clark, 2018; Rust & Rust, 2013).

2.8 Effects of crop production on soil organic matter

Increasing demand for food and fibre has sparked a global run for increased food production, thereby adversely influencing the environment and climate (Arthur & Okae-Anti, 2022; Obeka et al., 2024). These changes are accelerated by intensified monoculture production systems. Increasing SOM may increase yields in crops with relatively low nutrient demand, and has not yet realised recognition in staple high-nutrient crop (e.g., maize, wheat, and potatoes) production (He, 2020). Organic inputs that build SOM are limited in supply and have low nutrient content. Farmers thus require them in bulk, and this demands more labour compared to chemical fertilisers. Soil degradation in its many forms does not directly translate to mass starvation despite its contribution to declining yields globally (Mesele et al., 2025). This could be attributed to increasing availability and access to farm inputs like fertilisers and agrochemicals.

2.8.1 Management of soil organic carbon in croplands

Increasing cropping frequency and cultivating high-residue crops are two recommended management methods to increase SOC in croplands (Govaerts et al., 2009; Lavallee et al., 2020). Reduced soil tillage, although efficacy varies by soil type and crop, increases plant water and nutrient use efficiencies (Baker *et al.*, 2007). Sustainable crop rotation and irrigation management alongside the use of surface mulches can mediate soil C losses (van

Wijk *et al.*, 2020). Perennial grass/legume mixtures can help to assign a higher percentage of plant biomass C to below-ground soil C sequestration, extend the growing season, better utilise soil water, and reduce tillage disturbances (Lu *et al.*, 2020; Viaud, 2018; Zuo *et al.*, 2018). SOC sequestration rates on croplands can be increased to 1 Mg (106 g) C ha^{-1} yr^{-1} (Hinshaw & Wohl, 2023; Schweizer *et al.*, 2021). Higher conversion rates of annual croplands to perennial grasses and legumes as conservation set-asides or pastures are predictable herein (Tubiello *et al.*, 2015; Wachiye *et al.*, 2020b).

2.8.2 Conservation tillage and soil carbon

According to Govaerts *et al*. (2009), the continued use of traditional agricultural methods that involve heavy tillage and burning of crop wastes has increased soil deterioration and increased soil carbon losses through erosion. Conservation tillage requires that the residue covering on the soil surface be at least 30 %, although it does not specify an ideal amount of tillage (Baker et al., 2007; Rahman et al., 2021). Conservation agriculture further combines the following principles to address an improved notion of entire agricultural systems rather than focusing solely on the tillage component (Baker et al., 2007; Featherstone & Goodwin, 1993; Rahman et al., 2021).

2.8.2.1 Principles of conservation tillage

1. **Reduce soil disturbance:** Apply zero tillage (no till) or controlled tillage practices that do not disturb more than 20-25% of the soil surface. Tillage to a depth that just "covers" seeds to enable germination. This is important in maintaining soil biology, which helps with natural pedoturbation and aeration of the soil.

2. **Maintain soil cover:** Keep sufficient residue on the soil's surface to prevent erosion from wind, splash, water runoff, and evaporation. This helps to increase

water productivity and improve the physical, chemical, and biological soil attributes.

3. **Adopt crop rotation:** Employ economically viable, diversified crop rotations to help moderate/mitigate possible weed, disease, and pest problems and their associated diseases. Crop rotations are important in nutrient access and turnover by different root-depth diversity.

2.9 Agricultural greenhouse gas (GHG) emissions

Greenhouse gases (GHG) naturally trap radiation in the atmosphere to keep the globe warm and thus are key to life. The three GHGs (CO_2, CH_4, and N_2O), derived from various sectors, play a major role in regulating Earth's temperature (see **Figure 2**). At their initial levels, GHG ensured a maintained moderate global temperature that supports living organisms. Global temperatures have elevated and continue to do so to detrimental levels that threaten the very human existence. This has resulted from increased atmospheric concentrations of carbon dioxide (CO_2), methane (CH_4), and nitrous oxide (N_2O), trapping more heat to destabilise the planet's temperatures (Rahman *et al.*, 2021; Smith *et al.*, 2003a; Wachiye *et al.*, 2020a).

Agriculture encompasses both the crop and livestock sectors under different scales of operation**Error! Reference source not found.**. Cumulative GHG emission estimates should include direct and indirect sources. The application of farm machinery, agrochemicals, fertilisers, and inappropriate logging and deforestation all contribute indirectly to the emission of greenhouse gases. On the other hand, burning of fossil fuels, enteric fermentation, decomposition, respiration, and manure are direct sources of GHGs in agriculture (Tian *et al.*, 2020; Tubiello *et al.*, 2014).

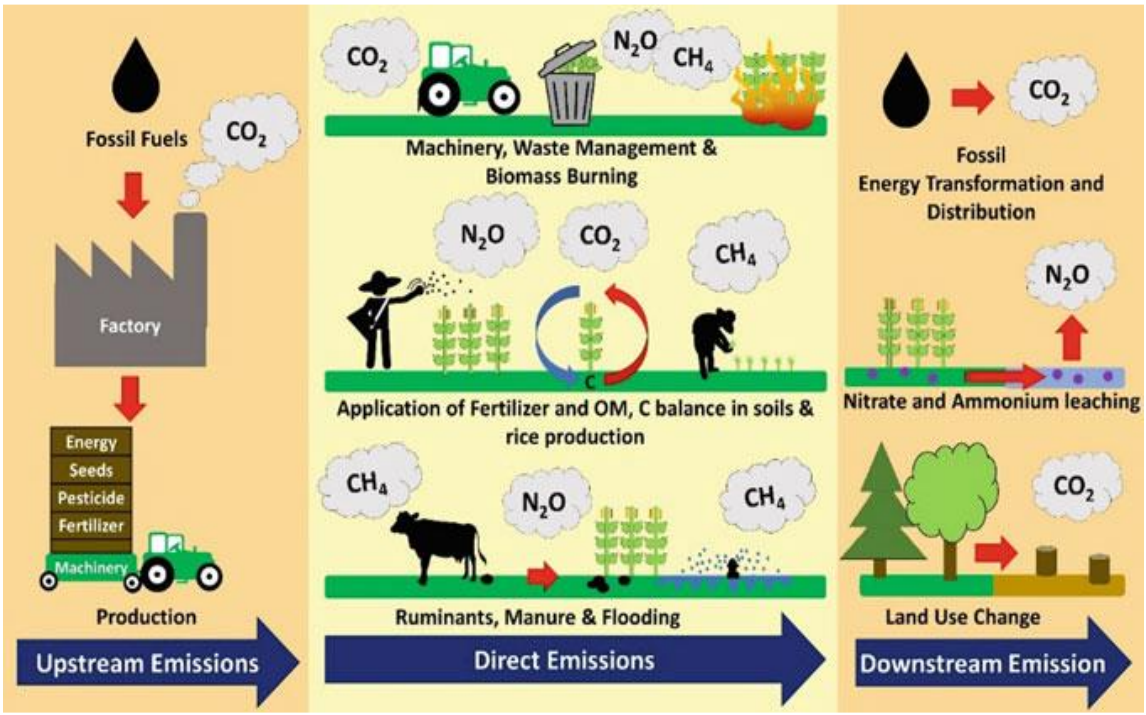

Figure 5: Agricultural greenhouse gas (GHG) emissions in their direct and indirect (Upstream and Downstream) sources. Key sources of GHG are the burning of fossil fuels (industrialisation) and agrifood systems. Adapted from (Fernández & Manuel, 2016).

2.9.1 Major GHG emissions from agricultural systems

The following gases are associated with agricultural systems;

2.9.1.1 Carbon dioxide (CO_2)

Carbon dioxide is the major GHG responsible for the increasing greenhouse effect (see **Figure 2**). Key natural sources of CO_2 include ocean–atmosphere exchange, respiration of animals, soils (microbial respiration) and plants, and volcanic eruption (Bhattacharyya *et al.*, 2022; Wachiye *et al.*, 2022). Major anthropogenic sources of CO_2 include the burning of fossil fuels (coal, natural gas, and oil), deforestation, and the cultivation of land that

increases the decomposition of soil organic matter and crop and animal residues (Chen & Gong, 2021; Clark *et al.*, 2020).

2.9.1.2 Methane (CH_4)

Methane (CH_4) is a significant GHG, which is emitted from both natural and anthropogenic processes. Ruminants such as cattle produce methane (CH_4) as part of their digestive processes (Bratti *et al.*, 2022; Ndung'u *et al.*, 2020). Ndung'u *et al.* (2020) also documented that this process, leading to enteric fermentation, is responsible for over 25 % of total agricultural emissions. Other natural sources of CH_4 emissions include the wetlands, termite activities, and the ocean. Paddy rice fields, livestock manure management, landfills, and fossil fuels are the main anthropogenic sources of CH_4 (Goopy *et al.*, 2020; Ndung'u *et al.*, 2020). CH_4 can be further produced by anaerobic mineralisation by methanogenic archaea in both natural and man-made systems (Sapkota *et al.*, 2018; Wollenberg *et al.*, 2016). Plants have also been shown to emit CH_4 (McNunn *et al.*, 2020; Musafiri *et al.*, 2020).

2.9.1.3 Nitrous oxide (N_2O)

Some management options for agricultural soils may lead to nitrogen build-ups in the soil, and therefore enhanced N_2O emissions (Hou *et al.*, 2016). Activities such as the application of synthetic and organic fertilisers, the growth of nitrogen-fixing crops, the drainage of organic soils, and irrigation practices enhance N_2O emissions (Israel *et al.*, 2020). Management of agricultural soils accounts for just over half of the GHG emissions from the sector (Hou *et al.*, 2016; Janssens-Maenhout *et al.*, 2017; Tubiello *et al.*, 2014). Besides being a major GHG, N_2O is a major ozone (O_3) depleting gas (Hou *et al.*, 2016). Oceans and soils with natural vegetation are non-anthropogenic sources of N_2O. At a global scale, N_2O emission is mostly caused by anthropogenic activities. The atmospheric concentration of N_2O has increased by more than 20% from ~271 ppb to 331 ppb since the industrial era (1750s) to 2018 (WMO 2019).

Over the last decade, the rate of N_2O increase was equal to 0.95 ppb yr^{-1} (Eggleston *et al.*, 2006; McNunn *et al.*, 2020) with an increasing trend (Hou *et al.*, 2016). In 2006, the total anthropogenic source of N_2O was 6.9 Tg N_2O-N. Out of which agricultural sources dominated at (4.1 Tg N_2O-N), while indirect emissions were 0.1-2.9 Tg N_2O-N (Nayak *et al.*, 2015). Such a large N_2O emission is attributed to various factors, including the intensification of agriculture and increased use of synthetic fertiliser, which was approximately 119.4 million tons of nitrogen (N) worldwide (2019). Anthropogenic emissions of GHGs are at their highest in history, according to data from the UN's Intergovernmental Panel on Climate Change (IPCC) (IPCC 2014a). Since 1990, the Earth's average air temperature has increased by about 0.8 °C, with much of it in the mid-1970s – early industrialisation (Roger & Belliethathan, 2016; Zandalinas *et al.*, 2021).

2.10 The global warming potential (GWP) of GHGs and the Kyoto Protocol

The global warming potential (GWP) of a particular GHG relates to the amount of heat trapped by a certain mass of that gas compared to the amount of heat trapped by a similar mass of CO_2 calculated over a 100-year time horizon (Calvin *et al.*, 2023; IPCC, 2014). For instance, the GWP of nitrous oxide (N_2O) is between 265 and 298, implying that if the same masses of N_2O and CO_2 were emitted into the atmosphere, N_2O would trap 265–298 times more heat than CO_2 over 100 years, as shown in **Table 1**. The Kyoto Protocol (1997) was negotiated by parties to the United Nations Framework Convention on Climate Change (UNFCCC) to stabilise the increasing global temperature consequent to elevated atmospheric GHG concentrations (Liu *et al.*, 2022; Zandalinas *et al.*, 2021). The protocol outlines GHG reduction foci for participating countries (Calvin *et al.*, 2023; IPCC, 1996). The signatories to the protocol, agreeably, were to develop and report on their annual

national inventory of anthropogenic GHG emissions as prescribed by the Intergovernmental Panel on Climate Change (IPCC, 2014). Country-specific emission data based on precise GHG measurements would therefore significantly contribute to carbon budget analyses and consequently applicable management options (Eggleston *et al.*, 2006; Friedlingstein *et al.*, 2020).

Table 1: Global warming potential (GWP) for some greenhouse gases (GHG) and their corresponding lifespan in the atmosphere. Source (IPCC 2023).

Global warming potentials of major GHGs			
Greenhouse Gas (GHG)	Chemical Formula	GWP in 100 years	Lifespan (years)
Nitrous Oxide	N_2O	265-310	114
Methane	CH_4	21-28	12
Carbon dioxide	CO_2	1	Variable
Water Vapour	H_2O	N/A	Variable
Ozone	O_3	N/A	Hours to days

GHG = greenhouse gas, GWP = Global warming potential

The GWP for CO_2 is 1 because it is the reference point. Variability in the lifespan of CO_2 is based entirely on the carbon cycle, with photosynthesis and respiration as key drivers. Estimates for GWP due to H_2O and O_3 do not have standardised estimates (IPCC, 2023a, 1996).

2.11 Gas movements in nature

2.11.1 The ideal gas laws

Gas exchanges between the soil and the atmosphere are typically highly variable in both time and space. Determining gas fluxes is therefore a complex and challenging task. Movement of gas molecules is due to either mass flow (advective transport) or molecular diffusion. Diffusive transport is described by Fick's law and is also affected by gas permeability, i.e., the ease with which gases move through the soil, as demonstrated in **Figure 6**. Diffusive transport, therefore, varies over orders of magnitude, subject to the shape, size, and orientation of the soil pores as well as soil moisture content (Livingston *et al.*, 2005). Advective transport of gas occurs in response to a difference in total pressure between the soil air and the atmosphere, which is described by Darcy's law (Farmani *et al.*, 2018).

The flow of gases in soil is significantly impacted by water. Although the rates vary for different gases, the diffusivity of gases is lower in water than in air (D'Odorico et al., 2003; Liao et al., 2024). The exchange of gases in the soil is influenced by the rhizosphere. Generally, the presence of plants causes an increase in the fluxes of gases into and out of the soil. In addition to acting as a direct conduit for the passage of trace gases through (often specialised) plant tissues, such as the aerenchyma system, plants (mostly vascular plants) may modify rhizosphere conditions, which can have a direct or indirect impact on gas generation and transport. Additionally, plants both produce and consume a variety of gases, such as N_2O (Dlamini, Cárdenas, et al., 2022; Höglund-Isaksson, 2012) and CH_4 (Bratti et al., 2022; Yuan et al., 2024). From a practical point of view, plants complicate

accurate flux determination compared to bare soil due to photosynthesis and biogeochemical processes in the rhizosphere.

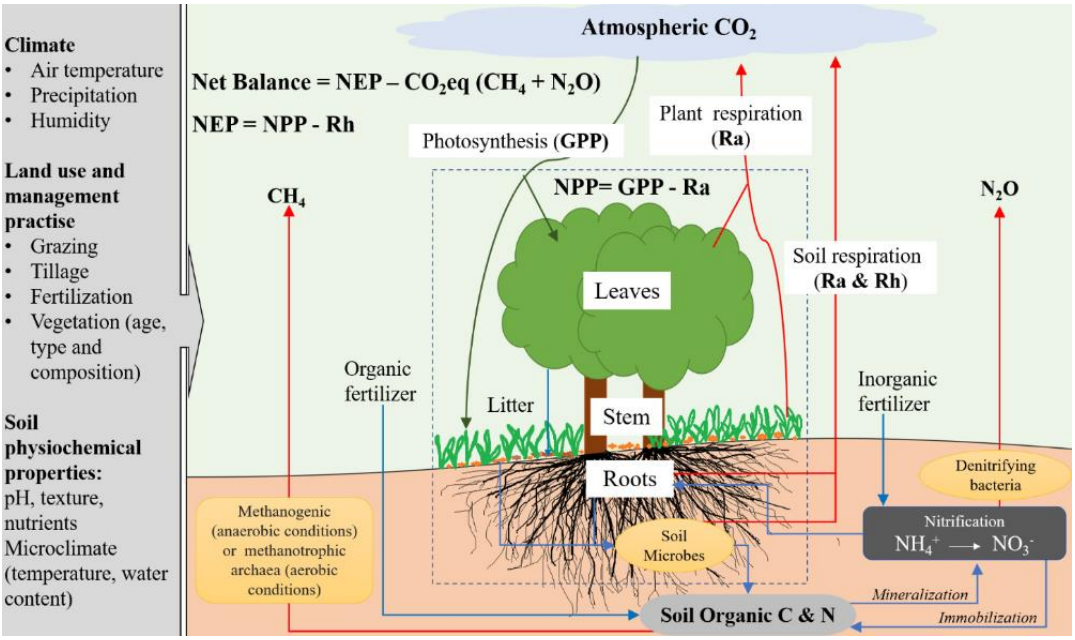

Figure 6:Conceptual diagram for carbon cycling in Afrotropical-savanna ecosystems. The red arrows show GHG emissions from the ecosystem. The abbreviations include: net ecosystem productivity (NEP), gross primary productivity (GPP), net primary productivity (NPP), autotrophic (Ra) and heterotrophic (Rh) respiration, carbon (C), and nitrogen (N). Adapted from (Wachiye, 2022).

2.12 GHG measurements using specialised chambers

2.12.1 Advantages of the static chamber method

1. Chambers are suitable for smallholder and plot-level research foci because they enable measurements at lower scales (< 1 m^2).

2. A variety of outdoor situations and experimental goals can be accommodated by chambers.

3. Because of its extreme sensitivity, chambers can monitor minuscule fluxes.

4. Chambers are easily transportable around the study region and are comparably inexpensive to buy, install, maintain, and operate.

5. Gas samples can be gathered and stored in chambers for subsequent examination.

2.12.2 Some limitations of the static chamber method

1. Labour-intensive due to the requirement for several chamber installations and repeated measurements.

2. When observations are made with plants present, it is challenging to interpret soil CO_2 flow data in the context of net GHG flux.

3. The use of chambers is restricted to bare soils or to soil with small-sized vegetation.

2.13 Agricultural GHG emission trends and policies

2.13.1 Agriculture in the phase of global change

According to FAO (2023), the agricultural sector employed 873 million people in 2021, compared to 1027 million in 2000. These figures represent 27 % and 40 % of the global workforce, respectively. While the difference of 154 million people should be a concern, agriculture remains a strong source of global livelihood. The largest GHG emitters in 2023 were the People's Republic of China, the United States, India, the EU27, Russia, and Brazil. These six economies jointly accounted for 49.8% of the global human population,

63.2% of the global GDP, 64.2% of the global fossil fuel consumption, and 62.7% of the global GHG emissions, as shown in **Figure 7**.

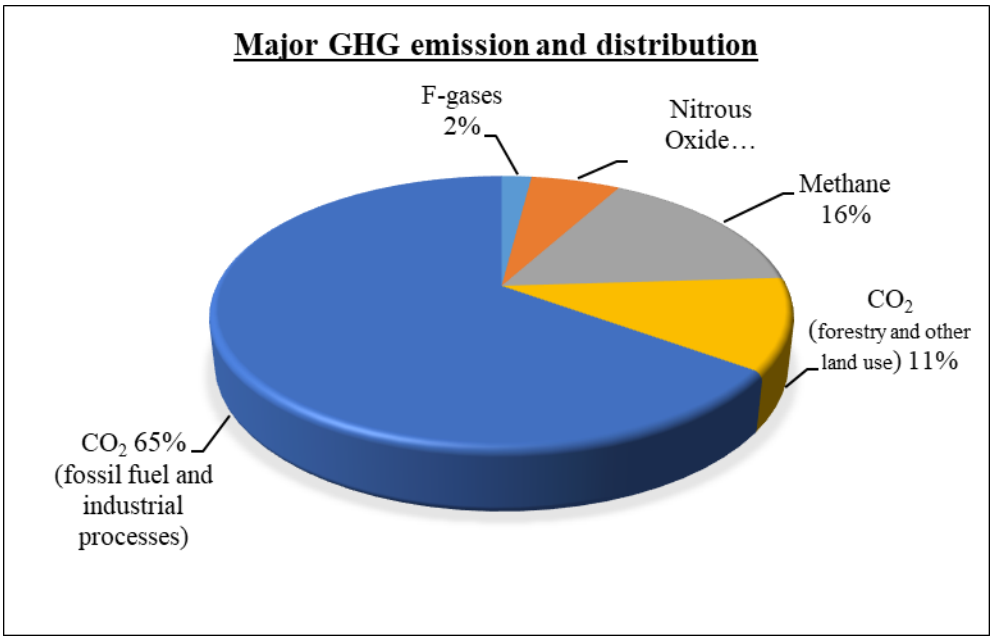

Figure 7: Distribution of major greenhouse gas emissions. CO_2 contributed the largest total share of global GHG emissions (76 %) while the agrifood systems accounted for 11 %. This underlines the role of agriculture in global change, focusing on enteric methane emissions. Source: *(IPCC, 2023a)*.

Africa is estimated to inhabit 1.55 billion people, with an annual growth rate of approximately 2.3 % (Winkler et al., 2021). The increasing population in Africa accelerates the region's threat of food and nutrition insecurity. Coupled with degrading arable land, a gap exists between domestic agrifood supply and demand. In Africa, 80% of farms are smallholder, which are critical as they account for up to 70% of the continent's food supply. This underscores the delicate balance between Africa's food demand and supply in the face of global change and limited resources. Relatively new farming technologies have been

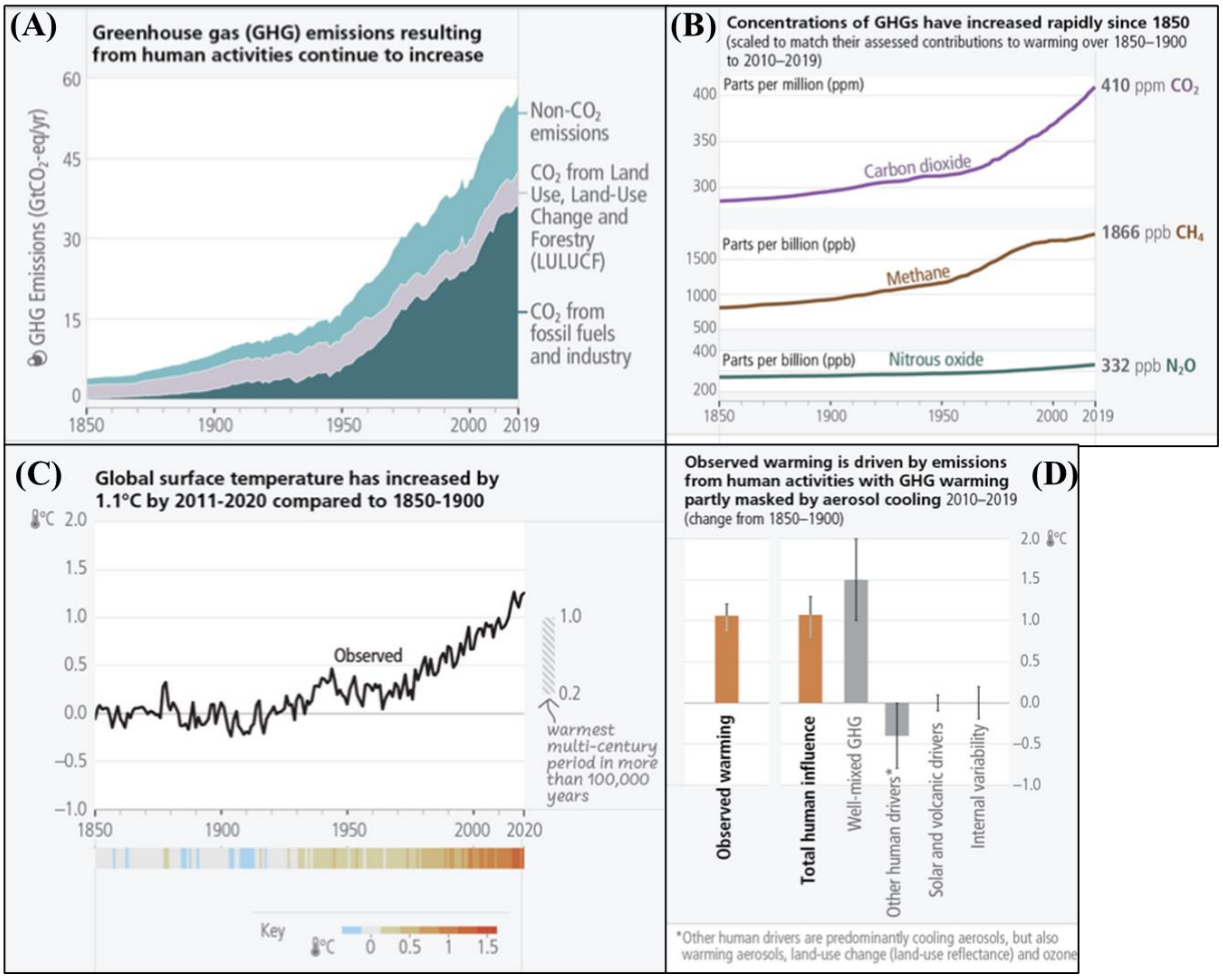

Figure 8: Global agricultural GHG Trends. Human activities are the centre of global change, and with increasing global populations, the activities are predicted to further increase (A). Industrialisation, building and construction, agriculture, and land use continue to exacerbate GHG emissions globally, as illustrated in (B). increasing GHG emissions due to increasing human activities further raise global temperatures, as recorded in (C and D). Sources: (Calvin *et al.*, 2023; Eggleston *et al.*, 2006)

proposed and widely advocated for in Africa. These strategies include climate-smart agriculture (CSA), integrated nutrient management, integrated pest and disease management, mixed or sustainable agriculture, and soil and water conservation, etc.

Limited access to and availability of flexible resource options hinder the adoption and investment in these resilience-oriented strategies. Consequently, most farms in Africa are rain-fed, dependent on manual labour, and relatively more vulnerable to the risks of climate change.

It is globally estimated that between 3.3 - 3.6 billion people live in environments that are highly vulnerable to climate change. A direct correlation indicates that both ecosystem and human vulnerability to climate risks are interdependent (see **Figure 8**). This is a call to action to strategise, shift, and adjust to more resilient farming approaches.

2.13.2 Agricultural GHG emission trends

A study by the IPCC (2023) justifies the increase of global temperatures by 1.5 °C above pre-industrial levels. The world's surface temperature was 1.09 °C higher in 2011–2020 than in 1850–1900. Larger increases were recorded over land (1.59 °C) than over the ocean (0.88 °C) (Calvin *et al.*, 2023). Cumulative CO_2 emissions between 1850 and 2019 were 2400 ± 240 $GtCO_2$. In 2019, atmospheric CO_2 concentrations (410 ppm) were higher than the previous records for at least 2 million years. The concentrations of methane (1866 ppb) and nitrous oxide (332 ppb) were higher than records back to 800,000 years, see **Figure 9*Figure 9***. At the global scale, net anthropogenic GHG emissions were estimated to be 59 ± 6.6 $GtCO_2$-eq (2019). This value was 12 % higher than emissions in 2010 and 54 % higher than emissions in 1990. During the 2010–2019 decade, GHG emissions were higher than in any previous decade on record. However, the annual emission growth rate in the same decade (1.3 %) was lower than that between 2000 and 2009 (2.1 %). In 2019. It was estimated that 22 % of GHG emissions were attributed to agriculture, forestry, and other land use (AFOLU) systems. The least developed countries (LDCs) and small island

developing states (SIDS) recorded much lower emissions per capita at 1.7 and 4.6 t CO_2-eq, respectively, compared to the global average of 6.9 t CO_2-eq. These per capita emissions exclude the contribution by land use, land use changes, and forestry (CO_2-LULUCF). The 10% of households with the highest per capita emissions contribute 34–45% of global consumption-based household GHG emissions, while the bottom 50% contribute 13–15%.

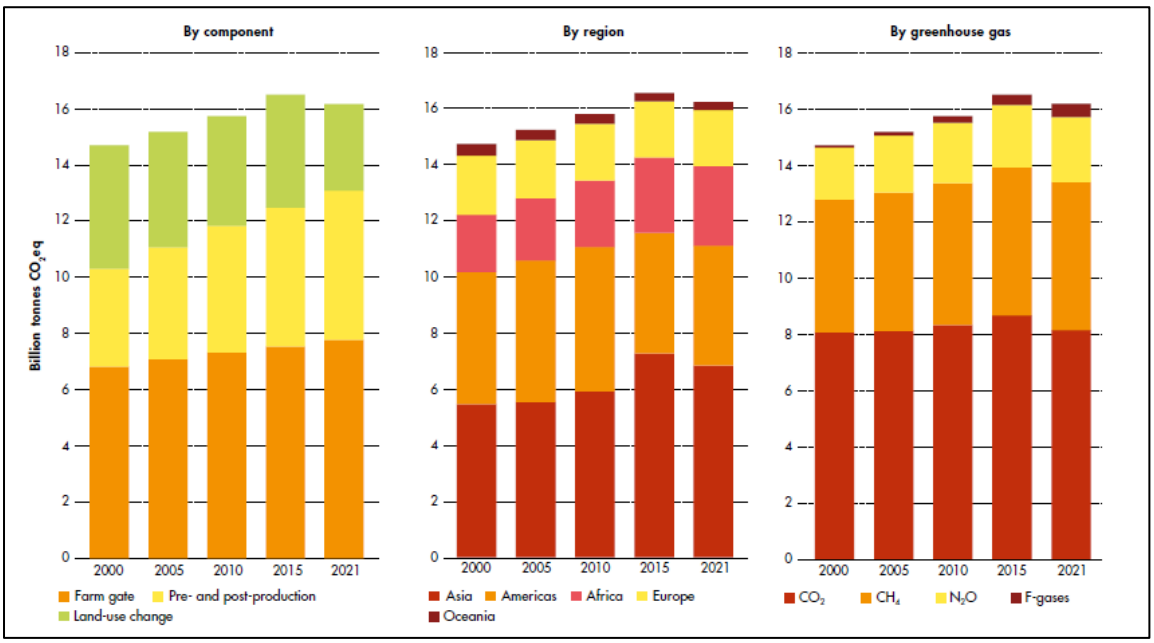

Figure 9: Global GHG emissions from agricultural systems. Increasing trends were observed in the farm-gate and pre- and post-production settings. Africa is not among the highest GHG-emitting regions, but it faces a critical climate change threat due to its climate dependency on agriculture. Source: (FAOSTAT, 2023).

2.14 GHG emissions from the livestock sector

The global cattle industry is vast and heterogeneous. Twenty (20) billion animals graze on about 30% of terrestrial land, and one-third of the world's cropland is utilised to provide

animal feed (Llonch *et al.*, 2017), and 32% of total freshwater is used by at least 1.3 billion farmers and retailers (Reisinger & Clark, 2018). Livestock provides up to 50% of worldwide agricultural GDP as an economic sector (Herrero *et al.*, 2016a; Rust & Rust, 2013). Over the last 40 years, milk and beef production have more than doubled, while the pig and poultry subsector has increased by a ratio of five or more, see **Figure 9**. Similarly, the global per capita consumption of cattle products has more than doubled (Ericksen & Crane, 2018; Gerber *et al.*, 2013). By 2040, the rising human population, earnings, and urbanisation will drive higher milk and meat consumption globally (Herrero *et al.*, 2016a). In Africa and Latin America, land expansion is a key component of production development (Critchley *et al.*, 2023). Notable greenhouse gas (GHG) increases, deforestation, biodiversity loss, and other severe environmental risks are looming if the current livestock industry trends are maintained (Symeon *et al.*, 2025; Herrero *et al.*, 2016a).

2.14 Mitigation options for GHG emissions in the livestock sector

Studied from a triple approach, livestock emissions can be mitigated from i. the intensification of livestock systems and accompanying structural modifications (Israel *et al.*, 2020), ii. technological and management initiatives (Symeon *et al.*, 2025), and iii. the moderation of livestock product demand, Technical and management interventions (Herrero *et al.*, 2016a; Janssens-Maenhout *et al.*, 2017). These options would potentially reduce a significant fraction of livestock-related emissions. According to Herrero (2016b), changes in the structure of livestock production systems and the enforcement of policies that reduce demand for animal protein may contribute to significant emissions reductions. This preposition was championed and referred to by related studies

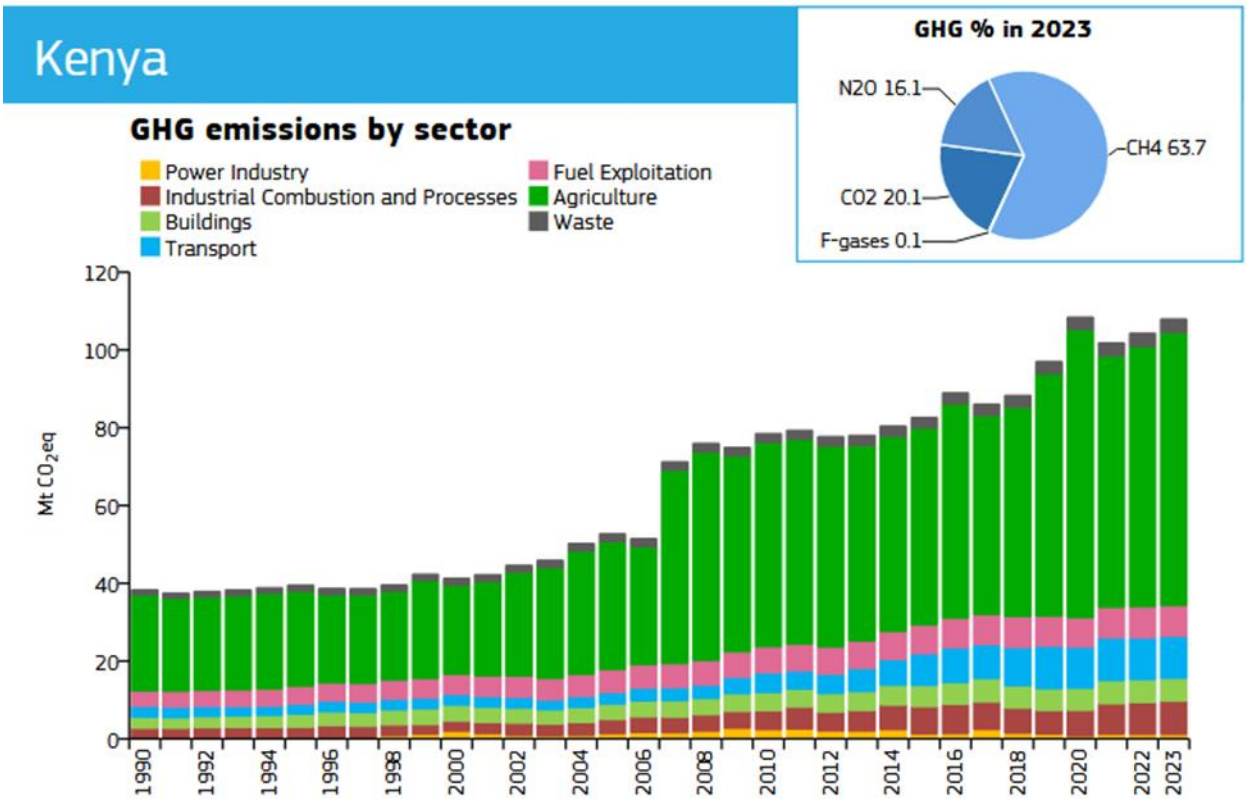

Year	GHG emissions Mt CO_2eq/yr	GHG emissions per capita t CO_2eq/cap/yr	GHG emissions per unit of GDP PPP t CO_2eq/kUSD/yr	Population
2023	107.977	1.881	0.344	57.395M
2015	82.647	1.750	0.375	47.236M
2005	52.719	1.462	0.383	36.048M
1990	38.350	1.639	0.401	23.402M

Figure 10: EDGAR's summary of key factors driving GHG emissions in Kenya. CH_4 dominates the emission at 63.7% while N_2O is the least (16.1%). Agriculture dominates the distribution, indicating that Kenya's economy is agro-based. Tabular GHG emissions per capita and population data extract for Kenya. Source (European Commission *et al.*, 2024).

(Ericksen & Crane, 2018; Reisinger & Clark, 2018). Mitigation options in the supply and demand segments were crucial for the multifaceted interactions in food systems and the evolution and regulation of GHG emissions (Graham et al., 2022; Herrero et al., 2013).

Inadequate investments in the SSA livestock sector, and a lack of effective policies or good political will to promote healthy production and consumption. Their economic mitigation potential may be far smaller, especially in developing countries and SSA (Herrero et al., 2016a). These may be attributed to economic adoption barriers, mass publicity, and the costs of technical options (Israel et al., 2020).

Total annual emissions from the livestock sector, as estimated between 1995 and 2005, were between 5.6 and 7.5 $GtCO_2e$ (Herrero *et al.*, 2016a; Reisinger & Clark, 2018). The most important sources of emissions were enteric CH_4 (1.6–2.7 $GtCO_2eq$, N_2O emissions associated with feed production (1.3–2.0 $GtCO_2e$, and land use for animal feed and pastures, including associated changes (~1.6 $GtCO_2e$) in land use (Gerber *et al.*, 2013; Gubamwoyo *et al.*, 2025). Even so, the levels of global livestock emissions differ considerably between studies due to estimates based primarily on Tier 1 approaches - using default global or regional emission factors (Gerber *et al.*, 2013), with Tier 2 approaches - using estimated regional or local emission factors, sometimes being used for enteric fermentation (Goopy *et al.*, 2020). Other studies estimate emissions by country and region, species, production system, and by products (i.e., milk, meat) (Herrero *et al.*, 2016a).

CHAPTER THREE

METHODOLOGY

3.1 Description of the study site

This research was carried out in the Bura and Wundanyi river basins in Taita Taveta County, southern Kenya (3^{o} 25' S, 38^{o} 20' E), see **Figure 11**. Taita Taveta County is a dryland area in Kenya, with approximately 89% of the land classified as arid or semi-arid lands (ASAL) (Wachiye *et al.*, 2020a). The Taita Hills' mountainous zone (Dawida, Kasigau, Sagalla), the Taita lowlands, and the foothills of Mt. Kilimanjaro are the three major geographical regions of the county. The County headquarters are located in Mwatate and have a population of ~363,990 people in 2023 (Taita Taveta County Government, 2023). Taita Taveta County has four sub-counties: Voi, Mwatate, Wundanyi, and Taveta, which also double up as the constituencies (Taita Taveta County Government, 2018, 2023).

Tsavo East and Tsavo West National Parks encompass 62 % of the county's total land size of 17,083.9 km^2, i.e., 11,100 km^2. Besides the national parks, the county's lowlands are home to farmlands, ranches, estates, and wildlife sanctuaries. There are roughly 25 ranches in the county, common smallholder farms, ranches, sisal estates, and water features that are heritage in Taita Taveta (Taita Taveta County Government, 2018). Hilltop woods range in size from small 500 m^2 areas with a few surviving trees to enormous 2 km^2 indigenous and exotic forest mountains. These forests are part of the Eastern Arc range of forests, which are largely located in eastern Tanzania, with the Taita Hills being the only Kenyan section (Pellikka *et al.*, 2013a, 2018b; Wachiye *et al.*, 2020a).

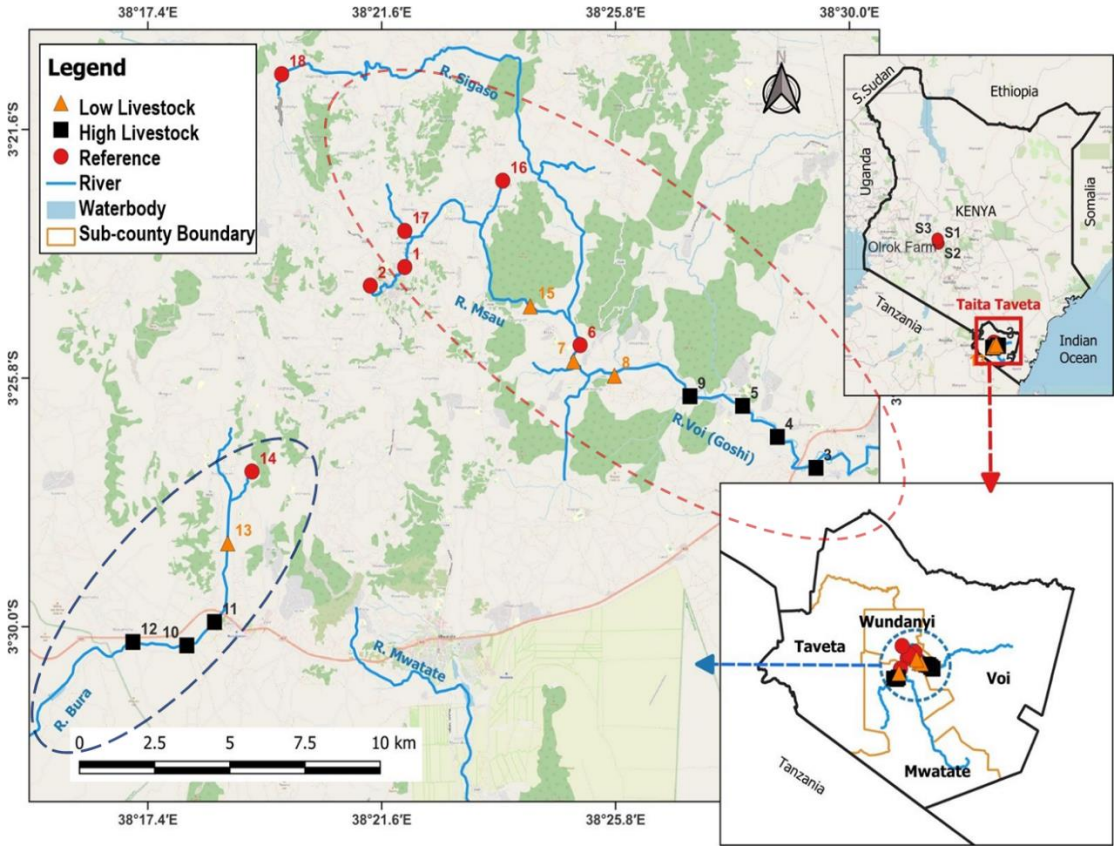

Figure 11: Map of the study site showing the sampling points in the Bura and Wundanyi catchments of Taita Taveta. Source: (Author 2025).

The Taita highland system features several tributaries with a dendritic drainage pattern. These streams originate from the summits and surrounding forests (e.g., Ngangao Forest), and drain into the Bura and Voi Rivers (Gubamwoyo *et al.*, 2025; Taita Taveta County Government, 2023). January and February are the hottest and driest months, while June through October are the coolest (Pellikka *et al.*, 2018a). The region's bimodal rainfall pattern is influenced by the intertropical convergence zone (ITCZ) with the long rains from March to June and the short rains from October to December (Hohenthal *et al.*, 2015; Owade *et al.*, 2025). Annual rainfall in highland areas of >1000 masl averages 1500 mm,

and the average temperature of 18 ^{o}C. The transitional (midland) zone (700 - 1000 m asl) records a mean temperature of 18 °C and a mean annual rainfall of 700 mm, while the lowlands (pastoral and rangelands, <700 m asl) experience 23 ^{o}C and rainfall of 500 mm. The rain shadow affects some hilly areas due to rapid altitudinal shifts (Abera *et al.*, 2022; Gubamwoyo *et al.*, 2025).

3.2 Study design

A survey was conducted to evaluate the ecological effects of livestock (goats, donkeys, cattle) access to watering points along the rivers. The mean livestock counts were used to classify sampling sites into three livestock production densities. Sites adjacent to homesteads with the highest mean livestock count were classified as high livestock density (HLD) sites, with livestock count ranging from 28 to 60. Low livestock density (LLD) sites had 14 to 27, while the zero livestock density (ZLD) sites had <13, with no subsequent watering points along the rivers. In ZLD sites, available livestock are raised at zero grazing units. In total, 18 sites were classified into the three broad categories based on livestock production system: ZLD (n = 7), LLD (n = 4), and HLD (n = 7). The sampling sites also occur along a precipitation gradient with altitude, thus related to land use and land cover attributes.

Season (Dry I, Dry II, Wet I, Wet II), topography (Upland, Midland, Lowland), and livestock density (HLD, LLD, ZLD) were key variables for this study. Due to conservation and wildlife in Taita Taveta, this study was conducted for all three topographies in Wundanyi, but only the Midland and Upland for the Bura catchment. The Bura lowland zone was inaccessible because it was a wildlife (elephants, buffalo, and crocodile) infested

region. Sampling was conducted four times to cover the dry and wet conditions. The sampling periods were in December 2021 during the peak of the rainy season (Wet I), February 2022 during the early dry season (Dry I), June 2022 during the peak of the dry season (Dry II), and November 2022 during the early wet season (Wet II). The sites were distributed across the two catchments, with the Bura catchment having five (5) sites and the Wundanyi catchment having thirteen (13) sites.

3.3 Theoretical framework for this study

A reconnaissance survey was conducted to i. identify potential sampling sites, ii. Familiarise with the dominant anthropogenic activities, iii. Analyse the landscape and terrain, iv. Conduct field tests and trials for study materials, and v. acquire field personnel to assist with project activities. When livestock access watering points, their trampling either loosens top soils when dry or compacts them when moist. This alters soil bulk densities and erosivity. Livestock are prone to unconditional defecation and urination at the water point, which introduces nutrients and organic matter on riparian lands. These nutrients are usually unmanaged and may undergo decomposition, dissolution, or absorption depending on external influences. This framework covers a broad landscape-scale sampling approach, factoring topography and land use typologies (LUT). Topography dictates the natural vegetation and agroecology (Abera *et al.*, 2022). Altitude (masl) was the key reference to the assignment of the three levels of topography, Upland (>1000 masl), Midland (700 – 1000 masl), and the Lowland (< 700 m asl). Earlier studies that adopted similar approaches have been used previously to conduct agroecological studies in Taita Taveta, see (Gubamwoyo *et al.*, 2025; MoALF, 2016; Pellikka *et al.*, 2013a; Watuma *et al.*, 2022).

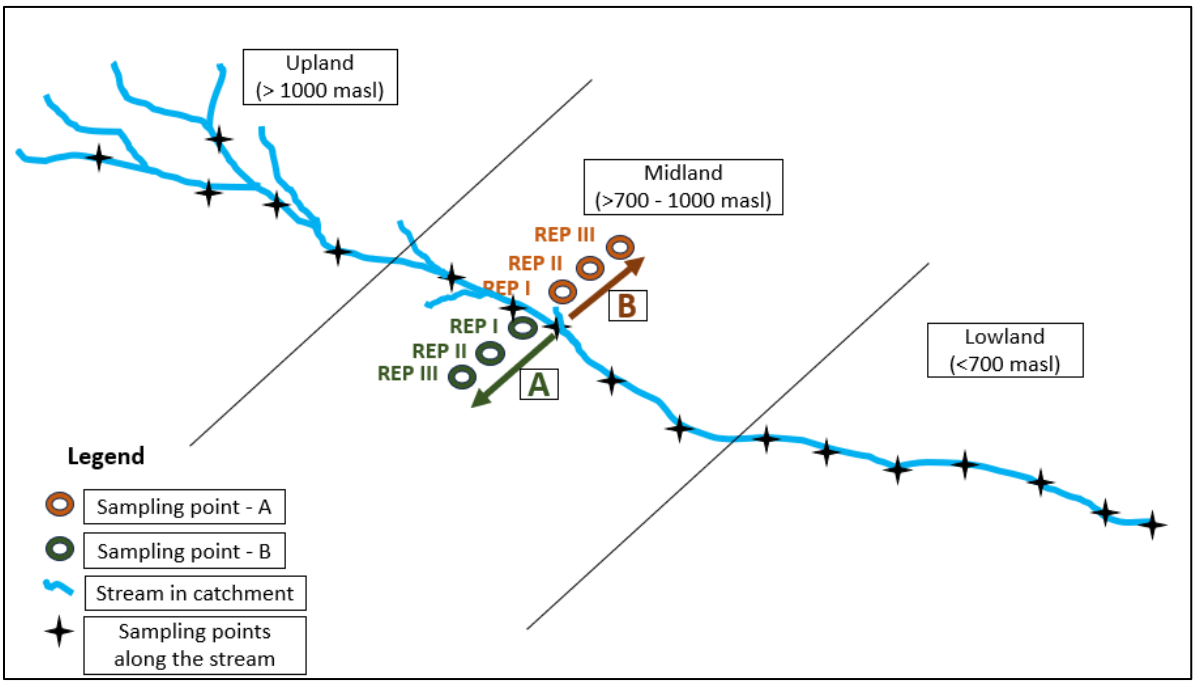

Figure 12: Visual illustration of multistage sampling locations. Note the three topographical classes (upland, midland, and lowland) along the catena, two adjacent sides of the stream (A and B) with strategic replications (REP I, II, and III) from the watering point. Source: (Author 2025).

3.4 GHG Sampling and Laboratory Analysis

3.4.1 Chamber installation and the gas pooling protocol

Static, dark (inhibiting photosynthesis) and reflective (reducing internal heating) gas-tight chambers were deployed in this study. This was the most appropriate sampling method, especially for the smallholder systems of Taita Taveta. Gas chambers will be placed on the riparian land surface at predefined spatial and temporal aspects. These chambers were vented to allow pressure equalisation between the headspace and the ambient air pressure and were operated manually. Nine chambers (measuring 27 * 37.2 * 12.5 cm) in a 3*3

arrangement (3 chambers per Replicate) were installed per sampling site. GHG samples were collected using the gas pooling technique, see **Figure 13** (Arias-Navarro *et al.*, 2013).

A 60 ml syringe with a one-way Luer lock and needle was adapted for gas pooling. The syringe was flushed in atmospheric air before drawing 20 ml of gas from each chamber at four 15-minute intervals (0, 15, 30, and 45 minutes). Both the LLD and HLD sites with sampled in doubles (A and B) to cater for livestock access from both sides of the stream. Each of the three chambers contributed 20 ml of sample, which was then mixed appropriately before pressure equilibration. The final 30 ml obtained after equalising atmospheric pressure was over-pressurised into 20 ml pre-evacuated glass vials with air-tight rubber seals. The samples were stored in a cool box and transported to ILRI's Mazingira Centre for GC concentration analysis. A total of 1392 gas samples were analysed for this study.

The timesteps were used to fit a slope that was used to calculate fluxes. The temperature within each chamber was recorded during each sampling time using a thermometer. Ambient air temperature, soil temperature, soil moisture, and air pressure were also recorded for use in flux calculations.

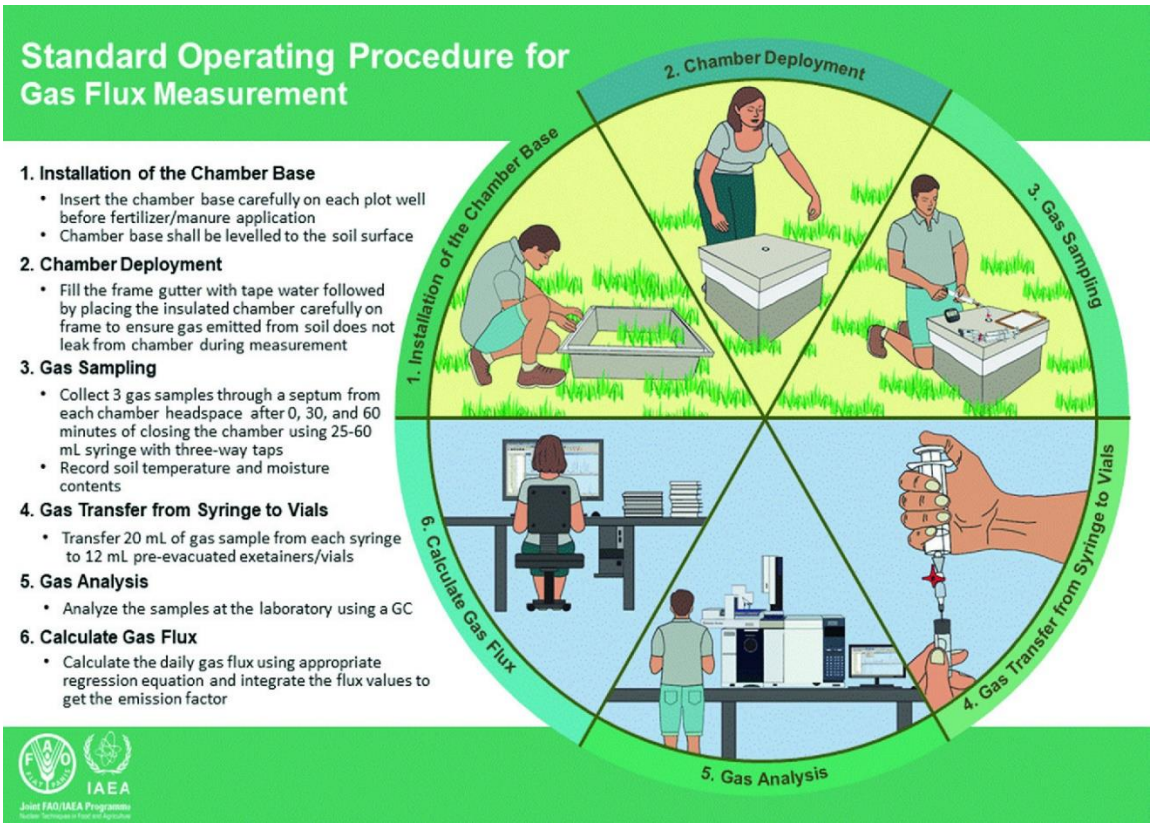

Figure 13: Protocol for GHG flux measurements showing chamber set-up (1 and 2), gas pooling (3 and 4), and the laboratory analytical procedure (5 and 6). This protocol highlights the 0-30-60 time period, which was adjusted to 0, 15, 30, and 45-minute time periods in our study. The design of the chambers and vials for GHG sampling may differ, but the deployment and operating principles are standardised. Source: (Zaman *et al.*, 2021).

3.4.2 Laboratory measurement of GHG concentrations

An SRI (8610C) gas chromatograph (SRI Instruments Europe GmbH, Bad Honnef, Germany) with two (HayeSep) D packed columns (3 m length, 1/8 in. diameter) was used to analyse gas samples. One of the columns led to an (^{63}Ni) electron-capture detector (ECD, temp = 350 °C) for the detection of N_2O, and another to a flame-ionisation detector (FID, temp = 350 °C) for the detection of CH_4 (Butterbach-Bahl *et al.*, 2016). The column oven temperature was adjusted to 70 °C, and the carrier gas was pure N_2 at both the FID and

ECD lines at a flow rate of 25 ml min^{-1}. N_2O and CH_4 mixtures in synthetic air were used for calibration (gas with known concentrations of CH_4, CO_2, and N_2O) at four different concentrations: 0.4–2.5 ppm for N_2O and 4–50 ppm for CH_4. After every 20 to 30 running samples, quadruplicates of the lowest concentration of the calibration gas were injected, and duplicates of the other three concentrations were injected every 20 to 30 samples (Leitner *et al.*, 2021; Wachiye *et al.*, 2020b). The gas concentrations of the samples were determined using the correlation between peak regions and calibration gas concentrations.

3.4.3 GHG flux calculations

The ideal gas law was used to compute gas flux rates. It is a fundamental equation in both physical chemistry and physics that relates the pressure, volume, temperature, and number of moles of an ideal gas (Lavenda, 2005a, 2005b). Using the change of gas concentration over time δConc/δTime (ppm min^{-1}), air pressure P at the sampling sites (mbar) corrected for air pressure at sea level (1013.25 mbar), chamber headspace temperature T (°C), atomic molar mass MM of the target compound (12 g mol^{-1} for CH_4-C, and 28 g mol^{-1} for N_2O-N since there are two atoms of N in one molecule of N_2O), the ideal gas volume (22.41 L mol^{-1}), total chamber volume V (m^2) and multiplied by 60 to convert from minutes to hours (Butterbach-Bahl *et al.*, 2016). The formula below summarises flux calculations (Leitner *et al.*, 2024).

$$F_{GHG} = \frac{\delta c}{\delta t} * \frac{P}{1013.25} * \frac{273}{(T + 273)} * \frac{MM}{22.41} * \frac{Ch.V}{Ch.A} * 60 \qquad \text{Equation 1}$$

Where;

$\frac{\delta c}{\delta t}$ – is the slope, gas concentration over time (ppb min^{-1})
MM – is the molecular mass of the target compound of the gas (g mol^{-1})
Ch. V – is the chamber volume (m^3)
P – is the pressure at the site (mbar) for pressure correction.
T – is the chamber temperature input for temperature correction.
Ch. A – is the chamber area (m^2)

R^2 values for flux data cleaning were calculated for δConc/δtime (slope). Fluxes with R^2 < 0.9 were discarded for N_2O and CO_2. We discarded 2 % of N_2O flux measurements in that regard. Similarly, R^2<0.7 values for CH_4 fluxes were discarded. Representing 7 % of the data. Flux data with R^2 below the threshold were attributed to leakages, either from the deployed chambers or vials. These hourly flux data were extrapolated to daily fluxes for reporting.

3.5 Soil sampling and laboratory analysis

3.5.1 Field sampling protocol

Soils were sampled from each replicate level containing three chambers. Soil samples were collected after GHG sampling to avoid alterations of soil temperature, induction of vibrations, and moisture dynamics, which would otherwise alter the ultrasensitive gases like N_2O and CH_4. For soil samples, the strategic distance from the water point accounted for erosional processes in riparian strips and fluctuations in water levels. Sampling was done at 20 cm depth from the central spot using Edelman's auger (Eijkelkamp Agrisearch Equipment, Giesbeek, The Netherlands). Additional core samples were obtained using core rings (volume = 100 cm^3) for the calculation of bulk density and porosity. For this study, three hundred and forty-eight (348) soil samples were collected. These samples were stored in a cooler box and transported to the University of Eldoret's Soil Science laboratory. Parameters of interest were *i*. total carbon (SOC) for SOC stocks, *ii*. total nitrogen (TN) for C:N ratio and inorganic N fractions, *iii*. bulk density and porosity, *iv*. available phosphorus (Olsen's), moisture for metabolism, and *v*. soil pH.

3.5.2 Laboratory determination of soil organic carbon (SOC)

SOC analysis was guided by the organic matter oxidation principle following the Walkley and Black oxidation procedure as outlined by Okalebo *et al.* (2002). About 0.3 ± 0.01 g of the fine ground (60 mesh) sample was weighed into clean and labelled carbon digestion tubes, followed by five (5) ml of 1N potassium dichromate ($K_2Cr_2O_7$). To this mixture, 7.5 ml of concentrated sulphuric acid (H_2SO_4), GPR grade, was carefully added while stirring. These mixtures were then heated (at 150 °C for 30 min) to enhance oxidation. These digests were then titrated against 0.2 M ferrous ammonium sulfate ($(NH_4)_2Fe(SO_4)_2 \cdot 6H_2O$) and the titre volumes used to calculate SOC. The reactions can be summarised as follows:

Reaction 1 $2Cr_2O_7^{2-} + 3C^0 + 16H^+ \text{<---> } 4Cr^+ + 3CO_2 + 8H_2O$

Reaction 2 $6Fe^{2+} + Cr_2O_7^{2-} + 14H^+ \text{<---> } 2Cr^{3+} + 6Fe^{3+} + 7H_2O$ Equation 2

Reaction 1 summarises carbon oxidation when block-heating the sample in chemical mixtures, while **Reaction 2** summarises the titration of residual potassium dichromate ($K_2Cr_2O_7$). Corrected titer volumes were then used to calculate soil SOC as shown in **Equation** (Okalebo *et al.*, 2002). These contents would then be quantitatively transferred into clean 100 ml conical flasks, followed by 0.3 ml of the diphenylamine indicator solution. Using a magnetic stirrer to ensure even mixing, these contents would be titrated against ferrous ammonium sulphate solution. After digestion, the acidified potassium dichromate ($K_2Cr_2O_7$) solution was dark green or yellowish-green due to excess dichromate, while at the endpoint, a sharp change to green via a blue-violet colour was observed. Titre volumes (T) were then recorded and corrected for their differences from the mean of 2 reagent blanks. SOC contents would then be calculated as shown in **Equation 3**;

$$\text{Total organic carbon (\%)} = \frac{\text{T} \times 0.2 \times 0.3 * 100}{\text{Sample Weight}} \qquad \text{Equation 3}$$

3.5.3 Calculation of SOC stocks

The computation of soil organic carbon (SOC) stock factors the TOC content (%), bulk density (BD), and the sampling depth (cm) (Hinshaw & Wohl, 2023). While methodologies for soil carbon quantifications are diverse (Dupla *et al.*, 2024), most studies sampled soils either up to a depth of 20 cm (K. Olson *et al.*, 2014) or up to 30 cm (Olson & Al-Kaisi, 2015), whereas others considered 0-50 cm depths (Harbo *et al.*, 2022). Interestingly, some depth ranges (0-5 cm; 5-15 cm; 10-20 cm, etc.) did not record significant carbon differences, but their combined depths (0-15 cm; 0-20 cm; 0-30 cm, etc.) did (K. R. Olson & Al-Kaisi, 2015; Raffeld *et al.*, 2024). This study adopted the 0-20 cm (Wolka *et al.*, 2021) sampling depth, which comprised the highest physical-chemical functions (0-5 cm) and the biological soil annexes (5-20 cm) (Molina *et al.*, 2024). SOC stock calculations were achieved as shown in **Equation 4** below (Xiao *et al.*, 2019).

$$SOC_{stock} = C\rho d \qquad \text{Equation 4}$$

3.5.4 Physical soil analyses

Soil bulk density (BD) and soil texture, which are critical for SOC and respiration, alongside moisture contents, were analysed. Soil core samples were taken from similar auger pits to minimise variations (Airori *et al.*, 2022). For bulk density, samples were collected at 30 cm depth using a soil bulk density ring (Eijkelkamp Agrisearch Equipment, Giesbeek, the Netherlands). Samples were immediately weighed onsite (fresh weight), stored in airtight polyethene bags, and kept in a cooler box before transportation for

laboratory analysis. Samples were oven-dried at 105 °C for 48 hours, after which gravimetric differences were used to calculate BD (Okalebo *et al.*, 2002).

Soil grain ratio is a key variable influencing both air, nutrient, and water dynamics. The hydrometer method for particle size analysis calculates the proportion of the three size classes: sand (2000 –50 μm), silt (50 – 2.0 μm), and clay (< 2.0 μm) based on the particles' settling rates in an aqueous solution (Okalebo *et al.*, 2002). The settling velocities are guided by the principle of sedimentation as described by Stokes' Law. This method uses an ASTM standard E126 hydrometer and is based on a standard temperature of 20 °C and a particle density of 2.64 g cm³ (Bouyoucos, 1962). Fractions for clay and silt were calculated using temperature-corrected hydrometer readings. The sand proportion was calculated arithmetically by subtracting the silt and clay percentage sum from 100 % (Bouyoucos, 1962; Okalebo *et al.*, 2002).

3.5.5 Subsidiary soil analyses

To potentially help comprehend and account for observations of patterns in soil and GHG measurements, this study further analysed total nitrogen (TN), ammonium nitrogen (NH-N), nitrate nitrogen (NO3-N), and available (Olsen) phosphorus. TN was analysed using the heat-enhanced digestion and colourimetry, and was key in extracting C:N ratios. NH_4^+-N and NO_3^--N fractions were analysed through extraction and were important in elucidating correlations. Phosphorus (Olsen) was an important element to analyse, especially due to its role in microbial substrate processing alongside carbon (C) and nitrogen (N). A site description sheet was also developed to record site details (ground cover, cloud cover, wind, shade, erosion, etc.) and events (crossing, livestock watering, rain, pumping, fetching, etc.) that occurred during the sampling time.

3.6 Statistical analysis

Data were managed and analysed in both MS Excel 2019 and R (Team, 2021). Separate analyses were conducted for the Bura and Wundanyi catchments to allow independent sub-catchment level assessments. Descriptive and inferential statistics were used to summarise SOC stocks. Data on SOC were analysed for significance using hierarchical analysis of variance (ANOVA). Tukey's post-hoc tests ($p < 0.05$) were used to analyse the significance of differences between treatments. Correlation between SOC stocks and soil parameters (TN, NO_3-N, NH_4-N, BD, and C:N) was done using the Pearson correlation test. The Shapiro-Wilk test was done to test for normality before log-transformations, where applicable, to improve normality and stabilise variances. For statistical modelling, ANOVA models were appropriately fitted with fixed effects (Season, Topography, Livestock density) and random effects (Sites). Estimated marginal means (EMM) were extracted to adjust for imbalances and other interactive factors. For post hoc multiple comparisons on GHG data, the confidence level was set at 0.95. Sidak's method was used to adjust confidence intervals for pairwise estimates, providing strong but efficient familywise error control without excessively widening intervals. Tukey's Honestly Significant Difference (HSD) adjustment was applied to rigorously control Type I error rates across all pairwise comparisons. A significance threshold of $\alpha = 0.05$ was used in this study.

CHAPTER FOUR

RESULTS

4.1 Greenhouse gas (GHG) fluxes in the Bura and Wundanyi Catchments

4.1.1 GHG fluxes in the Bura Catchment

4.1.1.1 Methane (CH_4) fluxes in the Bura midland

The Bura midland zone consisted of HLD and LLD, while the upland zone had the ZLD and LLD. Methane (CH_4) fluxes varied across topographic zones, livestock production systems (LPS), and seasons, with all mean values falling below zero except for the Wet I season, where 112.54 and 133.82 mg CH_4-C m^{-1} d^{-1} were recorded in the midland and upland zones, respectively. In the Midland zone, fluxes under HLD ranged from -264 to 112 mg CH_4-C m^{-1} d^{-1}. The LLD systems exhibited persistent net CH_4 uptake across all seasons, peaking at −0.58 mg CH_4-C m^{-1} d^{-1} in Wet I. Sites with ZLD recorded between -205 and -69.31 mg CH_4-C m^{-1} d^{-1}. Methane fluxes in the Bura catchment averaged at -141.81 mg CH_4-C m^{-1} d^{-1}, as contributed by the midland (-143.71 mg CH_4-C m^{-1} d^{-1}) and upland -139.91 mg CH_4-C m^{-1} d^{-1}) zones. Methane fluxes did not have a definite trend as opposed to both CO_2 and N_2O. No differences were recorded on a seasonal basis, except for CO_2 in the Wet II season.

4.1.1.2 Carbon dioxide (CO_2) fluxes in the Bura midland

Carbon dioxide (CO_2) fluxes in the Bura catchment recorded positive values across all observed topographic zones and livestock production systems (LPS), indicating net emissions (**Figure 14**b). In the Midland zone, fluxes under HLD ranged from 327.29 to 1345 CO_2-C m^{-2} d^{-1}, with the highest emissions recorded in Dry I. The LLD systems followed a similar seasonal trend, with generally lower fluxes ranging between 175.88 and

655.69 mg CO_2-C m^{-2} d^{-1}. The ZLD sites in the Midland showed the lowest observed emission of 176 mg CO_2-C m^{-2} d^{-1} during the Wet I season. Averaging across the LPS, the Midland zone recorded a seasonal mean ranging from 263 mg CO_2-C m^{-2} d^{-1} (Wet I) to 1000 mg CO_2-C m^{-2} d^{-1} (Dry I).

4.1.1.3 Nitrous oxide (N_2O) fluxes in the Bura midland

Nitrous oxide (N_2O) fluxes in the Bura catchment showed positive emissions across all measured sites (**Figure 14**c). In the Midland zone, HLD sites recorded the highest emissions, peaking at 322.4 µg N_2O-N m^{-1} d^{-1} during Dry I and declining to 80.9 µg N_2O-N m^{-2} d^{-1} in Wet I. LLD fluxes were lower overall, ranging from 69.3 to 198.8 µg N_2O-N m^{-2} d^{-1}, with peak emissions in Wet II. The ZLD site in the upland zone showed emissions of 61.6 µg N_2O-N m^{-2} d^{-1} in Dry I. Seasonal means in the Bura ranged from 67 to 107 µg N_2O-N m^{-2} d^{-1}, with an overall mean of 87 µg N_2O-N m^{-2} d^{-1}.

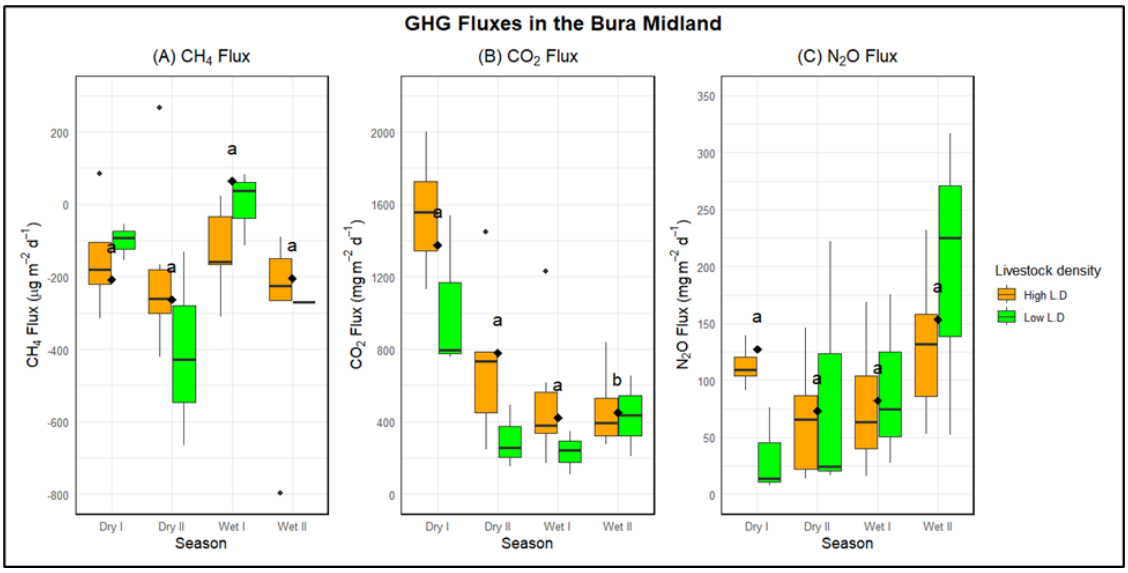

Figure 14: GHG fluxes in the Bura midland (>700 – 1000 m asl) zone. Both CO_2 and N_2O showed seasonal trends, showing an inverse and direct correlation with increasing moisture, respectively.

4.1.1.4 Methane (CH_4) fluxes in the Bura upland

In the Upland zone, HLD and LLD systems showed consistent CH_4 uptake, with mean values as low as -345.19 mg CH_4-C m^{-1} d^{-1}. Seasonal means for Upland ranged from -300.91 in Dry I to -21.53 mg CH_4-C m^{-1} d^{-1} in Wet I, with an overall average of -192.67 mg CH_4-C m^{-1} d^{-1}. Across both topographies, CH_4 fluxes were predominantly negative, indicating that the Bura landscape generally acted as a CH_4 sink during the sampling periods. The Bura catchment was generally a net sink of methane, as demonstrated by negative fluxes in 87.5 % (*n=16*) of the sites (see **Figure 15**a).

4.1.1.5 CO_2 fluxes in the Bura upland

In the Upland zone, LLD fluxes reached 865 mg CO_2-C m^{-2} d^{-1} (Dry II), while ZLD exhibited higher emissions across the seasons, peaking at 1213 CO_2-C m^{-2} d^{-1} in Dry II. The overall mean for Upland was 0.17 times higher than in Midland. The mean CO_2 Fluxes

averaged at 624 mg CO_2 m^{-2} d^{-1}. These patterns suggest strong CO_2 emissions in the Bura upland, particularly at high livestock density and during drier periods.

4.1.1.6 N_2O fluxes in the Bura upland

ZLD fluxes were measured at between 24 and 79 µg N_2O-N m^{-2} d^{-1}. LLD sites had higher values, ranging from 40 to 136 µg N_2O-N m^{-2} d^{-1} (ZLD, Wet II and LLD, Wet II). Seasonal means in Upland ranged from 47 to 82 µg N_2O-N m^{-2} d^{-1}, with an overall average of 87 µg N_2O-N m^{-2} d^{-1}. These results indicate generally higher N_2O emissions in the Midland relative to the Upland, especially in the presence of livestock (LLD) and during the dry season.

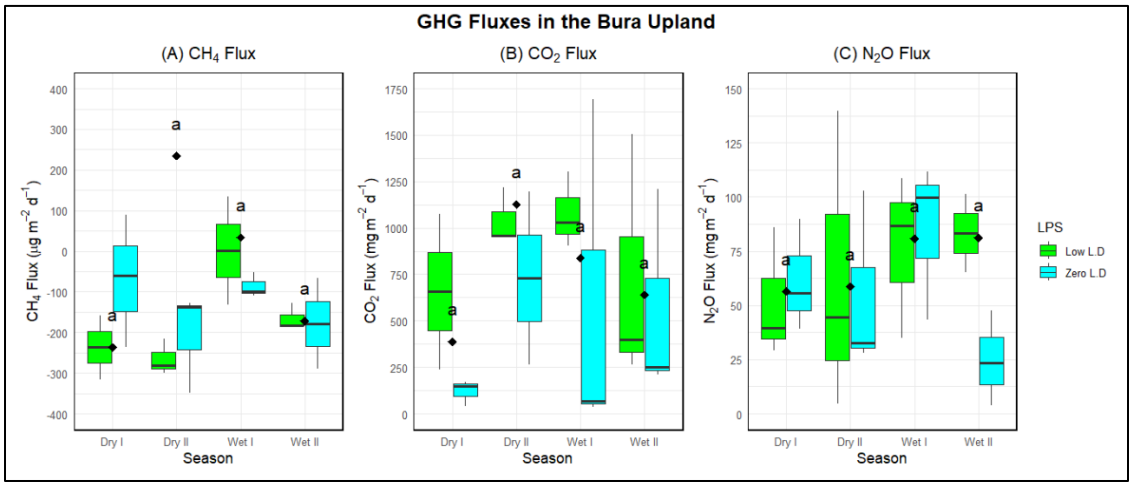

Figure 15: Seasonal GHG flux measurements in the Bura Upland zone. The GHG differed based on LPS categories (see CH_4 and CO_2 in Dry I, and N_2O in Wet II seasons) but not within seasons. Source: (Author 2025).

4.1.2 GHG Fluxes in the Wundanyi Catchment

4.1.2.1 Methane (CH_4) fluxes in the Wundanyi lowland

The Wundanyi lowland consisted of all livestock density levels, with the HLD zone recording the largest average methane at 160 µg CH_4-C m^{-2} d^{-1}. The fluxes reduced significantly with livestock density as the LLD recorded 34 µg CH_4-C m^{-2} d^{-1} while the ZLD recorded -197 µg CH_4-C m^{-2} d^{-1} (uptake). Both the Dry I and Wet II seasons recorded methane uptake (negative fluxes). The overall mean CH_4 flux for the entire lowland zone was -1.33 µg CH_4-C m^{-2} d^{-1}, indicating a general CH_4 uptake or low emissions. The mean CH_4 flux for the dry seasons was -14 µg CH_4-C m^{-2} d^{-1}, which increased for the wet seasons to 11.8 µg CH_4-C m^{-2} d^{-1} in the rainy (Wet I and Wet II) seasons. Statistical differences ($p = \leq 0.05$) were recorded while comparing fluxes between the three LPS levels, but not within seasons (**Figure 16**a).

4.1.2.2 CO_2 fluxes in the Wundanyi lowland

In the lowland zone**,** emissions ranged from 218 to 1899 mg CO_2-C m^{-2} d^{-1}, with the highest flux observed under zero livestock density (ZLD) during Wet I. The mean lowland flux averaged 746 CO_2-C m^{-2} d^{-1}, mainly contributed by the Wet season (63 % or 938 CO_2-C m^{-2} d^{-1}). Across all seasons, the lowland zone with ZLD recorded the highest seasonal mean (1004 mg CO_2-C m^{-2} d^{-1}), followed by HLD (842.53 CO_2-C m^{-2} d^{-1}) and LLD (394.25 CO_2-C m^{-2} d^{-1}). Mean CO_2 fluxes in the dry seasons stood at 555. 42 CO_2-C m^{-2} d^{-1} while the rainy seasons recorded 938 CO_2-C m^{-2} d^{-1}. HLD zones recorded more pronounced fluxes across the seasons.

4.1.2.3 N_2O fluxes in the Wundanyi lowland

Nitrous oxide in the Wundanyi lowland (< 700 masl) zone, wet seasons recorded higher average fluxes (130.87 µg N_2O-N m^{-2} d^{-1}) compared to the dry seasons (46.87 µg N_2O-N m^{-2} d^{-1}). This change represents a 2.8-fold increase between the wet and dry seasons. N_2O did not show a definite pattern with LPS. The HLD sites recorded an average of 91 µg N_2O-N m^{-2} d^{-1} while the ZLD sites recorded 32 µg N_2O-N m^{-2} d^{-1}, more than the LLD, which was 71.94 µg N_2O-N m^{-2} d^{-1}. The mean N_2O fluxes for the Wundanyi lowland were 88.87 µg N_2O-N m^{-2} d^{-1}, largely contributed by the Wet II season.

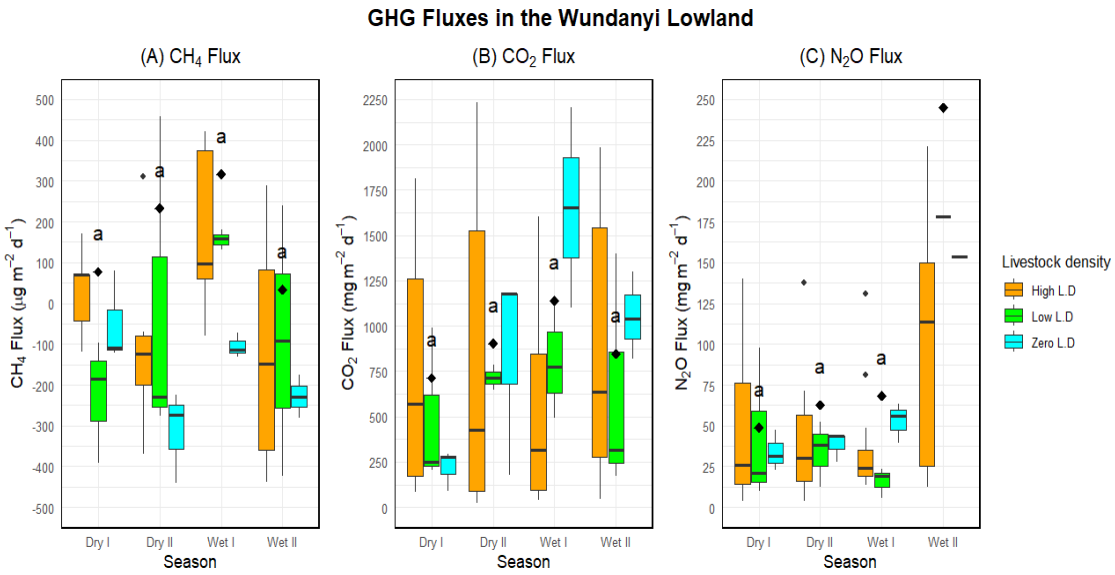

Figure 16: GHG flux measurements in the Wundanyi lowland zone. HLD areas recorded widespread fluxes (high SD), raising concerns about the fate of nutrient and carbon transfers and inputs by livestock.

4.1.2.4 CH_4 fluxes in the Wundanyi midland

CH_4 fluxes in the Wundanyi midland ranged between -190 and 772 mg CH_4-C m^{-2} d^{-1}, with 63 % of the measurements representing net uptake (negative flux values). All dry seasons recorded CH_4 uptake, whereas the rainy seasons recorded net emissions. The dry seasons averaged at -130 mg CH_4-C m^{-2} d^{-1} while the rainy seasons averaged 237 mg CH_4-C m^{-2} d^{-1}. N_2O fluxes increased rapidly with the presence of livestock, as the ZLD fluxes averaged -6.7 while LLD sites recorded a 113.38 mg CH_4-C m^{-2} d^{-1}. This difference is more than 100-fold. The average CH_4 fluxes in the Wundanyi midland were 53.34 mg CH_4-C m^{-2} d^{-1}, indicating that the region is a net source of methane gas (**Figure 17**a).

4.1.2.5 CO_2 fluxes in the Wundanyi midland

Higher CO_2 fluxes were recorded in the rainy seasons (mean 1048 mg CO_2-C m^{-2} d^{-1}) compared to the dry seasons (mean 818 mg CO_2-C m^{-2} d^{-1}). The biggest seasonal mean was recorded at 1293 mg CO_2-C m^{-2} d^{-1} in the Wet II season. Unlike CH_4, CO_2 fluxes decreased with increasing livestock influence, with the ZLD recording about 140 mg CO_2-C m^{-2} d^{-1} more than the LLD, which recorded 863 mg CO_2-C m^{-2} d^{-1}. CO_2 fluxes ranged between 1333 mg CO_2-C m^{-2} d^{-1} and 536 mg CO_2-C m^{-2} d^{-1} in the Wundanyi midland, with a zonal average of 933 mg CO_2-C m^{-2} d^{-1}.

4.1.2.6 N_2O fluxes in the Wundanyi midland

N_2O fluxes in the Wundanyi midland were generally low and ranged between 17.8 µg N_2O-N m^{-2} d^{-1} and 119.52 µg N_2O-N m^{-2} d^{-1}. Mean fluxes for this zone were 55.31 µg N_2O-N m^{-2} d^{-1}, mainly attributed to the Wet II season (107 µg N_2O-N m^{-2} d^{-1}). The Dry II season recorded the least mean (20 µg N_2O-N m^{-2} d^{-1}), followed by the Dry I (35 µg N_2O-N m^{-2}

d^{-1}) and the Wet I (59 µg N_2O-N m^{-2} d^{-1}) seasons. The Wet II season's mean was about twice that of the Wet I and 5-fold that of the Dry II. There were no huge mean differences between ZLD and LLD sites in the Wundanyi midland, as the latter recorded just 10 µg N_2O-N m^{-2} d^{-1} more than the former, which was 50.68 µg N_2O-N m^{-2} d^{-1}.

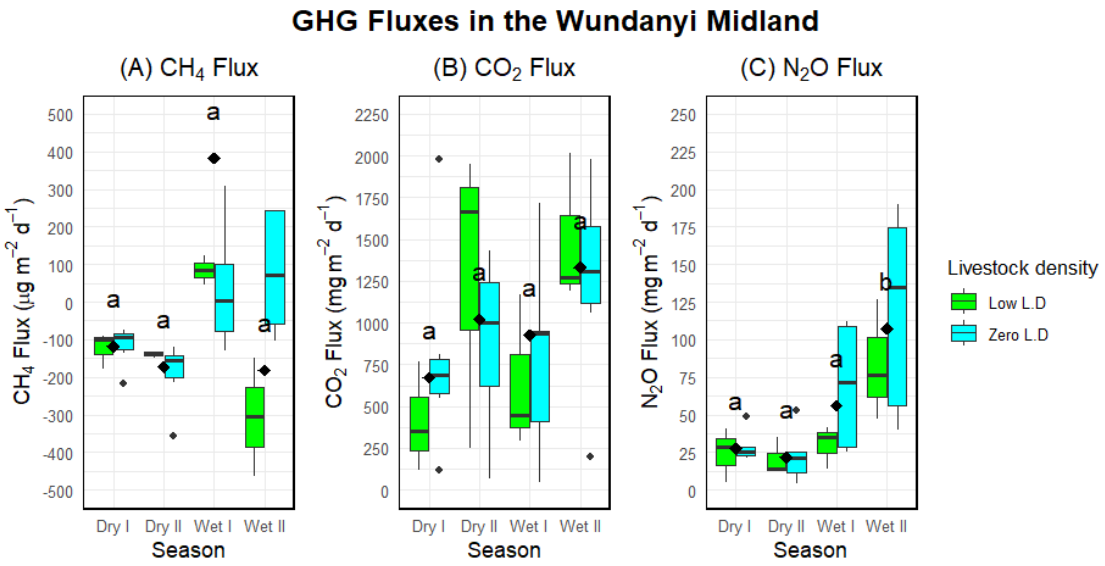

Figure 17: GHG flux measurements in the Wundanyi midland zone. No seasonal differences were recorded in means except for the N_2O fluxes in the Wet II season.

4.1.2.7 CH_4 fluxes in the Wundanyi upland

CH_4 fluxes in the upland were generally low and negative. The measured fluxes ranged between -201 and 120 mg CH_4-C m^{-2} d^{-1}, with a zonal mean of -58.5 mg CH_4-C m^{-2} d^{-1}. although both the dry and rainy seasons recorded negative fluxes (-40 and -76 mg CH_4-C m^{-2} d^{-1}, respectively), the Dry I season tended to show dominance. The Dry II and the Wet I seasons were notable net sources of methane gas (mean of 78 mg CH_4-C m^{-2} d^{-1}), whereas

the Dry I and Wet II were net sinks (mean of -196 mg CH_4-C m^{-2} d^{-1}), as shown in **Figure 18**.

4.1.2.8 CO_2 Fluxes in the Wundanyi midland

CO_2 fluxes ranged between 922 mg CO_2-C m^{-2} $d^{-1}$and 1298 mg CO_2-C m^{-2} d^{-1} in the Wundanyi Upland zone. The average for this zone was 1147 mg CO_2-C m^{-2} d^{-1} and was largely contributed by the rainy periods (mean 1203 mg CO_2-C m^{-2} d^{-1}). The dry episodes recorded 113 mg CO_2-C m^{-2} d^{-1} less than in the rainy seasons, accounting for a 10 % difference.

4.1.2.9 N_2O Fluxes in the Wundanyi midland

In the upland zone, N_2O emissions were generally moderate to high. The ZLD system produced a consistent upward trend across seasons, culminating in 112.8 µg N_2O-N m^{-2} d^{-1} during Wet I. The upland zone averaged 77 µg N_2O-N m^{-2} d^{-1}, 22 µg N_2O-N m^{-2} d^{-1} more than the midland (55 µg N_2O-N m^{-2} d^{-1}), and 12 µg N_2O-N m^{-2} d^{-1} less than the lowland mean (89 µg N_2O-N m^{-2} d^{-1}). Overall, N_2O emissions increased from the dry (52 µg N_2O-N m^{-2} d^{-1}) to rainy seasons (101 µg N_2O-N m^{-2} d^{-1}), with Wet I showing the highest seasonal average (112 µg N_2O-N m^{-2} d^{-1}).

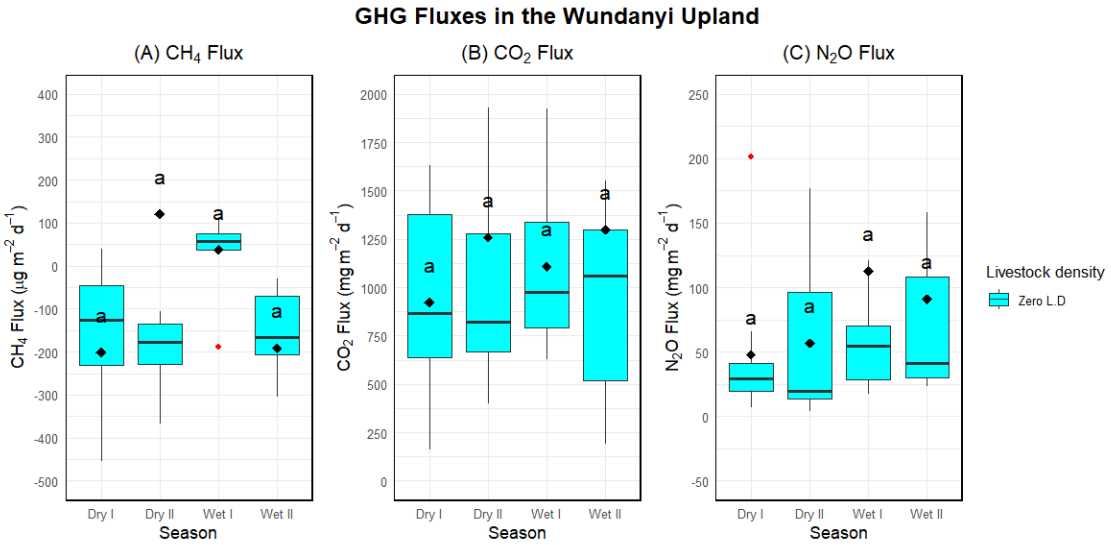

Figure 18: GHG fluxes in the Wundanyi upland zone, dominated by zero grazing units, high vegetation cover (including forests), and comparably stable riparian soils.

4.2 Soil organic carbon (SOC) stocks in the Bura and Wundanyi Catchments

SOC stocks varied between topographies and livestock density (LPS). SOC stocks increased from lowland zones to upland zones with the latter recording a mean of 7.61 Mg C ha^{-1}. This mean was 3 times larger than that of the lowland zone, and 40 % more than the midland zone. The mean SOC stocks were 4.86 Mg C ha^{-1} and were attributed to the upland zone. A negative correlation between SOC and LPS was observed, where increasing LPS levels resulted in lower SOC stocks. Mean SOC for the ZLD was the largest at 4.86 Mg C $ha^{-1,}$ which was 0.55 Mg C ha^{-1} more than the LLD and 38 % more than the HLD sites, as illustrated in **Figure 19** and further in **Figure 20**.

4.2.1 SOC stocks in the Bura catchment

The Bura catchment recorded a mean SOC stock of 6.80 Mg C ha^{-1}. The mean SOC stocks increased by 2.9 % between the Dry I and Dry II seasons. Similarly, an increase of 13.7 % was recorded between the Wet I and Wet II seasons. The dry seasons recorded a larger mean SOC stock of 7.69 Mg C ha^{-1} compared to the wet seasons' 5.92 Mg C ha^{-1}. The biggest seasonal mean (7.80 Mg C ha^{-1}) was recorded in the Dry II season, while the smallest mean (5.54 Mg C ha^{-1}) was recorded in the Wet I season. Carbon sequestration was thus highest in the LLD of the Bura catchment. The mean SOC stocks here were 7.67 Mg C ha^{-1}, which was 1.08 Mg C ha^{-1} more than the mean SOC stock in the HLD zones. In the reference (ZLD) zones, the smallest mean SOC stocks (4.16 Mg C ha^{-1}) were recorded. The Bura upland AEZ recorded a bigger SOC stock (7.40 Mg C ha^{-1}) than the midland AEZ (5.62 Mg C ha^{-1}). This was a 1.78 Mg C ha^{-1} difference, representing a 31.7 % increase between the midland and upland topographies. Mean SOC stocks in Bura increased with increasing distances from the watering point. The REP I recorded the smallest mean SOC stocks (6.20 Mg C ha^{-1}), while the Rep III range recorded the biggest mean (7.22 Mg C ha^{-1}), as shown in **Figure 19**. The Rep II recorded 12.6 % more SOC than Rep I and 3.4 % less SOC than Rep III. The LLD sites recorded larger SOC stock values in the midland and upland zones. In most sites, SOC stocks increased significantly from Rep I, to III in the midland zone. In the upland wet seasons, SOC stocks decreased with increasing replicates. Livestock density ($p = 4.69*10^{-3}$), altitude zones ($p = 1.04*10^{-2}$), and seasons ($p = 4.67*10^{-2}$) significantly influenced the SOC stocks measured in the Bura catchment.

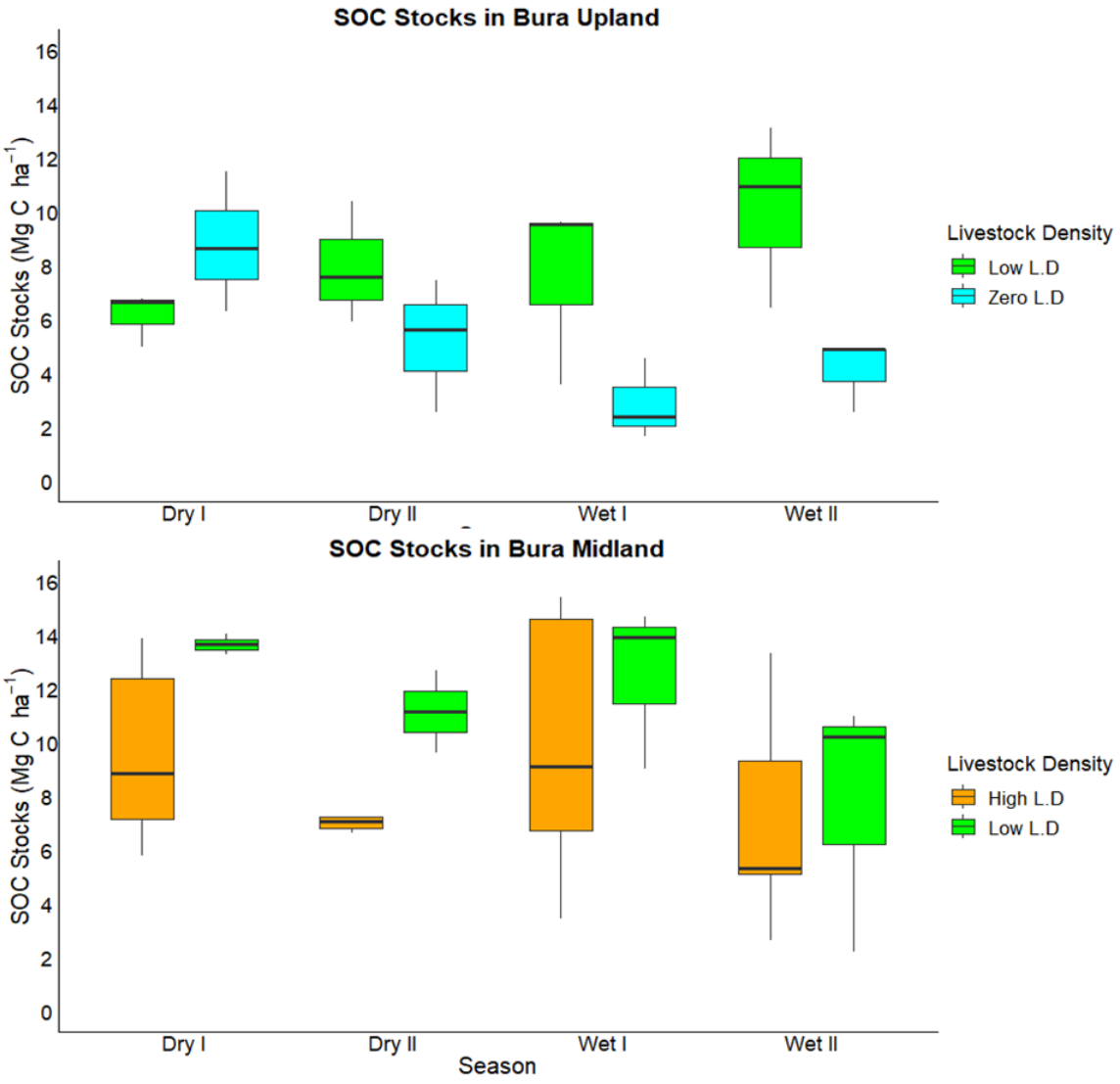

Figure 19: SOC stock measurements in the Bura sub-catchment. The presence of livestock reduced SOC stocks in the midland zone, but conversely increased SOC in the upland zone.

4.2.2 SOC stocks in the Wundanyi catchment

The Wundanyi catchment recorded a mean SOC stock of 3.10 Mg C ha^{-1}. The Dry I season recorded the largest mean (3.55 Mg C ha^{-1}), followed by the Wet II season (3.00 Mg C ha^{-1}). While the dry seasons recorded a large difference (0.71 Mg C ha^{-1}) in SOC stock means,

there was a 0.01 Mg C ha^{-1} difference between the two wet seasons in this study (**Figure 20**). The mean SOC stock in the dry seasons (3.195 Mg C ha^{-1}) was larger than in the rainy seasons (3.005 Mg C ha^{-1}). Based on altitude, the biggest mean SOC stock was recorded in the upland zone (6.10 Mg C ha^{-1}), followed by the midland zone (3.76 Mg C ha^{-1}) and lastly, the lowland zone (2.23 Mg C ha^{-1}). This implies that the upland agroecological zone sequestered more carbon than the combined midland and lowland zones. Mean SOC stock was greatest in the REP I (3.67 Mg C ha^{-1}) and smallest in the REP II (3.06 Mg C ha^{-1}). The REP III recorded 2.5 % less than REP I and 14.5 % more than REP II.. Saturation notably contributed to carbon sequestration in the REP I, where moisture levels were highest. The control sites with no livestock (ZLD) recorded the largest mean SOC stocks (4.63 Mg C ha^{-1}), followed by the LLD sites (3.0 Mg C ha^{-1}), and finally the HLD at 2.22 Mg C ha^{-1}. These means imply that carbon stocks, as hypothesised in this study, decreased with increasing livestock densities. Livestock density ($p = 1.5*10^{-12}$) and topography ($5.28*10^{-10}$) were the most influential factors in carbon sequestration. Topography was the key determinant of SOC stocks in the Wundanyi catchment ($p = <2.0*10^{-16}$). SOC stock in the Wundanyi upland zone was 1.6 times more than in the midland zone and 63.4 % higher than in the lowland zone.

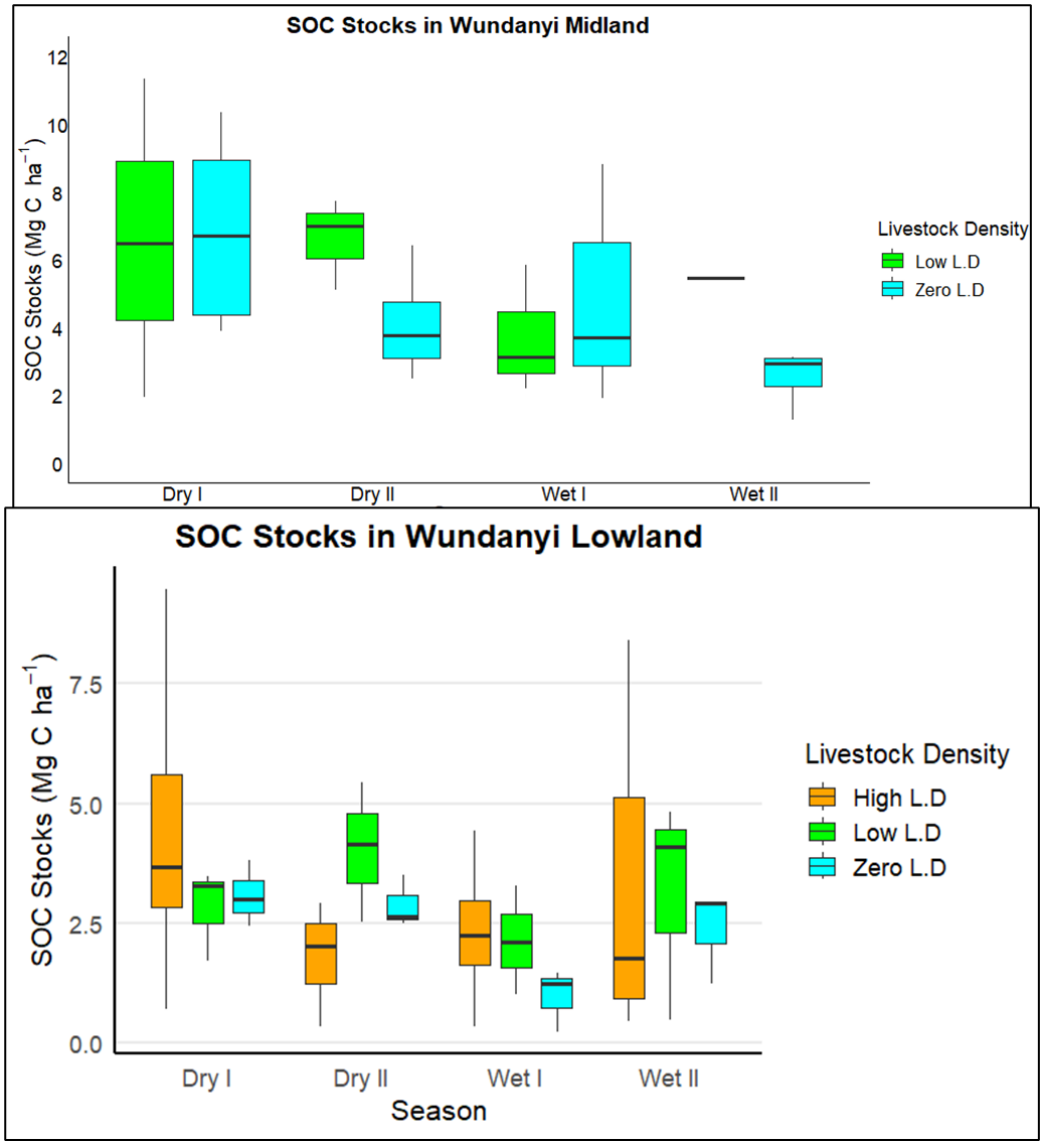

Figure 20: SOC stock measurements in the Wundanyi sub-catchment. In the lowlands, LLD sites recorded comparably bigger means, while the HLD sites had widely spread stock values.

4.3 Correlation between selected soil chemical attributes and GHG fluxes

A Pearson's correlation test result in the Bura catchment showed that SOC was weakly and negatively correlated with NH_4-N ($r = -0.027$, $p = 0.778$). SOC further showed a moderate positive and significant correlation with TN ($r = 0.286$, $p = 0.003$), indicating that with

increasing TN, SOC content also increases. SOC also showed a positive relationship with bulk density ($r = 0.277$, $p = 0.004$), indicating that SOC stock would slightly increase with an increase in soil bulk density. NO_3-N was weakly but significantly related to SOC ($r = 0.216$, $p = 0.025$), indicating that increased SOC accumulation may positively affect NO_3-N availability. SOC was positively and significantly correlated with NH_4-N in the Wundanyi catchment ($r = 0.199$, $p = 0.002$), with increased NH_4-N relating to increased SOC stocks. SOC was strongly and very significantly correlated with TN ($r = 0.601$, $p < 0.0001$). This suggests a strong linkage between TN availability and soil carbon sequestration. The correlation between SOC and bulk density was weak and non-significant ($r = 0.087$, $p = 0.190$), hence the minimal influence of bulk density on SOC in this catchment. NO_3-N had a weak but significant correlation with SOC ($r = 0.212$, $p = 0.001$), a trend similarly observed in Bura.

4.3.1 C:N Ratio attributions in Bura and Wundanyi

The results for the computation of C:N ratios showed that the mean C:N for the Bura upland zone was greater in the LLD (8.13) compared to the ZLD (7.13) sites. The mean C:N for the Bura catchment was 7.69. In the Bura midland zone, C:N was bigger in the HLD (9.16) compared to LLD sites, which was 16 % less. In the Wundanyi catchment, the upland zone recorded a mean C:N of 6.91, accounting for a 1.05 reduction from the Bura mean. In the upland zone, the ZLD zone recorded a mean C:N of 8.01. A big difference was recorded in the midland zone. The LLD recorded a C:N of 7.73 while the ZLD recorded 3.84, accounting for a 50 % decrease. In the Wundanyi lowland, the ZLD recorded the largest mean C:N (8.16), followed by the HLD at 7.40. The LLD zone recorded the smallest mean

C:N, 1.08 less than the HLD and 22.5 % less than the ZLD. C:N ratios were larger in the Wet II season for both catchments, 19.47 and 20.49 for the Bura and Wundanyi, respectively. The Wet II season was the largest, followed by the Dry I, Wet I, and Dry II seasons for both catchments. The smallest mean (Wet I) was 2.99 in Bura and 3.18 in Wundanyi, representing an 84.6 % and 84.5% reduction in their corresponding catchments. Other than the wet II seasons, which recorded means of 19 and 20, the seasonal mean C:N in all other seasons ranged between 6 and 2 for the Bura and Wundanyi catchments, respectively. Comparably, the C:N ratio was reduced with the reduction of livestock densities in the Bura catchment. The HLD averaged a bigger C:N (9.16), while the LLD recorded 7.78, and the lowest mean of 7.13 was recorded in the ZLD. In the Wundanyi catchment, the mean C:N of 8.08 was recorded in the ZLD, followed by 7.03 in the LLD, and 7.40 in the LLD.

4.4 Principal component analysis (PCA) for GHG fluxes and soil attributes in the Bura Catchment

PCA in the Bura Catchment was rather radial across seasons (**Figure *21***). PCA in the Dry I season accounted for 48.3 % variance (**Figure *21***b), while the Dry II season explained 41.8 % of the variance (**Figure *21***a). During the wet seasons, PCA accounted for 42.7 % (Wet I) and 45.4 % (Wet II) of the variances. Thus, plots b and d accounted for most of the seasonal variances of GHG and soil attributes in Bura. CH_4 fluxes contributed positively to PC1 and negatively to PC2, indicating an inverse correlation with TN, moisture, and NO_3^--N. CO_2 and N_2O fluxes were negatively related to PC1, indicating that they reduced the explanatory potential of the PCA. Available phosphorus strongly supported CO_2 fluxes

in Bura. Soil moisture, carbon stocks, and TN were strongly correlated. In wet environments, strong negative correlations were observed between CH_4 and N_2O fluxes. Soil pH, available P, and NO_3^--N were strongly and positively correlated. Most variables were strongly influential, except for porosity and soil moisture. CO_2 fluxes were positive on PC2 only and inversely correlated with carbon stocks and TN in wet conditions. Available P and moisture were strong antagonists.

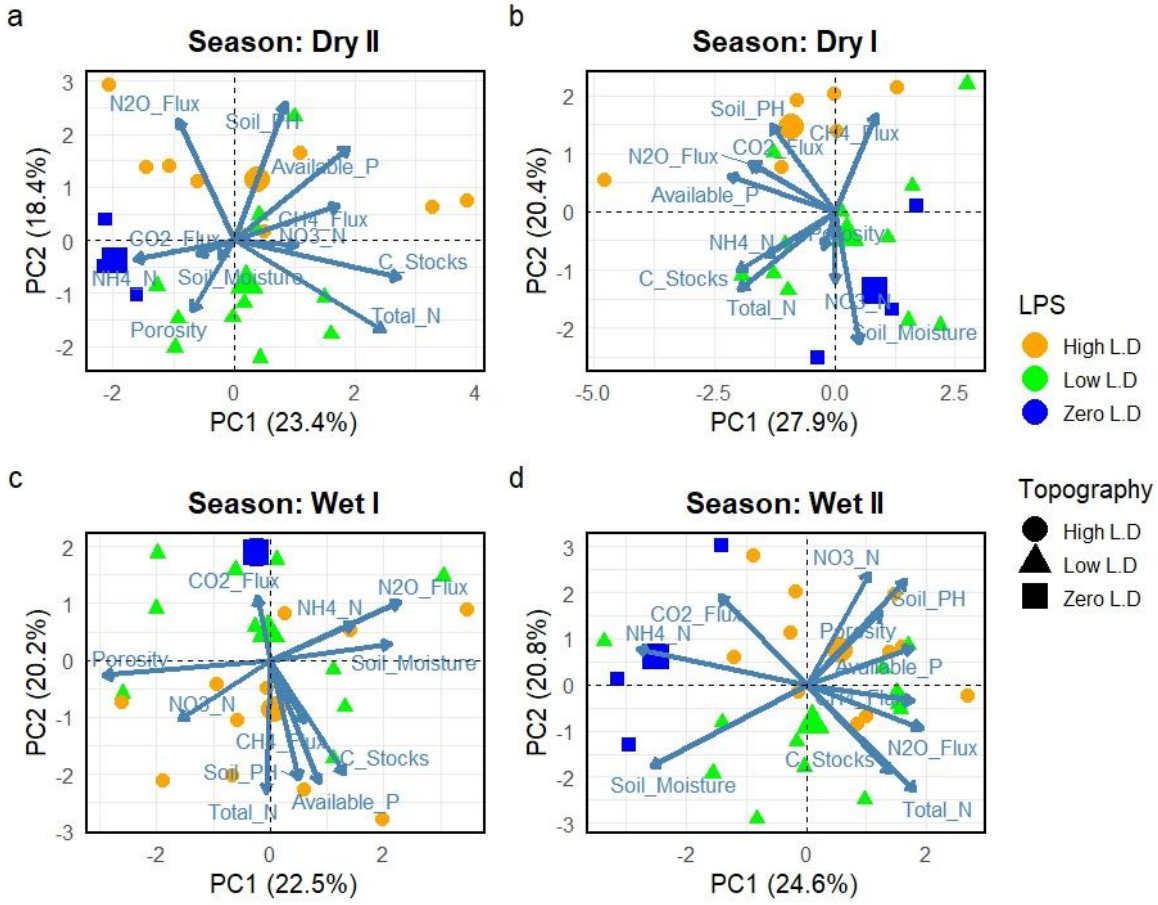

Figure 21: Principal component analysis (PCA) for seasonal GHG and soil physicochemical parameters in the Bura Catchment. Total nitrogen (TN) and SOC stocks were critical flux drivers in both seasons.

4.5 Principal component analysis (PCA) for GHG fluxes and soil attributes in the Wundanyi Catchment

In the Wundanyi catchment, the PCA for Dry I season explained 41.9 % of the variations, P1 26.4 %, and PC2 15.9 % (**Figure 22**). There were closer clusters in Dry II season, accounting for 45.4 % (PC1 32.9 % and PC2 12.5 %). In the wet seasons, the Wet I accounted for 40.4 % of the variations (PC1 23.8 % and PC2 16.6 %) while the Wet II explained 44.4 % of the variations (PC1 28.3 % and PC2 16.1 %). Accordingly, the Dry II and Wet II seasons better explained the variations between GHG and the selected soil parameters.

Porosity, available P, and NO_3^--N contributed positively to both PC1 and PC2, and showed strong positive correlations within the quadrant. All variables in this PCA were positively related to PC1, save for soil pH and moisture. While carbon stocks were strongly and positively correlated with PC1, it was neutral to soil moisture and available P, which were strongly negatively correlated. The Wet II season (**Figure 22**d) had dominant clusters positive to PC1. NH_4^+-N, carbon stocks, and TN were negatively correlated with PC2, while NO_3^--N, available P, and N_2O fluxes were positively to both PC1 and PC2. HLD and ZLD controlled most of the variations' direction and strength. CH_4 fluxes showed inverse correlation with NO_3^-- N, available P, and N_2O fluxes. CO_2 fluxes showed a strong positive correlation to TN, carbon stocks, and NH_4^+-N.

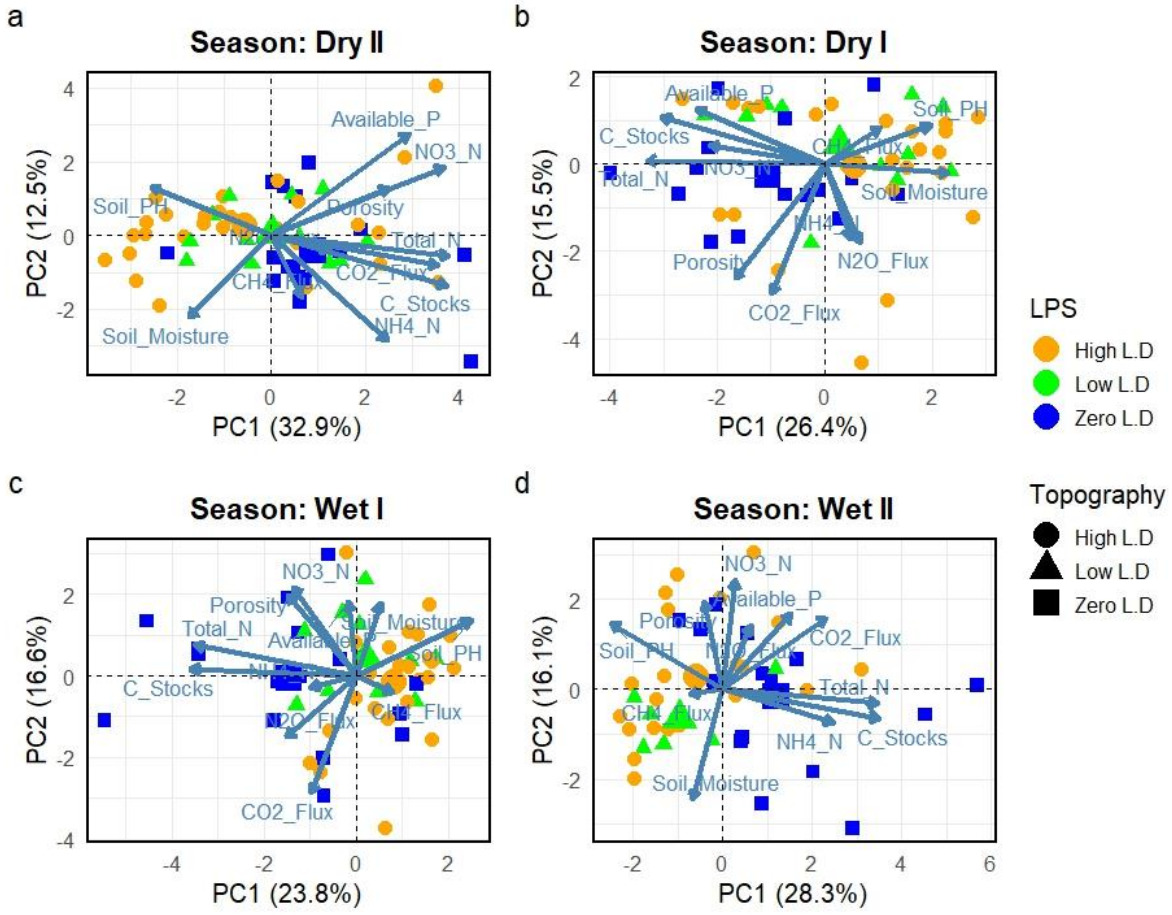

Figure 22: Principal component analysis (PCA) for seasonal GHG and selected soil physicochemical parameters in the Wundanyi Catchment. The role of phosphorus was clearly shown in the Wundanyi catchment, alongside total nitrogen (TN) and SOC stocks.

CHAPTER FIVE

DISCUSSIONS

5.1 GHG Fluxes in the Bura and Wundanyi Catchments

5.1.1 Methane fluxes

Methane fluxes in the Bura catchment were predominantly negative, identifying most measured sites as net methane sinks. Thus, underscoring the importance of low disturbance and well-aerated soils in promoting methane oxidation. Isolated cases of CH_4 emission were observed in the Midland HLD sites during the Wet I season. This suggests that methanogenic conditions, if they occurred at all, were likely short-lived and also microsite-specific. The consistently low or negative CH_4 emissions across HLD sites point to limited anaerobic conditions in Bura, likely due to dominant sand-sandy soils with high infiltration rates and low water retention capacity. These patterns align with Yan *et al.* (2022), who noted that well-drained tropical soils promote CH_4 oxidation over production, with the general understanding that methanotrophy thrives in aerobic-dry conditions. The presence of livestock did not substantially shift methane flux patterns in Bura because their dung and trampling were insufficient to create sustained anaerobic conditions suitable for methanogenesis. PCA analyses supported these findings, whereby CH_4 fluxes clustered near soil porosity and inversely with livestock pressure. This further reinforces the idea that soil texture and moisture regime, rather than livestock presence alone, play the dominant role in regulating methane dynamics in this semi-arid tropical catchment.

In contrast to Bura, CH_4 fluxes in the Wundanyi Catchment were highly variable, registering both CH_4 uptake and emission across the study variables. Average daily fluxes in Wundanyi were positive. These observations reflected a more complex linkage between

aerobic and anaerobic processes in the humid savanna landscape. The Dry I and Dry II seasons were marked by net CH_4 uptakes, particularly in Upland ZLD zones with strong soil aeration and active methanotrophy. Conversely, significant emissions were recorded in the Midland LLD and Lowland zones during Wet I. These emissions were attributed to increased soil moisture. Such conditions foster anaerobic microsites conducive to methanogenesis, especially in areas with high organic matter input from either litter or manure, as Dlamini *et al.* (2022) reported. In these zones, livestock activities may have compacted the soil and led to limited oxygen diffusion, which necessitates CH_4 production. Interestingly, some ZLD sites also emitted CH_4, particularly in Midland Wet I. This indicated that even without livestock, hydrologically active soils with organic substrates support methanogenesis. These findings aligned with the PCA outputs. CH_4 emissions were positively associated with soil moisture and livestock presence, particularly during the wet seasons. Correlation analysis further showed strong links between CH_4 fluxes and soil porosity. The coefficients suggest that soil structure may either facilitate CH_4 oxidation or shift microbial activity toward production when compacted. These findings highlight the sensitivity of CH_4 fluxes to livestock intensity and local hydrology in the ecosystem. Topographic position and moisture availability dynamically influence the balance between CH_4 uptake and emission.

The CH_4 flux dynamics observed in Bura and Wundanyi underscore the critical role of environmental and land-use contexts in shaping methane patterns as reported by Bratti et. al (2022), who studied the fluxes from an integrated perspective. In Bura, with its sandy soils, rapid infiltration, and low organic matter, methane uptake was dominant and stable, largely unaffected by livestock intensity. Conversely, Wundanyi's humid climate, variable

topography, and relatively organic-rich soils allowed for both uptake and significant emission, depending on season, livestock density, and microsite conditions. Livestock presence appeared to intensify CH_4 emissions in Wundanyi, particularly under HLD and wet conditions. Both catchments demonstrated that ZLD systems are not exempt from CH_4 emissions, especially during wetter periods with substrate (SOC) availability. This challenges the assumption that livestock-free areas universally function as methane sinks and calls for context-specific flux assessments in riparian landscapes. Studies by Butterbach-Bahl et al (2016) on GHG emissions from natural and managed soils confirm this. Conclusively, the study confirms that CH_4 fluxes are spatially and temporally variable among the three GHGs, governed not only by livestock densities but by a complex interplay of soil texture, hydrology, and organic matter availability, as proposed by Smith et. al (2003b). For policy and mitigation, this suggests that CH_4 monitoring should prioritise highland, humid catchments where emissions can spike under certain seasonal and land use combinations.

5.1.2 CO_2 fluxes in the Bura and Wundanyi Catchments

In the Bura catchment, CO_2 fluxes were comparably lower, with notable seasonal and spatial variability. These lower fluxes were attributed to the catchment's smaller coverage, smaller riparian strips, and more vegetated conditions. Bura had relatively limited soil erosion and livestock activities. The dry seasons exhibited reduced CO_2 emissions, consistent with moisture-limited biological processes. Among the topographic zones, upland and midland areas with HLDs exhibited relatively higher CO_2 fluxes, unlike the LLD and ZLD zones. This pattern suggests that grazing intensity influences carbon cycling through increased organic matter inputs such as manure, litter, and root turnover. This

aligns with Kindermann et. al (2025) who reported that at the ecosystem level, human disturbances influenced carbon storage, though in a non-linear trend. The variability across seasons indicates that soil moisture and temperature interactions play a key role in mediating microbial respiration. Accordingly, higher fluxes are likely during brief moisture pulses following rainfall, often referred to as the birch effect. While upland HLD zones in Bura occasionally recorded moderate fluxes, the midlands, especially under HLD, consistently released more CO_2. This may reflect increased microbial decomposition driven by organic inputs and disturbance-related aeration. These moderate emissions imply that Bura's sand soils were constrained by low organic carbon content and rapid infiltration, had a limited potential for CO_2 release under natural grazing conditions. The role of livestock in modulating CO_2 fluxes appears to be context-dependent, enhanced only under conditions of sufficient organic substrate and moisture availability, as shown by Rotich *et al.* (2020) and Wachiye *et al.* (2020b). Overall, carbon dioxide dynamics in Bura indicate that seasonal rainfall events, rather than grazing alone, are the dominant regulators of microbial CO_2 emissions in this dryland tropical catchment.

In contrast to Bura, CO_2 emissions in the Wundanyi catchment were consistently higher across all variables. These elevated fluxes are overall linked to Wundanyi's more humid conditions, higher organic matter content, and varied riparian strips. These attributes support greater microbial and root respiration and photosynthetic CO_2 release as inferred by (Konovalov *et al.*, 2025). Seasonal patterns showed peak emissions during the wet periods, particularly the Wet I season. At this time, soil moisture and temperature likely created optimal conditions for microbial activity and carbon mineralization. The consistently high CO_2 outputs from ZLD sites in both midland and upland zones suggest

that accumulated organic matter and reduced compaction support elevated respiration rates at the ecosystem level, as highlighted by Yang et. al (2025) in the Loess Plateau.

Topography also influenced CO_2 dynamics in Wundanyi. Upland zones under ZLD recorded some of the highest fluxes, likely due to cool, moist conditions that preserve organic matter while facilitating microbial decomposition. The vegetated uplands had high litter accumulation and relatively stable soils due to low soil erosion. The HLD sites in the Midlands registered high emissions during Dry I, which may reflect residual organic inputs or manure-enhanced microbial processes. These findings suggest that both site-specific land management and environmental conditions interact to shape carbon dynamics. In this regard, livestock presence influences fluxes more strongly when soils are moist and biologically active. Unlike Bura, where livestock impact was marginal, Wundanyi exhibited more pronounced land-use effects, particularly in wetter seasons and topographic zones where soil respiration is more responsive to disturbances and inputs. This aligns with a recent study linking surface processes to solute generation and CO_2 budgets by Slosson et. al (2025) and underscores the need for an integrated approach to GHG emission studies.

The contrasting CO_2 flux patterns between Bura and Wundanyi underscore the influence of climate, topography, and land use on soil biogeochemical processes. While Bura's dry conditions and sandy soils limit CO_2 production even under grazing, Wundanyi’s wetter, organic-rich soils support more active microbial communities and processes as well as greater respiration rates. In both catchments, seasonal moisture availability emerged as a dominant driver, modulated by livestock presence and topographic context. These findings support the notion that in tropical agroecosystems, CO_2 fluxes are tightly linked to soil-water-carbon interactions and are sensitive to both anthropogenic and natural gradients

across landscapes. This agrees with a satellite study in South Africa (Metz *et al.*, 2025) that showed significant variabilities at the landscape level.

5.1.3 N_2O fluxes in the Bura and Wundanyi Catchments

All sites in the Bura catchment were net sources of atmospheric N_2O, though Bura's emissions were generally lower than Wundanyi's. Like CH_4, fluxes here were governed by topography, livestock density, and especially seasonality. The highest average emissions were recorded in the midland HLD zones. This suggested a strong influence of livestock activity. Manure input likely enhanced nitrogen availability, while moderate moisture conditions influenced microbial nitrification and denitrification processes. This aligns with studies like (Bratti *et al.*, 2022; Zhu *et al.*, 2020) and indicates that grazing intensifies nitrogen turnover through both direct (manure) and indirect (soil compaction) mechanisms. This is common within short rainfall events. Both the Wet II and Dry I seasons recorded the highest emissions, implying that both moisture surpluses and the dry-season residual effects (e.g., accumulated organic N and microbially available substrates) influence N_2O dynamics. In contrast, emissions during Wet I and Dry II were moderate to low. This observation likely reflects fluctuating moisture conditions that could limit microbial activity or cause nitrogen leaching. Interestingly, ZLD sites emitted N_2O, albeit at lower rates. This suggests that legacy nitrogen, background mineralisation, and spontaneous vegetation can sustain microbial processes independent of recent livestock activities, as found by a study in China between 2021-2023 (Li *et al.*, 2025). The generally sandy soils with rapid infiltration in Bura, and the transient nature of wet conditions, appear to be the main limitation to a more sustained N_2O emission. Notably, under episodic rains, and

especially in the grazed midland zones, Bura's riparian soils can be significant sources of N_2O.

N_2O emissions in the Wundanyi catchment were higher and more spatially variable than Bura's. This highlights the disparities in soil moisture, organic matter, and land use intensity in these humid agroecosystems. Peak emissions were observed during Wet II, especially in lowland ZLD and HLD zones. These areas combine prolonged moisture retention, warm temperatures, and potential surface nitrogen accumulation (from litter, runoff, or anthropogenic inputs), creating ideal conditions for denitrification. The ZLD lowland sites recorded the highest emission events, indicating that substantial N_2O can be released from ungrazed but hydrologically active zones - a case similar to its CH_4 emissions. This is likely due to natural mineralization and soil organic N transformation as reported by Mwanake et. al (2019). The Upland ZLD sites produced elevated N_2O during Wet I, perhaps due to slower drainage and episodic saturation conditions. In the midlands, HLD zones exhibited significant emissions even during drier seasons (e.g., Dry I), potentially sustained by residual nitrogen from grazing and manure buildup. These findings point to a decoupling of moisture and fluxes under HLD, where biological N turnover can proceed at the slightest water availability. Meanwhile, LLD and ZLD midland sites showed more moderate, consistent emissions, suggesting resilience of lower input systems. The Wundanyi catchment illustrated how interactions between LPS, topography, and seasonality control N_2O production. In contrast to Bura, the influence of soil carbon and nitrogen cycling (subject to moisture availability) generates more dynamic flux responses. The elevated emissions from ZLD sites reinforce the idea that ungrazed landscapes are not

always low emitters and may play a disproportionate role under favourable hydrological conditions.

The Wundanyi's riparian strips support more active and seasonally amplified N_2O emissions than Bura. While livestock presence was associated with elevated N_2O fluxes, the Wundanyi's topographic complexity and longer moisture retention created more favourable conditions for denitrification. Significant emissions in the ZLD zones in both catchments emphasise that natural nitrogen cycling processes can sustain N_2O production even in the absence of livestock. Overall, the findings affirm that N_2O emissions in Afrotropical riparian zones are primarily regulated by soil moisture (seasonality), nitrogen availability, and land management. They also demonstrate the importance of topography in mediating these factors. The lowland zones were often the hotspots of flux activity. This has implications for GHG mitigation strategies in East African agroecosystems, especially as agriculture expands to protected riparian zones and climate profiles forecast more risks.

5.2 SOC stocks in the Bura and Wundanyi Catchments

In the Bura catchment, SOC stocks displayed notable spatial and seasonal variability, largely driven by soil texture, livestock density, and seasonal moisture variabilities. This suggests that moderate livestock activities may enhance organic matter retention and stabilization, particularly within favourable soil moisture, as supported by Hinshaw and Wohl, (2023). Conversely, HLD sites showed occasional SOC spikes in Midland HLD during Dry I, which were likely short-lived and subject to seasonal manure inputs or plant litter. The inherently low carbon stabilization potential of sandy soils limited long-term SOC retention. Furthermore, the dry seasons permitted organic residues to accumulate without immediate leaching, while the onset of wet seasons rapidly activated microbial

decomposition, mineralization, and erosion. These dynamics were also reported by Abbas et. al (2020) who reviewed the carbon footprints of anthropogenic activities. Despite these dynamics, LLD sites consistently outperformed HLD and ZLD zones in SOC retention across seasons, likely due to a balanced input-to-decomposition ratio under moderate grazing pressures. ZLD sites with cropping fields were likely subjected to the seasonal addition of SOM and manures for agricultural production. Descheermaeker et. al (2016) published on impacts, vulnerability, and knowledge gaps in the agricultural ecosystem, with similar input-output dynamics.

SOC dynamics in Wundanyi similarly reflected seasonal trends, with the Wet II season registering the highest carbon stocks across most topographic zones. However, due to the predominantly sandy soils (leaching) and steeper (erosion) gradients in Wundanyi, SOC values were comparably lower than in Bura. The lowland ZLD sites, characterised by loamy sand textures, had the highest mean SOC values, illustrating the potential of minimal soil disturbances to accumulate and sequester carbon as supported by Iteba et al (2021). Notably, the midland ZLD zones recorded lower SOC stocks, likely due to steep slopes promoting runoff and erosion. High SOC values in Upland ZLD areas during Wet II further emphasise the role of vegetation regeneration, minimal trampling, and episodic nutrient deposition from upper-slope erosion. Occasional SOC increases occurred in HLD zones, suggesting that manure deposition boosts short-term organic matter. However, this aspect is rarely maximised due to high turnover rates in coarse-textured soils, manure overwash into the stream, and continuous human disturbance (sand harvesting and cropping). Controlled grazing in Wundanyi, especially in community-managed conservancies under the Taita Taveta Wildlife Conservancies Association (TTWCA), has been shown to

improve vegetation recovery and potentially stabilize SOC under regulated conditions as reported by Wachiye et al (2022).

SOC stocks analysis in the Bura and Wundanyi catchments underscores the dominant role of seasonality, soil physicochemical attributes, and livestock densities in shaping SOC dynamics. Across the two catchments, the Wet II season consistently recorded the highest SOC accumulation, confirming that moisture enhances both input and stabilisation of organic matter. Hinshaw & Wohl (2023) measured and reported similar SOC stock trends in floodplains. The LLD zones maintained higher SOC across seasons and sites, indicating a stability phase. This observation supports the ecological benefits of moderate/controlled grazing in enhancing carbon sequestration. In contrast, HLD zones recorded high SOC stocks but were short-lived due to continuous vegetation removal, compaction, and hastened erosion, findings supported by the Rayne and Aula (2020) study. The interplay between slope, erosion potential, and livestock management was evident in Wundanyi. The ZLD sites in stable zones (e.g., forested uplands) outperformed midland zones (with or without livestock) in carbon retention. These findings affirm that sustainable livestock management, especially in zones with less stable soils and during the wet periods, is critical for enhancing SOC stocks. Riparian conservation strategies ought to integrate topographic sensitivity, regulate grazing intensity, and promote vegetation cover restoration to bolster SOC storage in ASAL ecosystems.

5.3 Soil attributes influencing carbon sequestration in riparian soils

A weak and non-significant correlation between SOC stocks and NH_4-N suggested that SOC dynamics in the Bura catchment were not directly influenced by soil NH_4-N concentrations. This could be due to rapid microbial assimilation, volatilisation, or leaching

of NH_4-N. However, the moderate and significant correlation between SOC and TN highlights the strong interdependence between ecosystem carbon and nitrogen cycles. Such observation was likely due to organic matter mineralisation, which consequently contributes to both SOC and TN accumulation. The positive correlation between SOC and bulk density in the Bura catchment suggests that increased carbon sequestration is associated with more stable soils. Harbo et al (2022) support this finding in their 0-50 cm measurement of bulk density and mineralogy study. This may be attributed to the influence of SOM bonding potentials or soil texture variations. However, higher bulk density limited root penetration and microbial activity in HLD sites. This was shown by bare lands in HLD sites, which may affect SOC sequestration in the long run. The weak but significant correlation between SOC and NO_3-N implies that SOC plays a significant role in NO_3 availability, possibly through the mineralisation processes or SOM decomposition. Since soil NO_3-N is highly mobile, its availability may also be subject to external factors like leaching.

Unlike Bura, the Wundanyi catchment exhibited a significant positive correlation between SOC and NH_4^+-N, indicating that NH_4^+-N retention potential may be higher. This could be due to differences in microbial activity, soil moisture, or clay content that enhance NH_4^+-N retention. Soil pH influenced both CH_4 and N_2O fluxes, with strong seasonal correlations. The strong correlation between SOC and TN in Wundanyi further confirms the close relationship between SOC and TN dynamics, reinforcing the role of organic matter as a reservoir of soil nutrients. Do et. al (2024) reported substantial soil transfer of organic carbon from the Korean (Rural Agriculture Development) RDA database. The weaker correlation between SOC and bulk density suggests that soil compaction slightly

enhances carbon storage in this catchment. This may be supported by livestock activity or inherent soil physical attributes like texture and structure. Like Bura, the correlation between SOC and NO_3^--N in Wundanyi was weak but significant. Thus, suggesting that SOC levels partly regulate NO_3^--N availability. However, other factors such as microbial nitrification and plant uptake may also contribute to soil NO_3^--N fluctuations.

5.4 Interactions of GHG and soil attributes in Bura and Wundanyi

Total nitrogen (TN), soil pH, and moisture exerted a strong influence during the dry periods. This observation suggests a co-regulatory role in influencing N transformations and microbial activity under moisture-limited conditions. Increased substrate availability and consequently microbial activities in the wet seasons prompted higher N_2O and CO_2 fluxes. These microbial settings are associated with wetter soils that favour nitrification, denitrification, and aerobic respiration. Porosity and moisture content emerged as dominant soil attributes in the Wet seasons, underscoring their fundamental roles in moderating gas diffusion, redox conditions, and microbial access to C and N substrates. These Bura observations showcase the role of both physical and chemical soil attributes in seasonal GHG fluxes and the need for integrated soil management strategies that factor hydrological and nutrient dynamics in ASAL agroecosystems.

In the Dry II season, total nitrogen (TN), available phosphorus (P), and soil moisture explained CH_4 and CO_2 emissions. This observation suggests that water limitations increased the influence of nutrients on microbial activity. A notable negative linkage between soil pH and SOC stocks also suggested the possibility of soil acidity limiting the breakdown of organic matter by altering microbial activities. Positive associations between CO_2 emissions and TN inform increased respiration and nitrogen turnover in the dry

season. In Wundanyi, SOC stocks, TN, soil moisture, and CO_2 flux remained the most influential variables in the Wet season. Increasing moisture availability and microbial activity. This resulted in enhanced ecosystem nutrient cycling and fluxes. The PCA captured more variation in the dry seasons, indicating that soil nutrients and moisture strongly influenced GHG fluxes when environmental conditions were limiting. This therefore underscores the need to manage nutrients and water more effectively in farming systems for ASAL regions. In a study by Liu et. al (2025), aligning ecological relationships between soil nutrients and the ecosystem functions was reported. This is the case for the PCA output in Bura and Wundanyi.

5.5 C:N ratio of riparian soils in Bura and Wundanyi

The seasonal variation in C:N ratios in Bura indicates strong seasonal influences on SOM decomposition and N mineralisation. The significantly higher C:N ratio in Wet II indicates enhanced build-up of organic residues, probably supported by reduced decomposition rates and increased biomass inputs. These findings align with Iteba et. al (2021), who reported that livestock are vectors of nutrients and therefore, in large numbers, can influence soil health. In the dry periods, leaf litter and manure are prone to build-ups in less disturbed areas, but are often washed away in wet periods. Consequently, the lower C:N ratios in the dry seasons (Dry I and Dry II) reflect enhanced microbial breakdown of organic matter (OM) and relatively faster mineralisation. The Midland HLD zones had the highest C:N ratio, indicating elevated OM input through livestock dung, manure, or vegetation litter. The C:N ratio was higher for the sandy loam soils of LLD zones compared with the sandy soil, scoring the better retention attribute of clays, as reported by Gul and Whalen (2022). Comparably, the C:N ratio in ZLD sites was relatively lower, probably due to limited OM

input from livestock or vegetation. As was in Bura, seasonal variation was the overriding factor on the C:N ratios in Wundanyi, with the highest values in Wet II and the lowest in Dry II. The trend agrees with the expected seasonality in the input of organic matter and decomposition rates. The Lowland ZLD recorded the highest C:N ratio, probably due to higher OM retention in loamy sand than in sand soils. The relatively lower C:N ratios in the Midland ZLD zone could be related to site-specific microbial activities and soil properties (Smith *et al.*, 2020). Higher C:N ratios imply elongated biodegradation periods. In the hydrolytic phase, N compounds generate ammonia as a by-product because the methanogens' toxicity inhibits the biodegradation process. Organic substrates with C:N ratio between 1 and 15 undergo rapid mineralisation and release N for plant uptake. Soil C:N ratio is therefore an important indicator of soil quality as reported by Evangelou & Giourga (2024).

CHAPTER SIX

CONCLUSIONS AND RECOMMENDATIONS

6.1 Conclusions

This study revealed that sites with high livestock density (HLD) exhibited markedly elevated CO_2 and CH_4 fluxes, as indicated by the PCA clustering results. These higher emissions were primarily driven by increased nutrient inputs from manure, urine, and agricultural amendments, which stimulate microbial respiration and methanogenesis. However, these same HLD sites also showed reduced soil organic carbon (SOC) stocks, likely due to accelerated decomposition, trampling, and soil disturbance. In contrast, zero (ZLD) and low livestock density (LLD) zones, particularly within the Wundanyi uplands, supported SOC accumulation. This underscores the dual role of livestock: while moderate grazing contributes to nutrient cycling and productivity, excessive stocking rates can intensify GHG emissions and undermine soil carbon sequestration efforts.

During wet seasons, elevated soil moisture and improved porosity created anaerobic microsites that enhanced CH_4 emissions, especially in midland and lowland landscapes. Conversely, under dry season conditions, the variability in CO_2 and N_2O fluxes was strongly influenced by mineral nitrogen fractions (NH_4^+ and NO_3^-) and SOC content, reflecting heightened mineralisation and nitrification under drier, aerobic environments. These seasonal shifts highlight the sensitivity of GHG dynamics to both moisture availability and nutrient status.

Higher SOC stocks were consistently recorded in upland zones, characterised by limited livestock access and minimal soil disturbance. These sites correspondingly exhibited lower

CH_4 and CO_2 fluxes, suggesting that topographic position and reduced anthropogenic pressure foster carbon retention and lower GHG emissions. In contrast, lowland areas associated with greater livestock concentration and moisture retention showed higher emissions and more variable SOC stocks, indicating a trade-off between productivity and carbon sustainability.

Overall, the findings reinforce that SOC stocks are pivotal for both long-term carbon sequestration and regulation of soil GHG emissions, through their interaction with nitrogen cycling and microbial processes. Sites with elevated SOC and total nitrogen (TN) demonstrated moderated CO_2 and N_2O fluxes under certain seasonal conditions, emphasising the buffering function of SOC in emission control. These integrated dynamics highlight that enhancing SOC through improved grazing management, organic amendments, and reduced disturbance can simultaneously sequester carbon and mitigate CO_2, CH_4, and N_2O emissions in smallholder livestock systems

6.2 Recommendations

Based on the findings of this study, I recommend the following:

i. **Promote ecosystem conservation and soil carbon restoration in riparian and cultivated zones**

Policymakers and extension agencies should actively promote manure management, regulated sand harvesting, and sustainable grazing practices within cultivated riparian strips and areas, especially with depleted SOC stocks and elevated CO_2 and CH_4 fluxes. These measures enhance soil organic matter (SOM) inputs, reduce erosion and sediment transport, and improve soil structure and moisture retention, creating conditions that favor

carbon sequestration and mitigate GHG emissions. Integrating these practices into local catchment management plans will strengthen the resilience of riparian ecosystems against degradation and climate impacts.

ii. Implement controlled grazing and optimized livestock stocking rates across production zones

In both high (HLD) and low livestock density (LLD) zones, enforcing controlled grazing regimes and maintaining sustainable stocking rates can significantly reduce extreme vegetation intakes, soil compaction, urine and manure deposition, and enhance vegetation recovery and pasture regeneration. These practices stabilize SOC levels, curb CO_2 and CH_4 emissions, and prevent the formation of anaerobic microsites that drive methanogenesis. Developing site-specific grazing schedules, supported by community-based rangeland monitoring, would ensure that livestock systems remain both productive and climate-smart.

iii. Prioritize agroforestry and re-vegetation in degraded landscapes

Given the pronounced SOC losses and land degradation, particularly in midland and lowland areas, policymakers and conservation programs should prioritize agroforestry, re-vegetation, and assisted natural ecosystem regeneration. These interventions enhance soil stability, improve biodiversity and microclimatic regulation, and increase ecosystem resilience to climate variability. In addition to sequestering carbon, these nature-based solutions contribute to sustained reductions in GHG emissions and foster balanced nutrient cycling at the landscape scale, aligning with national carbon neutrality and land restoration targets.

REFERENCES

Abbas, F., Hammad, H. M., Ishaq, W., Farooque, A. A., Bakhat, H. F., Zia, Z., Fahad, S., Farhad, W., & Cerdà, A. (2020). A review of soil carbon dynamics resulting from agricultural practices. *Journal of Environmental Management*, *268*, 110319. https://doi.org/10.1016/j.jenvman.2020.110319

Abera, T. A., Vuorinne, I., Munyao, M., Pellikka, P. K. E., & Heiskanen, J. (2022). Land Cover Map for Multifunctional Landscapes of Taita Taveta County, Kenya, Based on Sentinel-1 Radar, Sentinel-2 Optical, and Topoclimatic Data. *Data*, *7*(3), 36. https://doi.org/10.3390/data7030036

Airori, A. J., Baker, T. J., & Turk, J. K. (2022). The Impact of Sampling Methodology on Soil Bulk Density Measurement by the Clod Method. *Communications in Soil Science and Plant Analysis*, *53*(3), 317–326. https://doi.org/10.1080/00103624.2021.1993887

Arias-Navarro, C., Díaz-Pinés, E., Kiese, R., Rosenstock, T. S., Rufino, M. C., Stern, D., Neufeldt, H., Verchot, L. V., & Butterbach-Bahl, K. (2013). Gas pooling: A sampling technique to overcome spatial heterogeneity of soil carbon dioxide and nitrous oxide fluxes. *Soil Biology and Biochemistry*, *67*, 20–23. https://doi.org/10.1016/j.soilbio.2013.08.011

Arthur, A., & Okae-Anti, D. (2022). Variations in Soil Physico-Chemical Properties as Influenced by Landuse in a Toposequence. *Journal of Geoscience and Environment Protection*, *10*(8), Article 8. https://doi.org/10.4236/gep.2022.108008

Baker, J. M., Ochsner, T. E., Venterea, R. T., & Griffis, T. J. (2007). Tillage and soil carbon sequestration—What do we really know? *Agriculture, Ecosystems & Environment*, *118*(1), 1–5. https://doi.org/10.1016/j.agee.2006.05.014

Bhattacharyya, S. S., Leite, F. F. G. D., France, C. L., Adekoya, A. O., Ros, G. H., de Vries, W., Melchor-Martínez, E. M., Iqbal, H. M. N., & Parra-Saldívar, R. (2022). Soil carbon sequestration, greenhouse gas emissions, and water pollution under different tillage practices. *Science of The Total Environment*, *826*, 154161. https://doi.org/10.1016/j.scitotenv.2022.154161

Bird, S. B., Herrick, J. E., Wander, M. M., & Wright, S. F. (2002). Spatial heterogeneity of aggregate stability and soil carbon in semi-arid rangeland. *Environmental Pollution*, *116*(3), 445–455. https://doi.org/10.1016/S0269-7491(01)00222-6

Bouyoucos, G. J. (1962). Hydrometer Method Improved for Making Particle Size Analyses of Soils. *Agronomy Journal*, *54*(5), 464–465. https://doi.org/10.2134/agronj1962.00021962005400050028x

Brady, N. C., & Weil, R. R. (2016). *The nature and properties of soils* (Fifteenth edition, global edition). Pearson.

Bratti, F., Luiz Locatelli, J., Henrique Ribeiro, R., Renan Besen, M., Dieckow, J., Bayer, C., & Thiago Piva, J. (2022). Nitrous oxide and methane emissions affected by grazing and nitrogen fertilization in an integrated crop-livestock system. *Geoderma*, *425*, 116027. https://doi.org/10.1016/j.geoderma.2022.116027

Butterbach-Bahl, K., Sander, B. O., Pelster, D., & Díaz-Pinés, E. (2016). Quantifying Greenhouse Gas Emissions from Managed and Natural Soils. In T. S. Rosenstock, M. C. Rufino, K. Butterbach-Bahl, L. Wollenberg, & M. Richards (Eds.), *Methods for Measuring Greenhouse Gas Balances and Evaluating Mitigation Options in Smallholder Agriculture* (pp. 71–96). Springer International Publishing. https://doi.org/10.1007/978-3-319-29794-1_4

Calle, L., Canadell, J. G., Patra, P., Ciais, P., Ichii, K., Tian, H., Kondo, M., Piao, S., Arneth, A., Harper, A. B., Ito, A., Kato, E., Koven, C., Sitch, S., Stocker, B. D., Vivoy, N., Wiltshire, A., Zaehle, S., & Poulter, B. (2016). Regional carbon fluxes from land use and land cover change in Asia, 1980–2009. *Environmental Research Letters*, *11*(7), 074011. https://doi.org/10.1088/1748-9326/11/7/074011

Calvin, K., Dasgupta, D., Krinner, G., Mukherji, A., Thorne, P. W., Trisos, C., Romero, J., Aldunce, P., Barrett, K., Blanco, G., Cheung, W. W. L., Connors, S., Denton, F., Diongue-Niang, A., Dodman, D., Garschagen, M., Geden, O., Hayward, B., Jones, C., … Péan, C. (2023). *IPCC, 2023: Climate Change 2023: Synthesis Report. Contribution of Working Groups I, II and III of the Intergovernmental Panel on Climate Change. IPCC, Geneva, Switzerland.* https://doi.org/10.59327/IPCC/AR6-9789291691647

Carter, M. R. (1995). Analysis of Soil Organic Matter Storage in Agroecosystems. In *Structure and Organic Matter Storage in Agricultural Soils*. CRC Press.

Chen, S., & Gong, B. (2021). Response and adaptation of agriculture to climate change: Evidence from China. *Journal of Development Economics*, *148*, 102557. https://doi.org/10.1016/j.jdeveco.2020.102557

Cheng, S., Kumar, A., Lan, G., Zhang, W., Yu, Z., Zhang, S., Yu, Z.-G., Yao, M., & Lin, J. (2025). Thermal sensitivity and rising greenhouse gas emissions in riparian zone soils: Implications for ecosystem carbon dynamics. *Journal of Environmental Management*, *381*, 125194. https://doi.org/10.1016/j.jenvman.2025.125194

Clark, M. A., Domingo, N. G. G., Colgan, K., Thakrar, S. K., Tilman, D., Lynch, J., Azevedo, I. L., & Hill, J. D. (2020). Global food system emissions could preclude achieving the 1.5° and 2°C climate change targets. *Science*, *370*(6517), 705–708. https://doi.org/10.1126/science.aba7357

Clark, & Pellikka. (2009). Landscape analysis using multi-scale segmentation and object-oriented classification. In *Recent Advances in Remote Sensing and Geoinformation Processing for Land Degradation Assessment*. CRC Press.

Critchley, W., Harari, N., Mollee, E., Mekdaschi-Studer, R., & Eichenberger, J. (2023). Sustainable Land Management and Climate Change Adaptation for Small-Scale Land Users in Sub-Saharan Africa. *Land*, *12*(6), Article 6. https://doi.org/10.3390/land12061206

Dahl, M., McMahon, K., Lavery, P. S., Hamilton, S. H., Lovelock, C. E., & Serrano, O. (2023). Ranking the risk of CO2 emissions from seagrass soil carbon stocks under global change threats. *Global Environmental Change*, *78*, 102632. https://doi.org/10.1016/j.gloenvcha.2022.102632

Descheemaeker, K., Oosting, S. J., Homann-Kee Tui, S., Masikati, P., Falconnier, G. N., & Giller, K. E. (2016). Climate change adaptation and mitigation in smallholder crop–livestock systems in sub-Saharan Africa: A call for integrated impact assessments. *Regional Environmental Change*, *16*(8), 2331–2343. https://doi.org/10.1007/s10113-016-0957-8

Dlamini, J. C., Cardenas, L. M., Tesfamariam, E. H., Dunn, R. M., Evans, J., Hawkins, J. M. B., Blackwell, M. S. A., & Collins, A. L. (2022). Soil N2O and CH4 emissions from fodder maize production with and without riparian buffer strips of differing vegetation. *Plant and Soil*, *477*(1), 297–318. https://doi.org/10.1007/s11104-022-05426-0

Dlamini, J. C., Cárdenas, L., Tesfamariam, E. H., Dunn, R., Hawkins, J., Blackwell, M., Evans, J., & Collins, A. (2022). Soil methane (CH4) fluxes in cropland with permanent pasture and riparian buffer strips with different vegetation#. *Journal of Plant Nutrition and Soil Science*, *185*(1), 132–144. https://doi.org/10.1002/jpln.202000473

Do, M.-T. T., Van, L. N., Le, X.-H., Nguyen, G. V., Yeon, M., & Lee, G. (2024). National variability in soil organic carbon stock predictions: Impact of bulk density pedotransfer functions. *International Soil and Water Conservation Research*. https://doi.org/10.1016/j.iswcr.2024.04.002

D'Odorico, P., Laio, F., Porporato, A., & Rodriguez-Iturbe, I. (2003). Hydrologic controls on soil carbon and nitrogen cycles. II. A case study. *Advances in Water Resources*, *26*(1), 59–70. https://doi.org/10.1016/S0309-1708(02)00095-7

Don, A., Schumacher, J., & Freibauer, A. (2011). Impact of tropical land-use change on soil organic carbon stocks – a meta-analysis. *Global Change Biology*, *17*(4), 1658–1670. https://doi.org/10.1111/j.1365-2486.2010.02336.x

Dupla, X., Bonvin, E., Deluz, C., Lugassy, L., Verrecchia, E., Baveye, P. C., Grand, S., & Boivin, P. (2024). Are soil carbon credits empty promises? Shortcomings of current soil carbon quantification methodologies and improvement avenues. *Soil Use and Management*, *40*(3), e13092. https://doi.org/10.1111/sum.13092

Eggleston, H. S., Buendia, L., Miwa, K., Ngara, T., & Tanabe, K. (2006). *2006 IPCC Guidelines for National Greenhouse Gas Inventories*. https://www.osti.gov/etdeweb/biblio/20880391

Ericksen, P., & Crane, T. (2018). *The feasibility of low emissions development interventions for the East African livestock sector: Lessons from Kenya and Ethiopia*. 25.

European Commission, Joint Research Centre, Crippa, M., Guizzardi, D., Pagani, F., Banja, M., Muntean, M., Schaaf, E., Monforti-Ferrario, F., Becker, W. E., Quadrelli, R., Risquez Martin, A., Taghavi-Moharamli, P., Köykkä, J., Grassi, Rossi, S., Melo, J., Oom, D., Branco, A., … Pekar. (2024). *GHG emissions of all world countries* (p. 278). Publications Office of the European Union. https://data.europa.eu/doi/10.2760/4002897

Evangelou, E., & Giourga, C. (2024). Identification of Soil Quality Factors and Indicators in Mediterranean Agro-Ecosystems. *Sustainability*, *16*(23), Article 23. https://doi.org/10.3390/su162310717

FAO, F. (2018). *agriculture organization of the united nation. Africa sustainable livestock 2050, Country Brief Egypt., http*.

FAOSTAT. (2023). *World Food and Agriculture – Statistical Yearbook 2023*. FAO. https://doi.org/10.4060/cc8166en

FAOSTAT. (2024). *FAO 2024 Agricultural production statistics 2010-2023* (Brief No. 96; p. 16). https://openknowledge.fao.org/handle/20.500.14283/cd3755en

Farmani, Z., Azin, R., Fatehi, R., & Escrochi, M. (2018). Analysis of Pre-Darcy flow for different liquids and gases. *Journal of Petroleum Science and Engineering*, *168*, 17–31. https://doi.org/10.1016/j.petrol.2018.05.004

Featherstone, A. M., & Goodwin, B. K. (1993). Factors Influencing a Farmer's Decision to Invest in Long-Term Conservation Improvements. *Land Economics*, *69*(1), 67. https://doi.org/10.2307/3146279

Fernández, A., & Manuel, E. (2016). *The influence of management practices on the greenhouse gas balance of Mediterranean cropping systems: Identifying the climate change mitigation potential through quantitative review and life cycle assessment*. https://rio.upo.es/xmlui/handle/10433/3712

Friedlingstein, P., O'Sullivan, M., Jones, M. W., Andrew, R. M., Hauck, J., Olsen, A., Peters, G. P., Peters, W., Pongratz, J., Sitch, S., Le Quéré, C., Canadell, J. G., Ciais, P., Jackson, R. B., Alin, S., Aragão, L. E. O. C., Arneth, A., Arora, V., Bates, N. R., … Zaehle, S. (2020). Global Carbon Budget 2020. *Earth System Science Data*, *12*(4), 3269–3340. https://doi.org/10.5194/essd-12-3269-2020

Gerber, P., Steinfeld, H., Henderson, B., Mottet, A., Opio, C., Dijkman, J., Falcucci, A., & Tampio, G. (2013). *Tackling climate change through livestock: A global assessment of emissions and mitigation opportunities*. FAO.

Gitau, A. N., Onwonga, R. N., Mbau, J. S., Chepkemoi, J., & Mureithi, S. M. (2021). *Effect of Grazing Management and Land Cover Types on Mineral-Associated Organic Carbon and Particulate Organic Carbon in a Semi-arid Rangelands in Kenya* [Preprint]. In Review. https://doi.org/10.21203/rs.3.rs-768864/v1

Godde, C. M., de Boer, I. J. M., Ermgassen, E. zu, Herrero, M., van Middelaar, C. E., Muller, A., Röös, E., Schader, C., Smith, P., van Zanten, H. H. E., & Garnett, T. (2020). Soil carbon sequestration in grazing systems: Managing expectations. *Climatic Change*, *161*(3), 385–391. https://doi.org/10.1007/s10584-020-02673-x

Goopy, J. P., Onyango, A. A., Dickhoefer, U., & Butterbach-Bahl, K. (2020). Corrigendum to "A new approach for improving emission factors for enteric methane emissions of cattle in smallholder systems of East Africa – Results for Nyando, Western Kenya" [Agricultural systems volume (161) pp72–80]. *Agricultural Systems*, *184*, 102898. https://doi.org/10.1016/j.agsy.2020.102898

Govaerts, B., Verhulst, N., Castellanos-Navarrete, A., Sayre, K. D., Dixon, J., & Dendooven, L. (2009). Conservation Agriculture and Soil Carbon Sequestration: Between Myth and Farmer Reality. *Critical Reviews in Plant Sciences*, *28*(3), 97–122. https://doi.org/10.1080/07352680902776358

Graham, M. W., Butterbach-Bahl, K., du Toit, C. J. L., Korir, D., Leitner, S., Merbold, L., Mwape, A., Ndung'u, P. W., Pelster, D. E., Rufino, M. C., van der Weerden, T., Wilkes, A., & Arndt, C. (2022). Research Progress on Greenhouse Gas Emissions From Livestock in Sub-Saharan Africa Falls Short of National Inventory Ambitions. *Frontiers in Soil Science*, *2*. https://doi.org/10.3389/fsoil.2022.927452

Gross, C. D., & Harrison, R. B. (2019). The Case for Digging Deeper: Soil Organic Carbon Storage, Dynamics, and Controls in Our Changing World. *Soil Systems*, *3*(2), 28. https://doi.org/10.3390/soilsystems3020028

Gubamwoyo, S., Hein, T., Heiskanen, J., Kisha, D. G., Pellikka, P., Gruber, G., Omondi, V. A., Leitner, S. M., Weigelhofer, G., Mwamodenyi, J. M., Obonyo, A. O., & Gettel, G. M. (2025). Assessing land use changes and agricultural practices in highland valley-bottom wetlands in Taita Hills, Kenya. *Journal of Environmental Management*, *389*, 126122. https://doi.org/10.1016/j.jenvman.2025.126122

Gul, S., & Whalen, J. K. (2022). Chapter Six—Perspectives and strategies to increase the microbial-derived soil organic matter that persists in agroecosystems. In D. L. Sparks (Ed.), *Advances in Agronomy* (Vol. 175, pp. 347–401). Academic Press. https://doi.org/10.1016/bs.agron.2022.04.004

Guo, Y., Wang, X., Li, X., Wang, J., Xu, M., & Li, D. (2016). Dynamics of soil organic and inorganic carbon in the cropland of upper Yellow River Delta, China. *Scientific Reports*, *6*(1), 36105. https://doi.org/10.1038/srep36105

Hansen, M. C., Potapov, P. V., Moore, R., Hancher, M., Turubanova, S. A., Tyukavina, A., Thau, D., Stehman, S. V., Goetz, S. J., Loveland, T. R., Kommareddy, A., Egorov, A., Chini, L., Justice, C. O., & Townshend, J. R. G. (2013). High-Resolution Global Maps of 21st-Century Forest Cover Change. *Science*, *342*(6160), 850–853. https://doi.org/10.1126/science.1244693

Harbo, L. S., Olesen, J. E., Liang, Z., Christensen, B. T., & Elsgaard, L. (2022). Estimating organic carbon stocks of mineral soils in Denmark: Impact of bulk density and content of rock fragments. *Geoderma Regional*, *30*, e00560. https://doi.org/10.1016/j.geodrs.2022.e00560

He, Z. (2020). *Labile Organic Matter: Chemical Compositions, Function, and Significance in Soil and the Environment*. John Wiley & Sons.

Heinrich, S. (2025). *Soil Atlas Kenya Edition 2025* (p. 56). https://ke.boell.org/sites/default/files/2025-02/soilatlas-2025_-ke-edition-web.pdf

Herrero, M., Grace, D., Njuki, J., Johnson, N., Enahoro, D., Silvestri, S., & Rufino, M. C. (2013). The roles of livestock in developing countries. *Animal*, *7*, 3–18. https://doi.org/10.1017/S1751731112001954

Herrero, M., Henderson, B., Havlík, P., Thornton, P. K., Conant, R. T., Smith, P., Wirsenius, S., Hristov, A. N., Gerber, P., Gill, M., Butterbach-Bahl, K., Valin, H., Garnett, T., & Stehfest, E. (2016a). Greenhouse gas mitigation potentials in the livestock sector. *Nature Climate Change*, *6*(5), 452–461. https://doi.org/10.1038/nclimate2925

Herrero, M., Henderson, B., Havlík, P., Thornton, P. K., Conant, R. T., Smith, P., Wirsenius, S., Hristov, A. N., Gerber, P., Gill, M., Butterbach-Bahl, K., Valin, H., Garnett, T., & Stehfest, E. (2016b). Greenhouse gas mitigation potentials in the livestock sector. *Nature Climate Change*, *6*(5), 452–461. https://doi.org/10.1038/nclimate2925

Hinshaw, S., & Wohl, E. (2023). *Carbon sequestration potential of process-based river restoration*. https://www.authorea.com/users/602607/articles/633377-carbon-sequestration-potential-of-process-based-river-restoration

Höglund-Isaksson, L. (2012). Global anthropogenic methane emissions 2005-2030: Technical mitigation potentials and costs. *Atmospheric Chemistry and Physics*, *12*(19), 9079–9096. https://doi.org/10.5194/acp-12-9079-2012

Hohenthal, J., Owidi ,Emmah, Minoia ,Paola, & and Pellikka, P. (2015). Local assessment of changes in water-related ecosystem services and their management: DPASER conceptual model and its application in Taita Hills, Kenya. *International Journal of Biodiversity Science, Ecosystem Services & Management*, *11*(3), 225–238. https://doi.org/10.1080/21513732.2014.985256

Hou, Y., Velthof, G. L., Lesschen, J. P., Staritsky, I. G., & Oenema, O. (2016, December 20). *Nutrient Recovery and Emissions of Ammonia, Nitrous Oxide, and Methane from Animal Manure in Europe: Effects of Manure Treatment Technologies* (world) [Research-article]. ACS Publications; American Chemical Society. https://doi.org/10.1021/acs.est.6b04524

IPCC. (2014). Climate Change 2014: Synthesis Report. Contribution of Working Groups I, II and III to the Fifth Assessment Report of the Intergovernmental Panel on Climate Change. In *EPIC3Geneva, Switzerland, IPCC, 151 p., pp. 151, ISBN: 978-92-9169-143-2* (p. 151). IPCC. https://epic.awi.de/id/eprint/37530/

IPCC. (2023a). *Climate Change 2023: Synthesis Report. Contribution of Working Groups I, II and III to the Sixth Assessment Report of the Intergovernmental Panel on Climate Change [Core Writing Team, H. Lee and J. Romero (eds.)]. IPCC, Geneva, Switzerland.* (First). Intergovernmental Panel on Climate Change (IPCC). https://doi.org/10.59327/IPCC/AR6-9789291691647

IPCC (Ed.). (2023b). Emissions Trends and Drivers. In *Climate Change 2022—Mitigation of Climate Change* (1st ed., pp. 215–294). Cambridge University Press. https://doi.org/10.1017/9781009157926.004

IPCC (with Intergouvernemental panel on climate change & Groupe d'experts intergouvernemental sur l'évolution du climat). (1996). *Climate change 1995: The science of climate change*. Cambridge university press.

IPCC SPM (Ed.). (2023). Summary for Policymakers. In Climate Change 2022: Mitigation of Climate Change. Contribution of Working Group III to the Sixth Assessment Report of the Intergovernmental Panel on Climate Change. In *Climate Change 2022—Mitigation of Climate Change* (1st ed., pp. 3–48). Cambridge University Press. https://doi.org/10.1017/9781009157926.001

Israel, M. A., Amikuzuno, J., & Danso-Abbeam, G. (2020). Assessing farmers' contribution to greenhouse gas emission and the impact of adopting climate-smart agriculture on mitigation. *Ecological Processes*, *9*(1), 51. https://doi.org/10.1186/s13717-020-00249-2

Iteba, J. O., Hein, T., Singer, G. A., & Masese, F. O. (2021). Livestock as vectors of organic matter and nutrient loading in aquatic ecosystems in African savannas. *PLOS ONE*, *16*(9), e0257076. https://doi.org/10.1371/journal.pone.0257076

Janssens-Maenhout, G., Crippa, M., Guizzardi, D., Muntean, M., Schaaf, E., Dentener, F., Bergamaschi, P., Pagliari, V., Olivier, J. G. J., Peters, J. A. H. W., van Aardenne, J. A., Monni, S., Doering, U., & Petrescu, A. M. R. (2017). *Global Atlas of the three major GreenhouseGas Emissions for the period 1970–2012* [Preprint]. Data, Algorithms, and Models. https://doi.org/10.5194/essd-2017-79

Khatri-Chhetri, A., Wilkes, A., & Odhong', C. (2020). *Mitigation options and finance for transition to low-emissions dairy in Kenya* [Working Paper]. CGIAR Research Program on Climate Change Agriculture and Food Security (CCAFS). https://cgspace.cgiar.org/handle/10568/110568

Kim, Thomas, A. D., Pelster, D., Rosenstock, T. S., & Sanz-Cobena, A. (2016). Greenhouse gas emissions from natural ecosystems and agricultural lands in sub-Saharan Africa: Synthesis of available data and suggestions for further research. *Biogeosciences*, *13*(16), 4789–4809. https://doi.org/10.5194/bg-13-4789-2016

Kindermann, L., Sandhage-Hofmann, A., Amelung, W., Börner, J., Dobler, M., Fabiano, E., Meyer, M., & Linstädter, A. (2025). Natural and Human Disturbances Have Non-Linear Effects on Whole-Ecosystem Carbon Storage in an African Savanna. *Global Change Biology*, *31*(4), e70163. https://doi.org/10.1111/gcb.70163

Konovalov, I. B., Golovushkin, N. A., & Mareev, E. A. (2025). Using OCO-2 Observations to Constrain Regional CO2 Fluxes Estimated with the Vegetation, Photosynthesis and Respiration Model. *Remote Sensing*, *17*(2), 177. https://doi.org/10.3390/rs17020177

Lal, R. (2025). Managing Soil Health in Africa (MASHA) by Re-carbonization of Its Agroecosystems. *Egyptian Journal of Soil Science*, *65*(1), 301–320. https://doi.org/10.21608/ejss.2024.334426.1913

Lavallee, J. M., Soong, J. L., & Cotrufo, M. F. (2020). Conceptualizing soil organic matter into particulate and mineral-associated forms to address global change in the 21st century. *Global Change Biology*, *26*(1), 261–273. https://doi.org/10.1111/gcb.14859

Lavenda, B. H. (2005a). Thermodynamics of an ideal generalized gas: I. Thermodynamic laws. *Naturwissenschaften*, *92*(11), 516–522. https://doi.org/10.1007/s00114-005-0037-2

Lavenda, B. H. (2005b). Thermodynamics of an ideal generalized gas: II. *Naturwissenschaften*, *92*(11), 523–531. https://doi.org/10.1007/s00114-005-0038-1

Le Quéré, C., Moriarty, R., Andrew, R. M., Peters, G. P., Ciais, P., Friedlingstein, P., Jones, S. D., Sitch, S., Tans, P., Arneth, A., Boden, T. A., Bopp, L., Bozec, Y., Canadell, J. G., Chini, L. P., Chevallier, F., Cosca, C. E., Harris, I., Hoppema, M., … Zeng, N. (2015). Global carbon budget 2014. *Earth System Science Data*, *7*(1), 47–85. https://doi.org/10.5194/essd-7-47-2015

Leitner, S. M., Carbonell, V., Mhindu, R. L., Zhu, Y., Mutuo, P., Butterbach-Bahl, K., & Merbold, L. (2024). Greenhouse gas emissions from cattle enclosures in semi-arid sub-Saharan Africa: The case of a rangeland in South-Central Kenya. *Agriculture, Ecosystems & Environment*, *367*, 108980. https://doi.org/10.1016/j.agee.2024.108980

Leitner, S., Ring, D., Wanyama, G. N., Korir, D., Pelster, D. E., Goopy, J. P., Butterbach-Bahl, K., & Merbold, L. (2021). Effect of feeding practices and manure quality on CH4 and N2O emissions from uncovered cattle manure heaps in Kenya. *Waste Management*, *126*, 209–220. https://doi.org/10.1016/j.wasman.2021.03.014

Li, Z., Zhang, Q., Du, K., Liu, S., Li, F., Chen, G., Peng, J., & Bai, Y. (2025). Nitrous oxide emissions from rivers in agricultural area under different rainfall scenarios: The effect of typhoons in intensifying the release. *Environmental Pollution*, *376*, 126449. https://doi.org/10.1016/j.envpol.2025.126449

Liao, J., Zheng, W., Liao, Q., & Lu, S. (2024). Global latitudinal patterns in forest ecosystem nitrous oxide emissions are related to hydroclimate. *Npj Climate and Atmospheric Science*, *7*(1), 1–10. https://doi.org/10.1038/s41612-024-00737-8

Liu, Deng, Z., Davis, S. J., Giron, C., & Ciais, P. (2022). Monitoring global carbon emissions in 2021. *Nature Reviews Earth & Environment*, *3*(4), Article 4. https://doi.org/10.1038/s43017-022-00285-w

Liu, M., Lin, H., & Li, J. (2025). Are there links between nutrient inputs and the response of microbial carbon use efficiency or soil organic carbon? A meta-analysis. *Soil Biology and Biochemistry*, *201*, 109656. https://doi.org/10.1016/j.soilbio.2024.109656

Livingston, G. P., Hutchinson, G. L., & Spartalian, K. (2005). Diffusion theory improves chamber-based measurements of trace gas emissions. *Geophysical Research Letters*, *32*(24). https://doi.org/10.1029/2005GL024744

Llonch, P., Haskell, M. J., Dewhurst, R. J., & Turner, S. P. (2017). Current available strategies to mitigate greenhouse gas emissions in livestock systems: An animal welfare perspective. *Animal*, *11*(2), 274–284. https://doi.org/10.1017/S1751731116001440

Lu, T., Wang, X., Xu, M., Yu, Z., Luo, Y., & Smith, P. (2020). Dynamics of pedogenic carbonate in the cropland of the North China Plain: Influences of intensive cropping and salinization. *Agriculture, Ecosystems & Environment*, *292*, 106820. https://doi.org/10.1016/j.agee.2020.106820

Masese, F. O., Salcedo-Borda, J. S., Gettel, G. M., Irvine, K., & McClain, M. E. (2017). Influence of catchment land use and seasonality on dissolved organic matter composition and ecosystem metabolism in headwater streams of a Kenyan river. *Biogeochemistry*, *132*(1–2), 1–22. https://doi.org/10.1007/s10533-016-0269-6

McNunn, G., Karlen, D. L., Salas, W., Rice, C. W., Mueller, S., Muth, D., & Seale, J. W. (2020). Climate smart agriculture opportunities for mitigating soil greenhouse gas emissions across the U.S. Corn-Belt. *Journal of Cleaner Production*, *268*, 122240. https://doi.org/10.1016/j.jclepro.2020.122240

Mesele, S. A., Mechri, M., Okon, M. A., Isimikalu, T. O., Wassif, O. M., Asamoah, E., Ahmad, H. A., Moepi, P. I., Gabasawa, A. I., Bello, S. K., Ayamba, B. E., Owonubi, A., Olayiwola, V. A., Soremi, P. A. S., & Khurshid, C. (2025). Current Problems Leading to Soil Degradation in Africa: Raising Awareness and Finding Potential Solutions. *European Journal of Soil Science*, *76*(1), e70069. https://doi.org/10.1111/ejss.70069

Metz, E.-M., Vardag, S. N., Basu, S., Jung, M., & Butz, A. (2025). Seasonal and interannual variability in CO_2 fluxes in southern Africa seen by GOSAT. *Biogeosciences*, *22*(2), 555–584. https://doi.org/10.5194/bg-22-555-2025

MoALF. (2016). *Climate Risk Profile for Taita Taveta. Kenya County Climate Risk Profile Series.*

Molina, J. A., Martín-Sanz, J. P., Casermeiro, M. Á., & Quintana, J. R. (2024). Soil depth and vegetation type influence ecosystem functions in urban greenspaces. *Applied Soil Ecology*, *194*, 105209. https://doi.org/10.1016/j.apsoil.2023.105209

Morgan, J. A., Follett, R. F., Allen, L. H., Del Grosso, S., Derner, J. D., Dijkstra, F., Franzluebbers, A., Fry, R., Paustian, K., & Schoeneberger, M. M. (2010). Carbon sequestration in agricultural lands of the United States. *Journal of Soil and Water Conservation*, *65*(1), 6A-13A. https://doi.org/10.2489/jswc.65.1.6A

Muñoz-Rojas, M., Jordán, A., Zavala, L. M., De la Rosa, D., Abd-Elmabod, S. K., & Anaya-Romero, M. (2015). Impact of Land Use and Land Cover Changes on Organic Carbon Stocks in Mediterranean Soils (1956–2007). *Land Degradation & Development*, *26*(2), 168–179. https://doi.org/10.1002/ldr.2194

Musafiri, C. M., Macharia, J. M., Kiboi, M. N., Ng'etich, O. K., Shisanya, C. A., Okeyo, J. M., Mugendi, D. N., Okwuosa, E. A., & Ngetich, F. K. (2020). Soil greenhouse gas fluxes from maize cropping system under different soil fertility management technologies in Kenya. *Agriculture, Ecosystems & Environment*, *301*, 107064. https://doi.org/10.1016/j.agee.2020.107064

Mwanake, R. m., Gettel, G. m., Aho, K. s., Namwaya, D. w., Masese, F. o., Butterbach-Bahl, K., & Raymond, P. a. (2019). Land Use, Not Stream Order, Controls N2O Concentration and Flux in the Upper Mara River Basin, Kenya. *Journal of Geophysical Research: Biogeosciences*, *124*(11), 3491–3506. https://doi.org/10.1029/2019JG005063

Nayak, D., Saetnan, E., Cheng, K., Wang, W., Koslowski, F., Cheng, Y.-F., Zhu, W. Y., Wang, J.-K., Liu, J.-X., Moran, D., Yan, X., Cardenas, L., Newbold, J., Pan, G., Lu, Y., & Smith, P. (2015). Management opportunities to mitigate greenhouse gas emissions from Chinese agriculture. *Agriculture, Ecosystems & Environment*, *209*, 108–124. https://doi.org/10.1016/j.agee.2015.04.035

Ndung'u, P. W., Bebe, B. O., Ondiek, J. O., Butterbach-Bahl, K., Merbold, L., & Goopy, J. P. (2020). Corrigendum to: Improved region-specific emission factors for enteric methane emissions from cattle in smallholder mixed crop: livestock systems of Nandi County, Kenya. *Animal Production Science*, *60*(13), 1668. https://doi.org/10.1071/AN17809_CO

Nganga, W. B., Ng'etich, K. O., Macharia, M. J., Kiboi, N. M., Adamtey, N., & Ngetich, K. F. (2020). Multi-influencing-factors' evaluation for organic-based soil fertility technologies out-scaling in Upper Tana Catchment in Kenya. *Scientific African*, *7*, e00231. https://doi.org/10.1016/j.sciaf.2019.e00231

Obeka, B. M., Wacker, E., Shauri, H., & de Vries, W. T. (2024). Influence of Land Ownership Security on Land Use Changes in Mwatate Sub-County, Taita Taveta County, Kenya. *Tropical Conservation Science*, *17*, 19400829241247798. https://doi.org/10.1177/19400829241247798

Okalebo, J. R., Gathua, K. W., & Woomer, P. (2002). *Laboratory Methods of Soil and Plant Tissue Analysis*. 131.

Olson, K., Ebelhar, S. A., & Lang, J. M. (2014). Long-Term Effects of Cover Crops on Crop Yields, Soil Organic Carbon Stocks and Sequestration. *Open Journal of Soil Science, 2014*. https://doi.org/10.4236/ojss.2014.48030

Olson, K. R., & Al-Kaisi, M. M. (2015). The importance of soil sampling depth for accurate account of soil organic carbon sequestration, storage, retention and loss. *CATENA, 125*, 33–37. https://doi.org/10.1016/j.catena.2014.10.004

Owade, C. A. A., Kaiser, H., Simiyu, G. M., Owuor, G., Sicharani, E., Gettel, G. M., & Masese, F. O. (2025). Macroinvertebrate functional responses to human disturbance and flow cessation in Afromontane-savannah rivers. *Ecohydrology & Hydrobiology*, 100649. https://doi.org/10.1016/j.ecohyd.2025.100649

Paustian, K., Lehmann, J., Ogle, S., Reay, D., Robertson, G. P., & Smith, P. (2016). Climate-smart soils. *Nature*, *532*(7597), 49–57. https://doi.org/10.1038/nature17174

Pellikka, Clark, B. J. F., Gosa, A. G., Himberg, N., Hurskainen, P., Maeda, E., Mwang'ombe, J., Omoro, L. M. A., & Siljander, M. (2013a). Chapter 13—Agricultural Expansion and Its Consequences in the Taita Hills, Kenya. In P. Paron, D. O. Olago, & C. T. Omuto (Eds.), *Developments in Earth Surface Processes* (Vol. 16, pp. 165–179). Elsevier. https://doi.org/10.1016/B978-0-444-59559-1.00013-X

Pellikka, P. K. E., Clark, B. J. F., Gosa, A. G., Himberg, N., Hurskainen, P., Maeda, E., Mwang'ombe, J., Omoro, L. M. A., & Siljander, M. (2013b). Chapter 13—Agricultural Expansion and Its Consequences in the Taita Hills, Kenya. In P. Paron, D. O. Olago, & C. T. Omuto (Eds.), *Developments in Earth Surface Processes* (Vol. 16, pp. 165–179). Elsevier. https://doi.org/10.1016/B978-0-444-59559-1.00013-X

Pellikka, P. K. E., Heikinheimo, V., Hietanen, J., Schäfer, E., Siljander, M., & Heiskanen, J. (2018a). Impact of land cover change on aboveground carbon stocks in Afromontane landscape in Kenya. *Applied Geography*, *94*, 178–189. https://doi.org/10.1016/j.apgeog.2018.03.017

Pellikka, P. K. E., Heikinheimo, V., Hietanen, J., Schäfer, E., Siljander, M., & Heiskanen, J. (2018b). Impact of land cover change on aboveground carbon stocks in Afromontane landscape in Kenya. *Applied Geography*, *94*, 178–189. https://doi.org/10.1016/j.apgeog.2018.03.017

Pulido, M., Schnabel, S., Lavado Contador, J. F., Lozano-Parra, J., & González, F. (2018). The Impact of Heavy Grazing on Soil Quality and Pasture Production in Rangelands of SW Spain: Soil Quality and Pasture Production in Rangelands of SW Spain. *Land Degradation & Development*, *29*(2), 219–230. https://doi.org/10.1002/ldr.2501

Raffeld, A. M., Bradford, M. A., Jackson, R. D., Rath, D., Sanford, G. R., Tautges, N., & Oldfield, E. E. (2024). The importance of accounting method and sampling depth to estimate changes in soil carbon stocks. *Carbon Balance and Management*, *19*(1), 2. https://doi.org/10.1186/s13021-024-00249-1

Rahman, M. M., Aravindakshan, S., Hoque, M. A., Rahman, M. A., Gulandaz, Md. A., Rahman, J., & Islam, Md. T. (2021). Conservation tillage (CT) for climate-smart sustainable intensification: Assessing the impact of CT on soil organic carbon accumulation, greenhouse gas emission and water footprint of wheat cultivation in Bangladesh. *Environmental and Sustainability Indicators*, *10*, 100106. https://doi.org/10.1016/j.indic.2021.100106

Rayne, N., & Aula, L. (2020). Livestock Manure and the Impacts on Soil Health: A Review. *Soil Systems*, *4*(4), Article 4. https://doi.org/10.3390/soilsystems4040064

Reisinger, A., & Clark, H. (2018). How much do direct livestock emissions actually contribute to global warming? *Global Change Biology*, *24*(4), 1749–1761. https://doi.org/10.1111/gcb.13975

Roger, C., & Belliethathan, S. (2016). Africa in the global climate change negotiations. *International Environmental Agreements: Politics, Law and Economics*, *16*(1), 91–108. https://doi.org/10.1007/s10784-014-9244-7

Rotich, H. K., Onwonga, R. N., Mbau, J. S., & Koech, O. K. (2020). *Projected Changes in Soil Organic Carbon Stocks over a 50-Year Period under Different Grazing Management Systems in Semi- Arid Grasslands of Kenya*. *10*(4), 13.

Rowland, M. M., Nielson, R. M., Bohnert, D. W., Endress, B. A., Wisdom, M. J., & Averett, J. P. (2025). Modeling Riparian Use by Cattle – Influence of Management, Season, and Weather. *Rangeland Ecology & Management*, *98*, 419–431. https://doi.org/10.1016/j.rama.2024.08.023

Rust, J., & Rust, T. (2013). Climate change and livestock production: A review with emphasis on Africa. *South African Journal of Animal Science*, *43*(3), 255. https://doi.org/10.4314/sajas.v43i3.3

Sainepo, B. M., Gachene, C. K., & Karuma, A. (2018). Assessment of soil organic carbon fractions and carbon management index under different land use types in Olesharo Catchment, Narok County, Kenya. *Carbon Balance and Management*, *13*(1), 4. https://doi.org/10.1186/s13021-018-0091-7

Sapkota, T. B., Aryal, J. P., Khatri-Chhetri, A., Shirsath, P. B., Arumugam, P., & Stirling, C. M. (2018). Identifying high-yield low-emission pathways for the cereal production in South Asia. *Mitigation and Adaptation Strategies for Global Change*, *23*(4), 621–641. https://doi.org/10.1007/s11027-017-9752-1

Sapkota, T. B., Khanam, F., Mathivanan, G. P., Vetter, S., Hussain, Sk. G., Pilat, A.-L., Shahrin, S., Hossain, Md. K., Sarker, N. R., & Krupnik, T. J. (2021). Quantifying opportunities for greenhouse gas emissions mitigation using big data from smallholder crop and livestock farmers across Bangladesh. *Science of The Total Environment*, *786*, 147344. https://doi.org/10.1016/j.scitotenv.2021.147344

Schuman, G. E., Janzen, H. H., & Herrick, J. E. (2002). Soil carbon dynamics and potential carbon sequestration by rangelands. *Environmental Pollution*, *116*(3), 391–396. https://doi.org/10.1016/S0269-7491(01)00215-9

Schweizer, S. A., Mueller, C. W., Höschen, C., Ivanov, P., & Kögel-Knabner, I. (2021). The role of clay content and mineral surface area for soil organic carbon storage in an arable toposequence. *Biogeochemistry*, *156*(3), 401–420. https://doi.org/10.1007/s10533-021-00850-3

Six, J., Guggenberger, G., Paustian, K., Haumaier, L., Elliott, E. T., & Zech, W. (2001). Sources and composition of soil organic matter fractions between and within soil aggregates. *European Journal of Soil Science*, *52*(4), 607–618. https://doi.org/10.1046/j.1365-2389.2001.00406.x

Slosson, J. R., Larsen, I. J., Winnick, M. J., Marmolejo-Cossío, J. M., & Williams, K. H. (2025). Linking Surface Processes, Solute Generation, and CO2 Budgets Across Lithological and Land Cover Gradients in Rocky Mountain Watersheds. *Water Resources Research*, *61*(4), e2023WR036850. https://doi.org/10.1029/2023WR036850

Smith, K. A., Ball, T., Conen, F., Dobbie, K. E., Massheder, J., & Rey, A. (2003a). Exchange of greenhouse gases between soil and atmosphere: Interactions of soil physical factors and biological processes. *European Journal of Soil Science*, *54*(4), 779–791. https://doi.org/10.1046/j.1351-0754.2003.0567.x

Smith, K. A., Ball, T., Conen, F., Dobbie, K. E., Massheder, J., & Rey, A. (2003b). Exchange of greenhouse gases between soil and atmosphere: Interactions of soil physical factors and biological processes. *European Journal of Soil Science*, *54*(4), 779–791. https://doi.org/10.1046/j.1351-0754.2003.0567.x

Smith, P., Soussana, J.-F., Angers, D., Schipper, L., Chenu, C., Rasse, D. P., Batjes, N. H., van Egmond, F., McNeill, S., Kuhnert, M., Arias-Navarro, C., Olesen, J. E., Chirinda, N., Fornara, D., Wollenberg, E., Álvaro-Fuentes, J., Sanz-Cobena, A., & Klumpp, K. (2020). How to measure, report and verify soil carbon change to realize the potential of soil carbon sequestration for atmospheric greenhouse gas removal. *Global Change Biology*, *26*(1), 219–241. https://doi.org/10.1111/gcb.14815

Symeon, G. K., Akamati, K., Dotas, V., Karatosidi, D., Bizelis, I., & Laliotis, G. P. (2025). Manure Management as a Potential Mitigation Tool to Eliminate Greenhouse Gas Emissions in Livestock Systems. *Sustainability*, *17*(2), Article 2. https://doi.org/10.3390/su17020586

Taita Taveta County Government. (2018). *Taita Taveta County Integrated Development Plan II 2018-2022*. https://www.taitataveta.go.ke/wp-content/uploads/2024/05/CIDP-2018-2022.pdf

Taita Taveta County Government. (2023). *Taita Taveta County Integrated Development Plan III 2023-2027*. https://www.taitataveta.go.ke/wp-content/uploads/2024/05/Taita-Taveta-CIDP-2023-27.pdf

Team, R. S. (2021). *RStudio: Integrated development environment for R*. https://cir.nii.ac.jp/crid/1370580232391041538

Tian, H., Xu, R., Canadell, J. G., Thompson, R. L., Winiwarter, W., Suntharalingam, P., Davidson, E. A., Ciais, P., Jackson, R. B., Janssens-Maenhout, G., Prather, M. J., Regnier, P., Pan, N., Pan, S., Peters, G. P., Shi, H., Tubiello, F. N., Zaehle, S., Zhou, F., … Yao, Y. (2020). A comprehensive quantification of global nitrous oxide sources and sinks. *Nature*, *586*(7828), 248–256. https://doi.org/10.1038/s41586-020-2780-0

Tiegs, S. D., Costello, D. M., Isken, M. W., Woodward, G., McIntyre, P. B., Gessner, M. O., Chauvet, E., Griffiths, N. A., Flecker, A. S., Acuña, V., Albariño, R., Allen, D. C., Alonso, C., Andino, P., Arango, C., Aroviita, J., Barbosa, M. V. M., Barmuta, L. A., Baxter, C. V., … Zwart, J. A. (2019). Global patterns and drivers of ecosystem functioning in rivers and riparian zones. *Science Advances*, *5*(1), eaav0486. https://doi.org/10.1126/sciadv.aav0486

Tubiello, F. N., Salvatore, M., Ferrara, A. F., House, J., Federici, S., Rossi, S., Biancalani, R., Condor Golec, R. D., Jacobs, H., Flammini, A., Prosperi, P., Cardenas-Galindo, P., Schmidhuber, J., Sanz Sanchez, M. J., Srivastava, N., & Smith, P. (2015). The Contribution of Agriculture, Forestry and other Land Use activities to Global Warming, 1990–2012. *Global Change Biology*, *21*(7), 2655–2660. https://doi.org/10.1111/gcb.12865

Tubiello, F. N., Salvatore, M., Golec, R. D. C., Ferrara, A., Rossi, S., Biancalani, R., Federici, S., Jacobs, H., & Flammini, A. (2014). *Agriculture, forestry and other land use emissions by sources and removals by sinks*. *2*, 87.

Tubiello, F., Salvatore, M., Golec, R., Ferrara, A., Rossi, S., Biancalani, R., Federici, S., Jacobs, H., & Flammini, A. (2014). *Agriculture, Forestry and Other Land Use Emissions by Sources and Removals by Sinks: 1990-2011 Analysis*. https://doi.org/10.13140/2.1.4143.4245

van Gestel, N., Shi, Z., van Groenigen, K. J., Osenberg, C. W., Andresen, L. C., Dukes, J. S., Hovenden, M. J., Luo, Y., Michelsen, A., Pendall, E., Reich, P. B., Schuur, E. A. G., & Hungate, B. A. (2018). Predicting soil carbon loss with warming. *Nature*, *554*(7693), E4–E5. https://doi.org/10.1038/nature25745

van Wijk, M. T., Merbold, L., Hammond, J., & Butterbach-Bahl, K. (2020). Improving Assessments of the Three Pillars of Climate Smart Agriculture: Current Achievements and Ideas for the Future. *Frontiers in Sustainable Food Systems*, *4*, 558483. https://doi.org/10.3389/fsufs.2020.558483

Vermeulen, S., Bossio, D., Lehmann, J., Luu, P., Paustian, K., Webb, C., Augé, F., Bacudo, I., Baedeker, T., Havemann, T., Jones, C., King, R., Reddy, M., Sunga, I., Von Unger, M., & Warnken, M. (2019). A global agenda for collective action on soil carbon. *Nature Sustainability*, *2*(1), 2–4. https://doi.org/10.1038/s41893-018-0212-z

Viaud, V. (2018). *Landscape-scale analysis of cropping system effects on soil quality in a context of crop-livestock farming*. 12.

Wachiye, S. (2022). *SOIL GREENHOUSE GAS EMISSIONS FROM DOMINANT LAND USE TYPES IN LOWLANDS AND HIGHLANDS OF SOUTHERN KENYA*. https://helda.helsinki.fi/handle/10138/343704

Wachiye, S., Merbold, L., Vesala, T., Rinne, J., Räsänen, M., Leitner, S., & Pellikka, P. (2020a). Soil greenhouse gas emissions under different land-use types in savanna ecosystems of Kenya. *Biogeosciences*, *17*(8), 2149–2167. https://doi.org/10.5194/bg-17-2149-2020

Wachiye, S., Merbold, L., Vesala, T., Rinne, J., Räsänen, M., Leitner, S., & Pellikka, P. (2020b). Soil greenhouse gas emissions under different land-use types in savanna ecosystems of Kenya. *Biogeosciences*, *17*(8), 2149–2167. https://doi.org/10.5194/bg-17-2149-2020

Wachiye, S., Pellikka, P., Rinne, J., Heiskanen, J., Abwanda, S., & Merbold, L. (2022). Effects of livestock and wildlife grazing intensity on soil carbon dioxide flux in the savanna grassland of Kenya. *Agriculture, Ecosystems & Environment*, *325*, 107713. https://doi.org/10.1016/j.agee.2021.107713

Waters, C. M., Orgill, S. E., Melville, G. J., Toole, I. D., & Smith, W. J. (2017). Management of Grazing Intensity in the Semi-Arid Rangelands of Southern Australia: Effects on Soil and Biodiversity. *Land Degradation & Development*, *28*(4), 1363–1375. https://doi.org/10.1002/ldr.2602

Watuma, B. M., Kipkoech, S., Melly, D. K., Ngumbau, V. M., Rono, P. C., Mutie, F. M., Mkala, E. M., Nzei, J. M., Mwachala, G., Gituru, R. W., Hu, G.-W., & Wang, Q.-F. (2022). An annotated checklist of the vascular plants of Taita Hills, Eastern Arc Mountain. *PhytoKeys*, *191*, 1–158. https://doi.org/10.3897/phytokeys.191.73714

Wei, X., Shao, M., Gale, W., & Li, L. (2015). Global pattern of soil carbon losses due to the conversion of forests to agricultural land. *Scientific Reports*, *4*(1), 4062. https://doi.org/10.1038/srep04062

Wiesmeier, M., Urbanski, L., Hobley, E., Lang, B., von Lützow, M., Marin-Spiotta, E., van Wesemael, B., Rabot, E., Ließ, M., Garcia-Franco, N., Wollschläger, U., Vogel, H.-J., & Kögel-Knabner, I. (2019). Soil organic carbon storage as a key function of soils—A review of drivers and indicators at various scales. *Geoderma*, *333*, 149–162. https://doi.org/10.1016/j.geoderma.2018.07.026

Winkler, K., Fuchs, R., Rounsevell, M., & Herold, M. (2021). Global land use changes are four times greater than previously estimated. *Nature Communications*, *12*(1), Article 1. https://doi.org/10.1038/s41467-021-22702-2

Wolka, K., Biazin, B., Martinsen, V., & Mulder, J. (2021). Soil organic carbon and associated soil properties in Enset (Ensete ventricosum Welw. Cheesman)-based homegardens in Ethiopia. *Soil and Tillage Research*, *205*, 104791. https://doi.org/10.1016/j.still.2020.104791

Wollenberg, E., Richards, M., Smith, P., Havlík, P., Obersteiner, M., Tubiello, F. N., Herold, M., Gerber, P., Carter, S., Reisinger, A., van Vuuren, D. P., Dickie, A., Neufeldt, H., Sander, B. O., Wassmann, R., Sommer, R., Amonette, J. E., Falcucci, A., Herrero, M., … Campbell, B. M. (2016). Reducing emissions from agriculture to meet the 2 ℃ target. *Global Change Biology*, *22*(12), 3859–3864. https://doi.org/10.1111/gcb.13340

Xiao, D., Deng, L., Kim, D.-G., Huang, C., & Tian, K. (2019). Carbon budgets of wetland ecosystems in China. *Global Change Biology*, *25*(6), 2061–2076. https://doi.org/10.1111/gcb.14621

Yan, T., Kremenetska, Y., Zhang, B., He, S., Wang, X., Yu, Z., Hu, Q., Liang, X., Fu, M., & Wang, Z. (2022). The Relationship between Soil Particle Size Fractions, Associated Carbon Distribution and Physicochemical Properties of Historical Land-Use Types in Newly Formed Reservoir Buffer Strips. *Sustainability*, *14*(14), Article 14. https://doi.org/10.3390/su14148448

Yang, Y., Gunina, A., Cheng, H., Liu, L., Wang, B., Dou, Y., Wang, Y., Liang, C., An, S., & Chang, S. X. (2025). Unlocking Mechanisms for Soil Organic Matter Accumulation: Carbon Use Efficiency and Microbial Necromass as the Keys. *Global Change Biology*, *31*(1), e70033. https://doi.org/10.1111/gcb.70033

Yuan, J., Yao, Y., Guan, Y., Sadiq, M., Li, J., Liu, S., Lu, Y., Xu, G., Du, M., Li, G., & Yan, L. (2024). Effects of land use patterns on soil properties and nitrous oxide flux on a semi-arid environmental conditions of Loess Plateau China. *Global Ecology and Conservation*, *51*, e02899. https://doi.org/10.1016/j.gecco.2024.e02899

Zaman, M., Kleineidam, K., Bakken, L., Berendt, J., Bracken, C., Butterbach-Bahl, K., Cai, Z., Chang, S. X., Clough, T., Dawar, K., Ding, W. X., Dörsch, P., dos Reis Martins, M., Eckhardt, C., Fiedler, S., Frosch, T., Goopy, J., Görres, C.-M., Gupta, A., … Müller, C. (2021). Climate-Smart Agriculture Practices for Mitigating Greenhouse Gas Emissions. In M. Zaman, L. Heng, & C. Müller (Eds.), *Measuring Emission of Agricultural Greenhouse Gases and Developing Mitigation Options using Nuclear and Related Techniques: Applications of Nuclear Techniques for GHGs* (pp. 303–328). Springer International Publishing. https://doi.org/10.1007/978-3-030-55396-8_8

Zaman, M., Lee, H., & Christoff, M. (2021, January 30). *Methodology for Measuring Greenhouse Gas Emissions from Agricultural Soils Using Non-isotopic Techniques | SpringerLink*. https://link.springer.com/chapter/10.1007/978-3-030-55396-8_2

Zandalinas, S. I., Fritschi, F. B., & Mittler, R. (2021). Global Warming, Climate Change, and Environmental Pollution: Recipe for a Multifactorial Stress Combination Disaster. *Trends in Plant Science*, *26*(6), 588–599. https://doi.org/10.1016/j.tplants.2021.02.011

Zhu, Y., Merbold, L., Leitner, S., Xia, L., Pelster, D. E., Diaz-Pines, E., Abwanda, S., Mutuo, P. M., & Butterbach-Bahl, K. (2020). Influence of soil properties on N2O and CO2 emissions from excreta deposited on tropical pastures in Kenya. *Soil Biology and Biochemistry*, *140*, 107636.https://doi.org/10.1016/j.soilbio.2019.107636

Zuo, X., Zhang, J., Lv, P., Wang, S., Yang, Y., Yue, X., Zhou, X., Li, Y., Chen, M., Lian, J., Qu, H., Liu, L., & Ma, X. (2018). Effects of plant functional diversity induced by grazing and soil properties on above- and belowground biomass in a semiarid grassland. *Ecological Indicators*, *93*, 555–561. https://doi.org/10.1016/j.ecolind.2018.05.032

APPENDICES

Appendix I: The distribution of study sites for this study. The vast Wundanyi Catchment had more sites in the sampling campaigns compared to the Bura Catchment. The pie chart shows the distribution of sites by livestock densities in the two catchments.

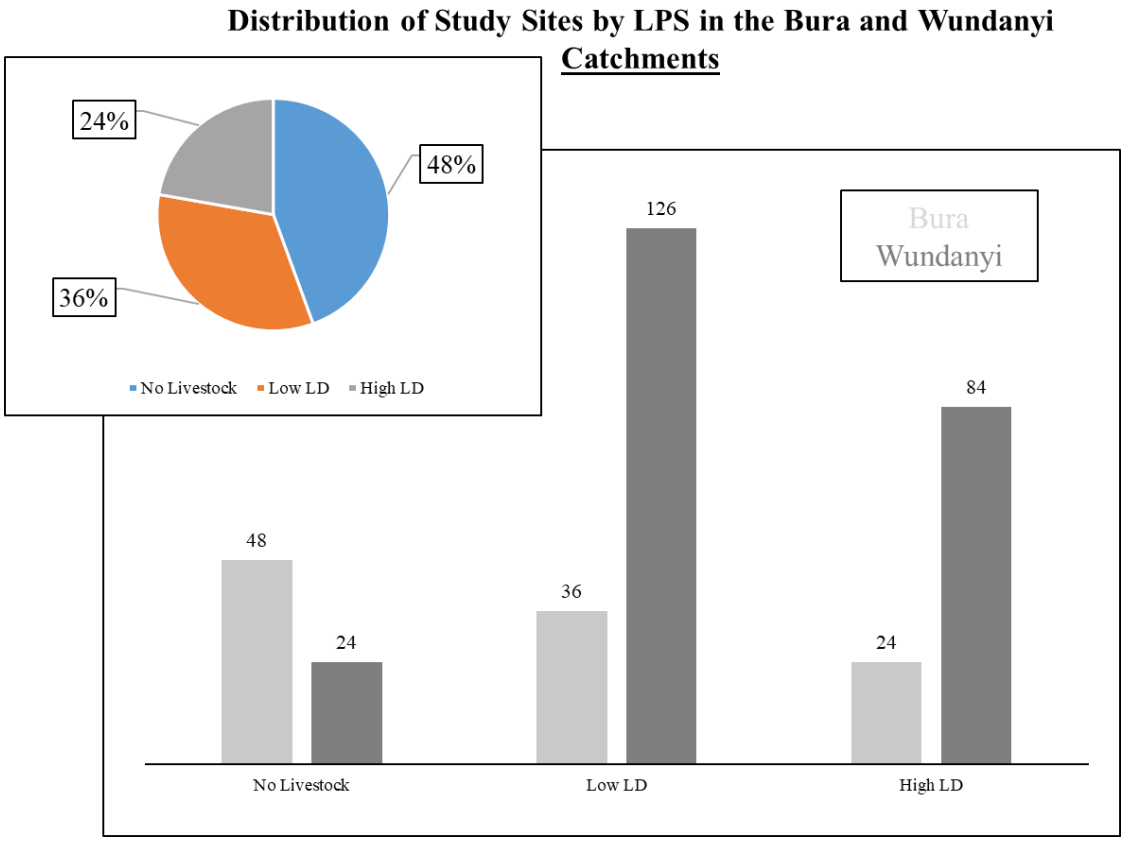

Appendix II: Summary statistics for the GHG fluxes in the Bura and Wundanyi Catchments. The Wundanyi Catchment generally recorded higher values for the six (6) summary categories.

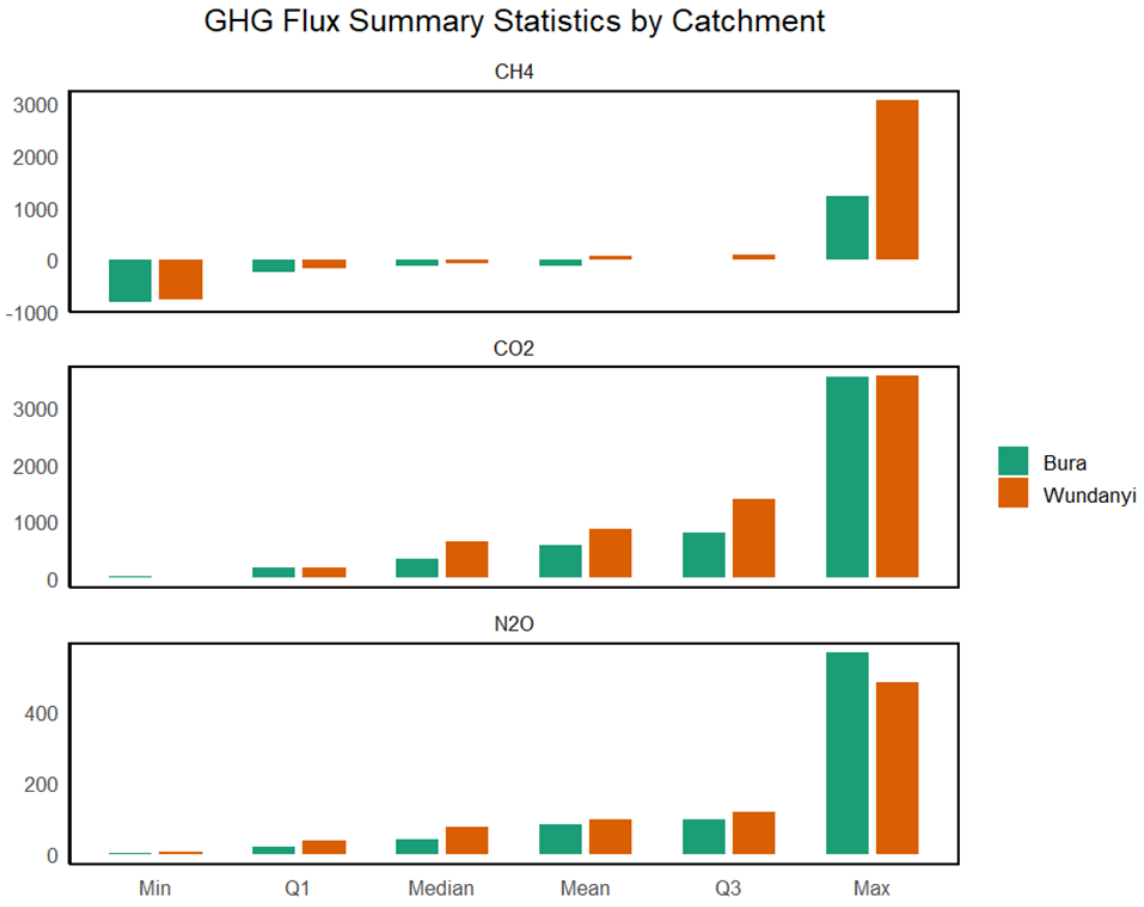

Appendix III: Means (EMM) for GHG fluxes in the Bura Catchment; an integrated agroecosystem approach.

BURA MIDLAND								
Topography	**GHG**	**LPS**	**Season**	**Mean**	**SE**	**Min**	**Max**	**n**
Midland	CH_4_Flux	ZLD	Dry I	-69.3072	93.70759	-235.994	88.2312	3
Mean				**-69.307**	**93.708**	**-235.994**	**88.231**	
Midland	CH_4_Flux	LLD	Dry I	-132.269	24.24092	-259.666	-40.716	9
Midland	CH_4_Flux	LLD	Dry II	-248.57	99.46893	-663.84	-61.752	6
Midland	CH_4_Flux	LLD	Wet I	-0.5768	31.95068	-113.954	82.3368	6
Midland	CH_4_Flux	LLD	Wet II	-248.69	265.0219	-801.478	966.7344	6

Mean				**-157.526**	**105.171**	**-459.734**	**236.651**	
Midland	CH_4_Flux	HLD	Dry I	-68.742	34.8804	-103.622	-33.8616	2
Midland	CH_4_Flux	HLD	Dry II	-175.619	100.3923	-823.082	531.5412	12
Midland	CH_4_Flux	HLD	Wet I	91.74573	119.1702	-310.699	1214.623	12
Midland	CH_4_Flux	HLD	Wet II	-252.971	92.61653	-820.21	223.6032	11
Mean				**-101.397**	**86.765**	**-514.403**	**483.977**	
Midland	CO_2_Flux	ZLD	Dry I	119.7888	40.14651	40.9344	172.32	3
Mean				**119.789**	**40.147**	**40.934**	**172.320**	
Midland	CO_2_Flux	LLD	Dry I	568.948	145.8744	145.428	1539.29	9
Midland	CO_2_Flux	LLD	Dry II	239.6848	65.15119	31.6608	494.5536	6
Midland	CO_2_Flux	LLD	Wet I	175.8772	43.25466	57.8232	346.9224	6
Midland	CO_2_Flux	LLD	Wet II	347.2776	77.99296	114.2064	653.4576	6
Mean				**332.947**	**83.068**	**87.280**	**758.556**	
Midland	CO_2_Flux	HLD	Dry I	1296.724	471.9276	824.796	1768.651	2
Midland	CO_2_Flux	HLD	Dry II	678.6423	203.257	61.1856	2440.889	11
Midland	CO_2_Flux	HLD	Wet I	350.0366	92.09801	71.7504	1230.701	12
Midland	CO_2_Flux	HLD	Wet II	328.1959	65.85287	63.0000	835.9536	11
Mean				**663.3996**	**208.2839**	**255.183**	**1569.049**	
			BURA UPLAND					
Upland	CH_4_Flux	ZLD	Dry II	-204.998	72.10546	-349.118	-128.522	3
Upland	CH_4_Flux	ZLD	Wet I	-86.5904	17.57101	-108.902	-51.9216	3
Upland	CH_4_Flux	ZLD	Wet II	-164.74	65.91194	-290.206	-66.9792	3
Mean				**-152.109**	**51.863**	**-249.409**	**-82.474**	
Upland	CH_4_Flux	LLD	Dry I	-345.189	197.7052	-740.412	-137.036	3
Upland	CH_4_Flux	LLD	Dry II	-215.401	41.68096	-299.362	-87.348	5
Upland	CH_4_Flux	LLD	Wet I	43.53453	96.53299	-137.036	461.8968	6
Upland	CH_4_Flux	LLD	Wet II	-160.038	30.49641	-311.026	-110.222	6
Mean				**-169.273**	**91.604**	**-371.959**	**31.823**	
Upland	CH_4_Flux	HLD	Dry I	-256.632	49.94778	-396.161	-70.2312	6
Mean				**-173.757**	**71.49396**	**-329.028**	**-23.7955**	
Upland	CO_2_Flux	ZLD	Dry II	1213.474	553.5672	263.7432	2181.106	3
Upland	CO_2_Flux	ZLD	Wet I	599.6496	547.3184	37.848	1694.158	3
Upland	CO_2_Flux	ZLD	Wet II	557.3096	326.4055	209.6856	1209.65	3
Mean				**790.144**	**475.764**	**170.426**	**1694.971**	
Upland	CO_2_Flux	LLD	Dry I	443.2768	322.2346	18.6288	1075.435	3
Upland	CO_2_Flux	LLD	Dry II	849.3202	203.3686	261.7896	1310.033	5
Upland	CO_2_Flux	LLD	Wet I	736.4392	178.2469	187.3584	1302.305	6
Upland	CO_2_Flux	LLD	Wet II	480.5204	207.3426	173.532	1504.351	6
Mean				**627.389**	**227.798**	**160.327**	**1298.031**	
Upland	CO_2_Flux	HLD	Dry I	961.6892	199.1965	254.484	1592.806	6
Mean				730.2098	317.21	175.8837	1483.73	
Midland	N_2O_Flux	ZLD	Dry I	61.6088	14.80967	39.336	89.6544	3
Mean				**584.503**	**177.072**	**156.568**	**1055.397**	

Midland	N_2O_Flux	LLD	Dry I	57.0712	21.90802	7.8648	222.228	9
Midland	N_2O_Flux	LLD	Dry II	69.34	35.43991	4.716	221.9256	6
Midland	N_2O_Flux	LLD	Wet I	82.7644	23.23989	21.168	175.6176	6
Midland	N_2O_Flux	LLD	Wet II	198.8272	34.75931	52.0656	316.4496	6
Mean				**102.001**	**28.837**	**21.454**	**234.055**	
Midland	N_2O_Flux	HLD	Dry I	322.4088	162.0672	160.3416	484.476	2
Midland	N_2O_Flux	HLD	Dry II	98.8546	31.40773	13.836	407.6496	12
Midland	N_2O_Flux	HLD	Wet I	80.9348	20.9646	16.1592	263.568	12
Midland	N_2O_Flux	HLD	Wet II	121.4852	24.87268	8.7744	275.9856	11
Mean				**155.921**	**59.828**	**49.778**	**357.920**	
Upland	N_2O_Flux	ZLD	Dry II	54.4728	24.20918	28.0392	102.8208	3
Upland	N_2O_Flux	ZLD	Wet I	84.9456	20.99442	43.4976	111.4872	3
Upland	N_2O_Flux	ZLD	Wet II	24.9016	12.58386	3.9912	47.4864	3
Mean				**54.773**	**19.262**	**25.176**	**87.265**	
Upland	N_2O_Flux	LLD	Dry I	76.5048	19.14606	39.6912	104.0376	3
Upland	N_2O_Flux	LLD	Dry II	39.56064	8.781183	4.7304	51.3264	5
Upland	N_2O_Flux	LLD	Wet I	79.3172	30.33267	8.5416	209.7984	6
Upland	N_2O_Flux	LLD	Wet II	136.1812	33.21895	35.8824	246.132	6
Mean				**82.891**	**22.870**	**22.211**	**152.824**	
Upland	N_2O_Flux	HLD	Dry I	109.1064	20.76316	40.3416	196.4016	6
Mean				**109.106**	**20.763**	**40.342**	**196.402**	

Appendix IV: Means (EMM) for GHG fluxes in the Wundanyi Catchment; an integrated agroecosystem approach.

WUNDANYI LOWLAND								
Topography	**GHG**	**LPS**	**Season**	**Mean**	**SE**	**Min**	**Max**	**n**
Lowland	CH_4_Flux	ZLD	Dry I	-50.317	64.978	-121.505	79.435	3
Lowland	CH_4_Flux	ZLD	Dry II	-313.103	65.724	-441.218	-223.577	3
Lowland	CH_4_Flux	ZLD	Wet I	-105.644	17.557	-131.316	-72.060	3
Lowland	CH_4_Flux	ZLD	Wet II	-319.955	96.048	-502.159	-176.155	3
Mean				**-197.255**	**61.077**	**-299.050**	**-98.089**	
Lowland	CO_2_Flux	ZLD	Dry I	218.15	65.49	87.52	291.79	3
Lowland	CO_2_Flux	ZLD	Dry II	845.95	334.64	176.66	1181.16	3
Lowland	CO_2_Flux	ZLD	Wet I	1899.03	402.78	1100.40	2389.62	3
Lowland	CO_2_Flux	ZLD	Wet II	1053.02	140.23	816.33	1301.65	3
Mean				**1004.038**	**235.785**	**545.227**	**1291.054**	
Lowland	N_2O_Flux	ZLD	Dry I	33.874	7.337	22.577	47.633	3
Lowland	N_2O_Flux	ZLD	Dry II	38.525	5.421	27.684	44.102	3
Lowland	N_2O_Flux	ZLD	Wet I	52.862	7.075	39.355	63.269	3
Lowland	N_2O_Flux	ZLD	Wet II	286.962	68.228	153.439	378.094	3
Mean				**103.056**	**22.015**	**60.764**	**133.274**	

Lowland	CH_4_Flux	LLD	Dry I	-313.056	137.323	-784.390	78.887	6
Lowland	CH_4_Flux	LLD	Dry II	394.740	354.654	-276.019	2075.057	6
Lowland	CH_4_Flux	LLD	Wet I	122.838	21.902	45.096	179.890	6
Lowland	CH_4_Flux	LLD	Wet II	-62.972	175.850	-623.477	562.322	6
Mean				**35.387**	**172.432**	**-409.697**	**724.039**	
Lowland	CO_2_Flux	LLD	Dry I	314.511	138.967	36.797	988.121	6
Lowland	CO_2_Flux	LLD	Dry II	435.048	126.916	137.407	787.488	6
Lowland	CO_2_Flux	LLD	Wet I	458.389	179.968	101.498	1166.326	6
Lowland	CO_2_Flux	LLD	Wet II	368.852	210.258	41.515	1397.278	6
Mean				**394.200**	**164.027**	**79.304**	**1084.803**	
Lowland	N_2O_Flux	LLD	Dry I	33.203	13.373	9.691	97.459	6
Lowland	N_2O_Flux	LLD	Dry II	52.538	13.865	12.506	102.468	6
Lowland	N_2O_Flux	LLD	Wet I	50.906	30.090	3.941	196.219	6
Lowland	N_2O_Flux	LLD	Wet II	151.101	64.645	12.710	345.785	6
Mean				**71.937**	**30.493**	**9.712**	**185.483**	
Lowland	CH_4_Flux	HLD	Dry I	12.96	41.62	-199.19	720.26	23
Lowland	CH_4_Flux	HLD	Dry II	138.97	127.11	-497.68	2555.53	30
Lowland	CH_4_Flux	HLD	Wet I	331.62	136.54	-227.81	2857.55	28
Lowland	CH_4_Flux	HLD	Wet II	99.48	132.62	-718.38	2847.82	26
Mean				**145.757**	**109.474**	**-410.764**	**2245.290**	
Lowland	CO_2_Flux	HLD	Dry I	572.130	144.861	76.560	2998.726	23
Lowland	CO_2_Flux	HLD	Dry II	864.366	181.358	16.051	3474.197	30
Lowland	CO_2_Flux	HLD	Wet I	861.185	202.199	12.288	3550.445	28
Lowland	CO_2_Flux	HLD	Wet II	812.088	168.629	41.479	3232.061	26
Mean				**777.442**	**174.262**	**36.595**	**3313.857**	
Lowland	N_2O_Flux	HLD	Dry I	39.973	7.626	3.605	136.877	23
Lowland	N_2O_Flux	HLD	Dry II	65.489	19.116	4.046	512.513	30
Lowland	N_2O_Flux	HLD	Wet I	82.172	20.394	12.550	418.567	28
Lowland	N_2O_Flux	HLD	Wet II	183.256	31.297	5.861	570.149	26
Mean				**92.722**	**19.608**	**6.515**	**409.526**	
WUNDANYI MIDLAND								
Midland	CH_4_Flux	HLD	Dry I	302.513	326.816	-243.876	1914.845	6
Mean				**302.513**	**326.816**	**-243.876**	**1914.84**	
Midland	CH_4_Flux	LLD	Dry I	-104.967	10.719	-125.774	-90.096	3
Midland	CH_4_Flux	LLD	Dry II	-129.232	45.048	-219.986	80.827	6
Midland	CH_4_Flux	LLD	Wet I	772.108	502.337	26.911	3064.529	6
Mean				**179.30**	**186.034**	**-106.28**	**1018.42**	
Midland	CH_4_Flux	ZLD	Dry I	-115.357	22.251	-217.493	-73.603	6
Midland	CH_4_Flux	ZLD	Dry II	-190.514	35.352	-355.682	-121.435	6
Midland	CH_4_Flux	ZLD	Wet I	35.788	66.746	-128.098	308.309	6
Midland	CH_4_Flux	ZLD	Wet II	188.486	178.170	-104.755	1064.587	6
Mean				**-20.399**	**75.630**	**-201.507**	**294.464**	
Midland	CO_2_Flux	HLD	Dry I	1038.811	300.431	66.259	1815.278	6

Midland	CO_2_Flux	LLD	Dry I	318.426	224.781	67.114	766.898	3
Midland	CO_2_Flux	LLD	Dry II	893.818	353.965	29.258	1952.282	6
Midland	CO_2_Flux	LLD	Wet I	536.019	163.687	153.941	1169.508	6
Mean				**696.768**	**260.716**	**79.143**	**1425.992**	
Midland	CO_2_Flux	ZLD	Dry I	804.268	254.501	118.361	1977.806	6
Midland	CO_2_Flux	ZLD	Dry II	885.734	209.385	66.360	1432.694	6
Midland	CO_2_Flux	ZLD	Wet I	1070.271	347.359	44.256	2367.158	6
Midland	CO_2_Flux	ZLD	Wet II	1253.064	247.824	201.026	1976.906	6
Mean				**1003.334**	**264.767**	**107.501**	**1938.641**	
Midland	N_2O_Flux	HLD	Dry I	128.296	37.498	46.325	283.085	6
Mean				**128.296**	**37.498**	**46.325**	**283.085**	
Midland	N_2O_Flux	LLD	Dry I	18.369	11.391	4.606	40.973	3
Midland	N_2O_Flux	LLD	Dry II	17.798	6.051	3.158	37.462	6
Midland	N_2O_Flux	LLD	Wet I	48.190	23.445	14.153	163.186	6
Mean				**28.119**	**13.629**	**7.306**	**80.540**	
Midland	N_2O_Flux	ZLD	Dry I	28.670	4.202	20.906	48.638	6
Midland	N_2O_Flux	ZLD	Dry II	22.357	6.959	4.399	52.697	6
Midland	N_2O_Flux	ZLD	Wet I	69.243	17.874	24.979	112.054	6
Midland	N_2O_Flux	ZLD	Wet II	119.522	28.121	39.521	189.559	6
Mean				**59.948**	**14.289**	**22.451**	**100.737**	
		WUNDANYI UPLAND						
Upland	CH_4_Flux	LLD	Dry I	-72.129	69.010	-176.875	58.080	3
Upland	CH_4_Flux	ZLD	Dry I	-201.382	69.585	-592.771	40.207	9
Upland	CH_4_Flux	ZLD	Dry II	116.307	336.545	-532.745	2770.176	9
Upland	CH_4_Flux	ZLD	Wet I	42.672	30.094	-188.503	113.472	9
Upland	CH_4_Flux	ZLD	Wet II	-131.536	63.613	-502.464	78.887	9
Mean				**-49.214**	**113.769**	**-398.672**	**612.164**	
Upland	CO_2_Flux	LLD	Dry I	1057.98	529.02	348.78	2092.56	3
Upland	CO_2_Flux	ZLD	Dry I	922.34	173.05	160.48	1629.47	9
Upland	CO_2_Flux	ZLD	Dry II	1259.47	231.41	399.79	2224.98	9
Upland	CO_2_Flux	ZLD	Wet I	1107.86	134.98	626.61	1922.70	9
Upland	CO_2_Flux	ZLD	Wet II	1298.25	297.59	192.04	2923.40	9
Mean				**1129.179**	**273.2109**	**345.54**	**2158.622**	
Upland	N_2O_Flux	LLD	Dry I	63.386	26.029	28.128	114.185	3
Upland	N_2O_Flux	ZLD	Dry I	47.837	19.982	6.876	201.098	9
Upland	N_2O_Flux	ZLD	Dry II	56.800	22.252	4.186	176.868	9
Upland	N_2O_Flux	ZLD	Wet I	112.820	57.755	17.059	566.371	9
Upland	N_2O_Flux	ZLD	Wet II	90.871	27.832	23.350	274.015	9
Mean				**74.343**	**30.770**	**15.920**	**266.508**	

Appendix V: Pictorial presentations

Plate II: Human influence on riparian lands in the Wundanyi Upland zone. Plate A shows agricultural interventions in crop production and forestry. Plate B shows active sand harvesting, which is often unregulated. Source: (Author 2025).

Plate III: The gas chromatography (GC) laboratory at Mazingira Centre. Plate A shows the GC equipment, while plate B shows GHG samples delivered for analysis of concentrations. Source: (Author 2025).

Plate IV: The role of livestock and human activities in the riparian zones of Taita Taveta. Plate A illustrates a looming water crisis in the Msau lowland region. There is active competition for domestic use, irrigation, and livestock watering. Plate B features dung deposition by livestock on the riparian zones. Source: (Author 2025).

Plate V: Seasonal roles of riparian lands in Taita Taveta. Livestock watering from a pond in the rainy season (left) and water competition between livestock and irrigation pumps in the dry season (right). Source: (Author 2025).

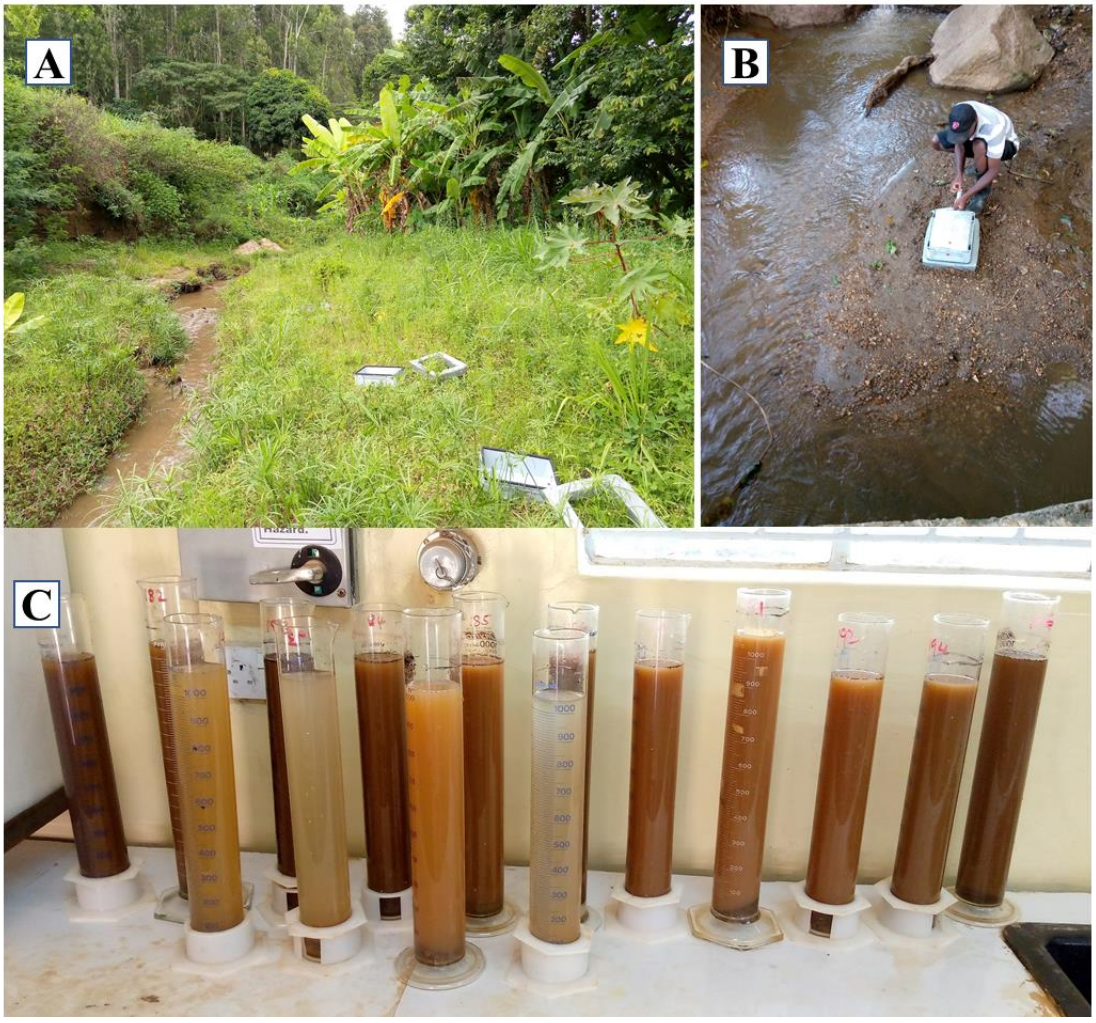

Plate VI: GHG sampling and soil analysis. Sampling in the Upland zone characterized by forest and mixed farming, with smaller streams in (A). Instream greenhouse (GHG) sampling in a Midland zone (B), and clay content analysis (C). Source: (Author 2025).

Appendix VI: Similarity report

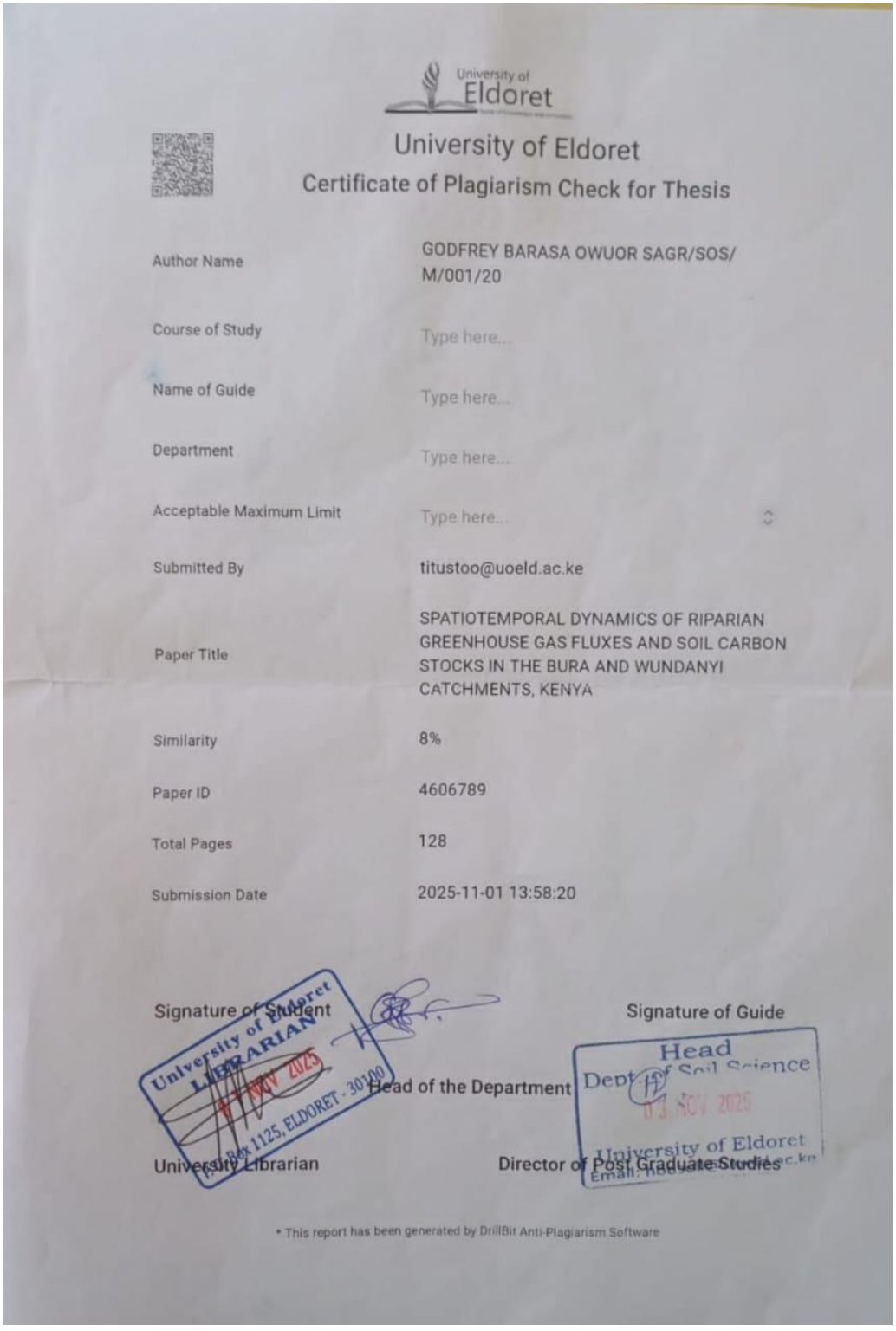

University of Eldoret

University of Eldoret

Certificate of Plagiarism Check for Thesis

Author Name	GODFREY BARASA OWUOR SAGR/SOS/ M/001/20
Course of Study	Type here...
Name of Guide	Type here...
Department	Type here...
Acceptable Maximum Limit	Type here...
Submitted By	titustoo@uoeld.ac.ke
Paper Title	SPATIOTEMPORAL DYNAMICS OF RIPARIAN GREENHOUSE GAS FLUXES AND SOIL CARBON STOCKS IN THE BURA AND WUNDANYI CATCHMENTS, KENYA
Similarity	8%
Paper ID	4606789
Total Pages	128
Submission Date	2025-11-01 13:58:20

Signature of Student

Signature of Guide

University of Eldoret LIBRARIAN 04 NOV 2025 P. O. Box 1125, ELDORET - 30100

Head of the Department

Head Dept. of Soil Science 03 NOV 2025 University of Eldoret

University Librarian

Director of Post Graduate Studies

* This report has been generated by DrillBit Anti-Plagiarism Software